Spring 2022

Comparative Assessment of the Fate and Toxicity Of Chemically and Biologically Synthesized Silver Nanoparticles Toward Juvenile Clams, *Mercenaria Mercenaria*

Amar Yasser Al-Rshim

COMPARATIVE ASSESSMENT OF THE FATE AND TOXICITY OF CHEMICALLY AND BIOLOGICALLY SYNTHESIZED SILVER NANOPARTICLES TOWARD JUVENILE CLAMS, *MERCENARIA MERCENARIA*

by

Amar Yasser Al-Rshim

Bachelor of Food and Dairy Technology
University of Basrah, 2001

Master of Food Sciences and Biotechnology
University of Basrah, 2010

Submitted in Partial Fulfillment of the Requirements

For the Degree of Degree of Doctor of Philosophy in

Environmental Health Sciences

The Norman J. Arnold School of Public Health

University of South Carolina

2021

Accepted by:

Mohammed Baalousha, Major Professor

Geoffrey I. Scott, Committee Member

Dwayne E. Porter, Committee Member

Yeomin Yoon, Committee Member

Tracey L. Weldon, Interim Vice Provost and Dean of the Graduate School

DEDICATION

I dedicate my dissertation to the soul of my beloved father and to the martyrs of Iraq.

ACKNOWLEDGEMENTS

In the first place, after spending a long hard time through the journey of realizing this thesis, thank Allah for allowing me to complete this thesis.

I would like to personally acknowledge all those who supported me and helped to come to the end of this work. I am grateful to so many who made it possible for me to undertake doctoral research at the University of South Carolina: To Dr. Mohammed Baalousha, my advisor, mentor, and friend—thank you for your guidance and patience, and for creating a research environment that values personal growth, exploration, and fundamental understanding. Special thanks to Dr. Geoff Scott, Dr. Yoon, Dr. Dwayne Porter for their support, expertise, and advice throughout the design and implementation of this research.

There is, unfortunately, no research without money, so I express much gratitude to the sponsor for this study, the Ministry of Higher Education and Scientific Research and Iraqi Cultural Office in Washington DC.

I am grateful to the core faculty, fellows, and administrators of the University of Basrah, Marine Science Centre, and the SmartState Center for Environmental Nanoscience and Risk (CENR) to create many opportunities for interdisciplinary research professionals' development.

To my family, my mother deserves special thanks for her continued praying, support, encouragement, and steadfast belief in me. Without you, I would not be

who I am today. Thanks also to my siblings and their families, my parents-in-law and brothers-in-law.

The person I would like to thank the most is my amazing wife, Nesami, who has been exceptionally supportive of me throughout the travails, absences, tantrums, and impatience I've experienced. She gave me love and made countless sacrifices to help me get to this point. She also supported the family during much of my graduate studies. I am deeply grateful for her love and undying support and owe her everything. Along with her, I would like to acknowledge my daughters and sons. They are both beautiful sources of love and relief from my scholarly endeavors.

ABSTRACT

Engineered nanomaterials (ENMs) with unique nanoscale properties, including novel optical behavior and superparamagnetic, are continually being developed for biomedical and industrial applications. In specific biomedical applications, ENMs are surface-functionalized using polymers, proteins, and other stabilizing agents to facilitate their resistance to salt-induced aggregation. Since their colloidal stability in high ionic-strength matrices, functionalized ENMs are anticipated to be persistent aquatic contaminants. Despite their potential environmental significance, the persistence of surface-functionalized ENMs as individually stabilized nanoparticles in marine environments is largely unknown. Further, few studies have investigated the fundamental factors that influence ENMs uptake and fate/transport processes in ecologically susceptible aquatic biota, such as filter-feeding bivalves, which ingest and accumulate a broad range of dissolved- and particulate-phase contaminants.

This study was aimed to explain a comprehensive approach to prepare and rigorously characterize ENM test suspensions to facilitate fundamental examinations of nanoparticle toxicity and fate/behavior processes in marine bivalves. We have investigated the synthesis and characterization of AgNPs through chemical and biological approaches. The chemical approach (cit-AgNPs) is based on the reduction of ionic silver using sodium borohydride (NaBH4) as a reducing agent and trisodium citrate ($Na_3C_6H_5O_7$) as a reducing agent. The

biological synthesis approach (bio-AgNPs) is based on the reduction of ionic silver using biomolecules extracted from the fungi *Aspergillus parasiticus* strain AFS10. The biomolecules also act as a capping agent. The physicochemical properties of the synthesized AgNPs were determined using UV-vis Spectrophotometer, dynamic light scattering (DLS), laser Doppler electrophoresis, inductively coupled plasma-atomic mass spectroscopy (ICP-MS), transmission electron microscopy (TEM), asymmetric flow-field flow fractionation (AF4-ICP-MS), and single-particle (SP-ICP-MS). Both synthesis approaches generated spherical AgNPs. The core and hydrodynamic diameters (9.72 ± 0.1 nm and 21.5 ± 0.1 nm) of the chemically synthesized AgNPs were slightly smaller than those (15.85 ± 0.8 nm and 38.6 ± 0.1 nm) of the biologically synthesized AgNPs. The chemical synthesis approach produced AgNPs with narrower size distributions (more monodispersed) than those generated through the biological synthesis approach. The magnitude of the zeta potential of the chemically synthesized AgNPs was higher than those of the biologically synthesized AgNPs.

The environmental behavior (i.e., aggregation and dissolution) and toxicity (i.e., mortality) of commercially powder AgNPs (Ag-*n*-powder), cit-AgNPs, bio-AgNPs, and dissolved silver ($AgNO_3$) to Juvenile *Mercenaria mercenaria* (0.820 – 1.2 mm) at 24-h exposure. The hydrodynamic diameter of cit-AgNPs, bio-AgNPs, Ag-*n*-powder in stock suspensions, determined by dynamic light scattering, were 21.5 ± 0.1, 38.6 ± 0.1, and 132 ± 2.0 nm, respectively. All AgNPs formed aggregates in natural seawater. The dissolution of AgNPs in natural seawater (the toxicological test media) was measured by an inductively coupled plasma-mass

spectrometer following ultrafiltration (3kDa). The dissolved Ag concentration increased with the increases in AgNP concentration over a range of environmentally relevant concentrations: 0.2, 0.35, 0.6, 1.0, 1.5, and 2.6 mg-Ag L^{-1}. Mortality (%) of juvenile clams decreased following the order $AgNO_3$ (24-h mean LC50 value of 0.24 mg L^{-1}, 95% confidence intervals: 0.22–0.27 mg L^{-1}) > cit- AgNPs (24-h LC50 of 0.7 mg L^{-1}, 95% confidence intervals: 0.645–0.87) > and bio-AgNPs (24-h LC50 of 1.05 mg L^{-1}, 95% confidence intervals: 0.90–1.36 mg L^{-1}) > powder-AgNPs (24-h LC50 of 2.44 mg L^{-1}, 95% confidence intervals: 1.81–2.43 mg L^{-1}). Dissolved Ag could not explain the toxicity of AgNPs, indicating that the toxicity of AgNPs can be attributed to a combined effect of dissolved ions and the AgNPs.

TABLE OF CONTENTS

LIST OF TABLES

LIST OF FIGURES

CHAPTER 1

BACKGROUND AND PROBLEM STATEMENT

1.1 Nanoscience and Nanotechnology

Nanotechnology is the manipulation and control of matter at the nanoscale; that is 1-100 nm in order to achieve control and exploit the novel properties of materials that manifest themselves in the nanoscale domain for many technological and consumer applications. Nanotechnology is expected to influence all aspects of our lives, from how we generate energy to remedy health disorders. However, these novel material properties may also pose a risk to environmental and human health.

Since Feynman's seminal speech in 1960, nanotechnology has advanced by leaps and bounds due to scientific and technological advancement such as the invention of the scanning tunneling microscope that enabled the control of matter atom by atom and the improvement of the transmission electron microscope that enabled imaging materials at the atom in scale.

1.2 Definitions

Defining a nanoparticle or nanomaterial has been a subject of discussion over the past two decades, and there are currently numerous definitions from different national and international agencies. Nanoparticles are defined as materials having a dimension of approximately 1–100 nm, where this unit represents 10^{-9} meters in length (Nowack and Bucheli 2007). An easier way to image the nanoscale size range is by comparing this scale to common objects in our life of nanomaterials. For instance, a 1 nm nanoparticle is 100,000 times smaller than the diameter of a human hair or paper thickness and 7000 times

smaller than a red blood cell (Dowling et al. 2004). Figure 1.1 shows the length of the nanometer compared to other objects.

Even though the definition of nanomaterials above has been widely used, still, nanomaterials' pragmatic and apparent definition has not been agreed upon because of the different existing viewpoints of various stakeholders (Kreyling et al. 2010). Other definitions, therefore, have also been suggested. Different organizations proposed and adopted slightly different meanings of nanomaterials (NMs) (Boverhof et al. 2015).

A working group of the Europaische Akademie (Schmid et al. 2003) states the recent definition forwarded by: *"Nanotechnology is dealing with functional systems based on the use of sub-units with specific size dependent properties of the individual sub-units or of a system of those"*.

Following definitions of 'nanoscience' and 'nanotechnologies' are given by 2004 the Royal Society and Royal Academy of Engineering as: *"Nanoscience is the study of phenomena and manipulation of materials at atomic, molecular and macromolecular scales, where the properties differ significantly from those at a larger scale"; "Nanotechnologies are the design, characterisation, production and application of structures, devices and systems by controlling shape and size at nanometre scale".*

According to The US Food and Drug Administration (UDFDA 2011), *“Materials that have at least one dimension in the range of approximately 1 to 100 nm and exhibit dimension dependent phenomena”*

The Environmental Protection Agency (EPA, 2012) also denotes to NMs as "*NMs can exhibit unique properties dissimilar than the equivalent chemical compound in a larger dimension*" (Jeevanandam et al. 2018).

1.3 Classification of nanomaterials

Nanomaterials can be organized into four categories based on their composition:

Carbon-based nanomaterials: These NMs contain carbon, commonly speaking, and are present in different morphologies, including hollow tubes and ellipsoids. Examples are carbon nanotubes (CNTs) and their derivatives like Fullerenes, which are a 60-carbon atom hollow sphere, also known as the Buckyball (Kroto et al. 1985), carbon nanofibers, carbon black, graphene (Gr), and carbon nano-onions (Kumar and Kumbhat 2016). Carbon-based materials are used in components in electronics, aircraft, aerospace, and automotive industries, vehicles, sensors, plastics, conductive coatings, composites, and batteries and fuel cell electrodes, super-capacitor devices, water purification devices, orthopedic implants. Expanded production of carbon-material results in an increased possibility for release to the environment, either accidentally in spillages or intentionally in discharges, and a greater potential of adverse environmental effects (Klaine et al. 2008).

Inorganic-based nanomaterials: These nanomaterials, composed of metal and metal oxide materials, have received considerable attention, and have a wide spectrum of applications. Metal and metal oxide nanomaterial such as Au,

Ag, TiO_2, ZnO can be synthesized relatively easily within the capacity of most chemical laboratories (Gu and Soucek 2007). Owing to their ultraviolet blocking capabilities and the visible limpidity of nanomaterials, zinc oxide, and TiO_2 are used widely in sunscreens, cosmetics, and bottle coatings. Inorganic NMs also include semiconductor nanocrystals, also known as quantum dots (QDs), which possess a reactive core that dominates their optical properties (Dabbousi et al. 1997).

***Organic-based nanomaterials*:** These nanomaterials are nanosized polymers constructed from organic matter and branched units, excluding carbon- or inorganic-based nanomaterials. The noncovalent (weak) interactions utilizing for the self-assembly and design of molecules help transform the organic NMs into desired forms such as dendrimers, liposomes, micelles, and polymer Nanoparticles. Dendrimer's surface contains multiple chain terminations and can be tailored to achieve certain chemical functions. This property might be valuable for catalysis, and it may also be useful for drug delivery because three-dimensional dendrimers contain interior cavities into which other molecules could be placed.

***Composite nanomaterials*:** The nanocomposites field includes the study of multi-phase materials, which have at least one of the constituent phases is less than 100 nm in length (Ajayan 2003). Nanocomposites are materials that either combines two different types of NMs or NMs with larger or bulk- materials (e.g., hybrid nanofibers), or more complicated structures. Composite nanomaterials may have any compositions of carbon-based, metal-based, or organic-based NMs with any form of metal, ceramic, or polymer bulk materials. Examples of

polymer/ceramic nanocomposites of technological interest are formed by ceramic nanoparticles such as barium strontium titanate phase in a matrix with low dielectric loss (Zhou et al. 2008) or nickel-zinc ferrite, dispersed in a polymeric matrix such as vulcanized natural rubber (Ismail et al. 2007).

1.4 Main Sources of nanomaterials

Nanomaterials are used in many products that we use in our daily life, and thus we are constantly exposed to various types of nanomaterials. NMs can be classified into three main categories based on their origin, including natural, incidental, and engineered NMs.

1.4.1 Natural nanomaterials

Natural nanomaterials are materials produced by natural processes such as soil erosion, dust, volcanic activities, and ashes, but also some organisms show sizes of range 1-1000 nm (Buzea et al. 2007). Although the biggest number of particles generated in a dust storm show sizes of a little micrometer, they also include a fraction of particles <100 nm. The quantity of nano- and microparticles can be so large that it can be observed by satellites. Natural colloids (and nanoparticles) are omnipresent in the environment and might originate from geogenic or biogenic sources (Buffle et al. 1998). Natural nanomaterials are found as suspended particles smaller than 25 nm in marine surfaces and groundwater (Lead et al. 2005; Baalousha and Lead 2007). The ashes created during a forest fire, or a volcanic eruption are also a source of nano-and micromaterials. Organisms like viruses and some bacteria also show sizes of a few nanometers

up to a few hundred nanometers, making them part of the nanomaterial regime, which can be found in the air. Nano/micro scale materials can be found not only outdoors but also indoors. According to the US Environmental Protecting Agency, indoor air can be ten times more polluted than outdoor air (USEPA 2010). Indoor sources of NMs include cooking, smoking, dust, skin particles, spores, and combustion (e.g., candles). According to The World Health Organization worldwide, 1.6 million people die annually because of indoor air pollution (WHO 2010).

1.4.2 Incidental nanomaterials

They are produced by physical, chemical, biological, mechanical, or hybrid methods. By-products of industrial processes, including nanoparticles formed from vehicle exhaust engine, fumes of welding and combustion, and even natural processes such as forest fires, are generated unintentionally. Platinum and rhodium NMs were un-intended released with traffic density and drive speed by the automotive catalytic converters because of factors that regulate their concentration level (Levard et al. 2012; Lowry et al. 2012). Carbon Black, an incidentally industrial form of soot which is commonly used filler in rubber compounds such as those used for automobile tire.

1.4.3 Engineered nanomaterials

Engineered nanomaterials (ENMs) are manufactured purposefully by humans with controlled properties such as size, shape, coating, composition in order to exploit their novel properties for the desired applications. Engineered

nanomaterials can be synthesized by physical, chemical, biological, or hybrid methods. ENMs could be carbon-based such as carbon nanotubes and fullerenes or based upon inorganic materials such as metals (gold, silver, and iron), metal oxides (ceria, titania, zinc, and iron), and quantum dots (cadmium sulfide and cadmium selenide) which are present in sporting goods, toothpaste, sunscreen, and commercial cosmetics. Such synthesized NMs are thus new genera of NMs that are able to pose adverse effects on the environment and human health(Jeevanandam et al. 2018). The pivotal challenge is whether existing knowledge of engineered nanomaterials is adequate to predict their behavior or if ENMs exhibit a distinct fate in the environment that differs from natural and Incidental nanomaterials (Wagner et al. 2014).

1.5 Physicochemical properties of nanoparticles

The physicochemical properties of NM, such as size, composition, specific surface area, and surface energy, play a vital role in regulating NM behavior and generally differ for each class of NMs. Nanomaterials have unique properties comparing to their bulk counterparts, which impart beneficial characteristics to NMs. Paradoxically, these novel properties of NMs may pose risks to environmental and human health. Generally, it is thought that the toxicity of NMs arises from their surface area, size, shapes, composition, etc. (Gatoo et al. 2014). NM properties are critical to understanding their fate and transformations and their risk assessment (Lead et al., 2018). Figure 1.2 depicts the most relevant NM properties to their environmental fate and effects, such as particle size, surface area, charge, coatings, different shapes, and materials.

Particle size and surface area: size is the most significant property of NMs as it influences other properties of NMs. Decreases in particle size results in increases in increases in the specific surface area (i.e., surface area per unit mass), leading to increased surface reactivity and energy. Due to the increased surface area, NMs possess massive surface energy and subsequently are thermodynamically unstable (Rama et al. 2021).

The small size of NMs prevents their gravitational settling in environmental matrices such as air or water. Thus, nanomaterials remain in suspension and settle only if their size increases by agglomeration. Therefore, size and surface area are essential properties that greatly influence the behavior and transport of ENMs in the environment as well as their interaction with the biological system (Nel et al. 2006; Aillon et al. 2009).

In terms of the environment and public health, it is well known that the fate and effects of NMs differ from their bulk counterparts (Nel et al. 2006). The size-dependent toxicity of NMs is due to their ability to penetrate the biological systems and then modify the structure of various macromolecules, thereby interfering with vital biological functions (Lovrić et al. 2005; Aggarwal et al. 2009). In the human respiratory tract, NM size has been shown to affect their translocation and dissemination, which in effect determines their toxicity. Asgharian and Price have observed that NMs less than 10 nm occur only in the tracheobronchial region, while larger particles with a diameter larger than 100 nm deposit in all regions (Asgharian and Price 2007). The toxicity of gold and silver NMs has been tested on zebrafish in different sizes ranging from 3, 10, 50, and 100 nm. AgNMs exhibited size-

dependent mortality, whereas the behavior of AuNMs was independent of size (Seaton and Donaldson 2005).

Surface charge and agglomeration degree: The surface charge is a significant characteristic of NMs and has a substantial impact on the fate and behavior of NMs. NM surface charge cannot be measured directly, and thus, zeta potential is the potential at the slipping plane or surface of the shear plane (hydrodynamic shear), which is used as a proxy of surface charge. Surface charge is a key property influencing NM colloidal stability. NMs (mostly positively charged ones) strongly influence NM interactions with biological systems such as blood-brain barrier integrity, the permeability of the transmembrane, and NMs selective adsorption (Georgieva et al. 2011; Pietroiusti et al. 2011).

1.6 Transformations and fate of engineered NMs

The intrinsic properties of NM such as high surface area, surface energy, and surface atom availability makes NMs very reactive to their surrounding environment, leading to many NM transformations (Dwivedi et al. 2015; Abbas et al. 2020), including surface coating replacement (e.g., degradation or replacement by natural organic matter), oxidation, dissolution, sulfidation, advection, diffusion, hetero-and homo-aggregation/disaggregation, and sedimentation/ resuspension (Figure 1.3). NM transformation processes can be grouped as physical, chemical, and biological transformation processes.

1.6.1 Chemical transformation

Nanomaterials undergo various chemical transformation processes such as dissolution, oxidation-reduction (redox), degradation, adsorption, complexation, and photochemically induced reactions. These transformations occur due to the presence of inorganic and/or organic ligands and other constituents of terrestrial and aquatic systems(Abbas et al. 2020). Oxidation and reduction transformations define the transfer of electrons (loss or gain) between reacting chemical moieties in the natural environment. Redox reactions are governed by different environmental conditions such as pH and the existence of electron donors (reducing agent) or acceptors (oxidizing agent) (Nowack et al. 2012). Metallic and metal oxide NMs (e.g., Ag, Cu, nZVI, and Fe oxides) are susceptible to undergo oxidation-reduction transformations (Mudunkotuwa et al. 2012; Mitrano et al. 2016).

Dissolution is the release of water-soluble ions or molecules from NMs, which is a crucial chemical transformation process determining NM's environmental fate and effects. NMs can be categorized into highly soluble (Ag, Cu/CuO, FeO, QDs, Zn/ZnO), poorly soluble (CeO_2, TiO_2), and insoluble (CB, CNTs, graphene, fullerenes) materials. The oxidative dissolution of AgNMs occurs in surface water and well-aerated soil. Ag^o converts into silver ions (Ag^+) due to surface atoms' chemical oxidation (Dwivedi et al. 2015).

Their high affinity to organic and inorganic sulfide ligands to soft metals (e.g., Ag, Cu, Zn) usually causes the sulfidation of NMs made of these soft metals.

In contrast, their dissolution leads to the production of partially soluble metal oxides (Figure 1.4). Dissolution and sulfidation processes significantly impact NM surface properties, persistence, and toxicity. The sulfidation of metals induces their aggregation owing to the formation of an insoluble metal-sulfide on their surface that alters NM surface charges. On the other side, dissolution leads to the release of toxic ions, reduces NM stability and persistence, and increases their toxicity (Levard et al. 2011).

Adsorption of macromolecules and organic and inorganic ligands on NMs alters NM behavior and surface chemistry radically. For example, the dissolution, charge, and stability of NMs are influenced considerably by the adsorption of organic ligands having thiol groups. Moreover, polymer coating adsorption to NMs increases their mobility and, consequently, their removal from drinking water (Fauconnier et al. 1997; Deonarine et al. 2011).

1.6.2 Physical transformation

Aggregation/agglomeration and sedimentation/deposition can occur at all stages of the life cycle of NMs (Peijnenburg et al. 2015). Typically, aggregation/agglomeration phenomena are interchangeably utilized because distinguishing between them is not easy-going. Agglomerates are “collection of loosely bound particles or aggregates, or mixtures of the two having external surface area similar to the sum of the surface areas of the individual components” and “weak forces (van der Waals forces) as well as simple physical entanglement holds an agglomerate together” (British Standards Institution 2007). Aggregation

is, theoretically, an irreversible path that binds particles together by electrostatic or strong chemical forces, resulting in a reduction in surface area.

Once NMs have been released into the environment, they undergo homo-aggregation, which occurs between the same kind of NMs, or hetero-agglomeration, between organic and inorganic colloids or other surrounding particles in the environment (Lei et al. 2018). Agglomeration contributes to increasing the size of NMs, which in turn impacts their reactivity, sedimentation, transportation, and toxicity (Figure 1.4).

In environmental matrices (aquatic and terrestrial), NMs' interactions with natural colloids such as clay minerals, organic matter, Fe and Mn hydrous oxides, and extracellular polymeric substances (EPS) lead to modulation of the stability and agglomeration state of ENMs.

Despite NMs being kinetically stable in suspensions, they are still thermodynamically unstable due to the collision of NMs (Brownian motions) (Handy et al. 2008). Thus, collisions can lead to peri-kinetic aggregation, Differential settling of particles with different sizes, and fluid movement.

Because of the Brownian motions, the particles are in constant motion and collide with each other. They agglomerate when the attractive van der Waals force balances repulsive electrostatic force. Agglomeration, alternatively, is a reversible phenomenon that binds particles together by van der Waals forces without impacting the surface as they remain separate entities (Nichols et al. 2002).

According to Derjaguin-Landau-Verwey-Overbeek (DLVO) theory, the agglomeration rate of NMs is regulated by surface charge, particle size, Hamaker constant, and media ionic strength (Tourinho et al. 2012; Goswami et al. 2017). Also, non-DLVO-related processes, such as hydration effects, steric barriers, polymers, and hydrophobicity interactions, donate significantly to the agglomeration process of NMs in the environmental media (Thompson et al. 2009; Wagner et al. 2014).

Between agglomeration and sedimentation is a logical relation. The agglomeration processes increase the size of particle flocks over time. Thus, NMs number concentration reduces in the suspensions, which favor the deposition of large, agglomerated particles. Because of the gravity force regulated by Stoke's law, which helps remove NMs, agglomerated particles tend to settle more than to diffuse from aquatic environments (Hartmann et al. 2014).

1.6.3 Biological transformation

Biological transformations of nanomaterials in the environment include biodegradation, the formation of NMs by reducing biomolecules, the formation of bio-corona, and nano-bio-interactions. These processes' rates and relative importance are based on the interaction of NMs with extracellular enzymes, extracellular polymeric substances (EPS), and microbes. Nanomaterials' properties such as the activity, surface charge, aggregation state, and toxicity will be altered through these transformations (Lowry et al. 2012) (Figure 1.5).

In the natural environment, various tissue extracts containing macromolecules (biomolecules) are present, produced, and secreted by diverse flora and fauna (Xu 2011). The metal ions can be transformed into the NMs due to the existence of reductive enzymes and functional groups in the secreted tissue extracts (Oza et al. 2020). Bacteria such as Geobacter and Shewanella have demonstrated their redox reactions, which reduced Ag^{+} from solution and formed silver NMs (Law et al. 2008). It is also established that the biological transformations of bioavailable polyethylene glycol (PEG) coatings on NMs have led to their aggregation (Kirschling et al. 2011).

Overall, NMs do not have the same behavior and toxicity in aquatic environments as they change marine and fresh water at high dilutions. For example, the introduction of suspended particulate matter and natural colloids into marine environments leads to various behaviors that change due to the receiving estuarine systems (Guzman et al. 2006). It was established that NM transformation processes depend primarily on the receiving water body's chemical and environmental characteristics (Ju-Nam and Lead 2008).

1.7 Silver Nanoparticles

Silver nanoparticles (AgNPs) are used in a wide range of applications, including pharmaceuticals, cosmetics, medical devices, food products, clothing, and water purification, among other uses (Choi et al., 2008). Due to AgNPs' novel properties and their increasing applications in many aspects and commercial sectors, multiple synthesis protocols have been studied and can be grouped into the so-called top-down and bottom-up methods (Ju-Nam and Lead 2008). AgNPs

can be synthesized using various approaches including chemical, physical, and biological. Although chemical and physical methods of synthesis require a short period of time to synthesize a large quantity of nanoparticles, however, the chemical and physical processes of AgNPs production involve the use of toxic and hazardous chemicals, which may pose potential environmental and biological risks. Thus, the need for environmentally and economically feasible approaches to synthesize AgNPs leads to the developing interest in biological methods that are free from the use of toxic chemicals as by-products. To this end, there is an increasing demand for green nanotechnology (Singhal et al. 2011). To date, numerous biological procedures for extracellular and intracellular nanoparticle synthesis have been stated using microorganisms, including bacteria, fungi, etc., as well as plants (Mukherjee et al. 2001; Mohanpuria et al. 2008).

Biosynthesis of AgNPs is a bottom-up approach that mostly involves reduction/oxidation reactions. The three major components involved in synthesizing nanoparticles using biological methods are the solvent medium for synthesis, the environmentally friendly reducing agent, and a nontoxic stabilizing agent (Prabhu and Poulose 2012). Towards this end, the use of fungal extracts to synthesize AgNPs becomes an option that is feasible compared with bacteria. Because fungi are known to secrete much higher amounts of bioactive substances, which directly translate to higher nanoparticle productivity (Narayanan and Sakthivel 2010), the extracellular biosynthesis using fungi could make downstream processing much easier than bacteria (Mohanpuria et al. 2008).

1.8 Nanoparticle toxicity

A zero-risk approach to environmental regulation is not economically feasible. Management of chemical risks to predict ecological effects is thus the primary focus of regulatory policy. The rising use of manufactured nanoparticles increases the likelihood that nanoparticles will enter the environment. Research has indicated that materials considered benign in the bulk form may show toxic or adverse effects when nano-sized (Adams et al. 2006; Grassian et al. 2007).

The primary reasons for releasing nanomaterials into the environment are the processing, production, use, disposal, and waste treatment of products containing nanoproducts. Human skin usually blocks foreign substances, whereas lungs and gastrointestinal tract organs are vulnerable to foreign substances. Given NMs are similar viruses in size, Inhaled NMs can effortlessly reach the bloodstream and other organs within the human body, including the liver, heart, or blood cells. It's necessary to note that NMs' toxicity depends on their sources. Some look to be nontoxic, and others have positive health effects (Gnach et al. 2015). NMs are cytotoxic and are also likely hazardous to environmental and ecological health, depending on bioavailability. Therefore, environmental risk assessment analysis is vital so as to understand the environmental impact of NMs. Independent assessments of NMs exposure and NMs hazard need to be performed, and how this may change under different conditions.

1.9 Marine bivalves as sentinel organisms: uptake and cytotoxicity

There are around 7,500 species in the Bivalvia class, including animals with two shell valves(Gosling 2003). These species are diverse and abundant and are found in most aquatic as freshwater, estuarine water, and marine environment. Marine and freshwater bivalves are column water and sediment filter feeders and can be found at all latitudes and depths, though none of them are planktonic. Filter feeders are a sub-group of organisms fed by straining food particles and suspended matter from water, usually from passing the water throw a specialized filtering structure. Due to their filtrating mechanisms in aquatic ecosystems, bivalves are vulnerable to environmental pollutants' adverse effects. They are particularly beneficial to quantify pollutant contamination in water systems as keystone or indicator species (Doherty 1990). To this end, bivalves are broadly utilized as biological sentries for detecting and tracking a broad spectrum of environmental contaminants, including metals, persistent organic pollutants, asbestos fibers, biocides, protozoan parasites, and bacteria (Croteau and Luoma 2005; Miller et al. 2006; Mcleod et al. 2008).

In realistic environmental scenarios, the self-aggregation of NMs into larger masses and incorporating NMs into aggregate materials might increase the bioavailability and toxicity of aquatic organisms such as algae, phytoplankton, filter feeders and benthic deposit, and detrital feeders. According to Navarro et al., 2008, inorganic NM toxicity, such as AgNM and ZnONM, appears to be related to solubility or the release of toxic metal ions from the NMs instead of aggregation.

With a view to investigating presumed ecological impairments caused by AgNPs, it is necessary to select species that have a vital role in ecosystems' structure and functioning and are recognized as valuable models for biomonitoring purposes. In this way, marine invertebrates such as hard clam *Mercenaria mercenaria* suitable candidates. The hard clam *Mercenaria mercenaria* is a common inhabitant of estuarine sediments and a critical United States fishery species. The hard clam, *M. mercenaria*, is a marine filter-feeding, infaunal mollusk (Dillon and Manzi 1989). A juvenile clam toxicity bioassay has illustrated this species' sensitivity compared to other commonly used test organisms (Chung et al. 2007). Because bivalves in estuarine systems play a significant role in the ecological and economic aspects, the juvenile clam is a vital representative test species.

1.10 Dissertation organization

The overall of the research performed in this dissertation is to evaluate the environmental fate and effects of commercially available, chemically synthesized, and biosynthesized AgNMs toward the clam *Mercenaria Mercenaria*, which was performed under four specific objectives. First, synthesize silver nanoparticles using chemical and biological approaches. Second, characterize the physicochemical properties of the synthesized AgNPs by using multi-methods. Third, assess the acute toxicity of the synthesized AgNMs toward marine organisms. Fourth, quantify AgNP behavior (colloidal stability and dissolution) in the exposure media, i.e., natural seawater. To accomplish these goals, I set out the following chapters.

This dissertation contains five chapters, including the overall dissertation organization and this introductory chapter (**Chapter 1**).

Chapter 2 provides a general overview of NPs characterization, environmental fate, and effect. It also describes two approaches for the synthesis of silver nanoparticles by: (i) chemical rout (cit-AgNPs) using sodium citrate coated as reducing agent, (ii) biological rout (bio-AgNPs) using fungal extracts (reducing agent) of *Aspergillus parasiticus*. It also provides full characterization data of synthesized AgNPs by multi-technique.

Chapter 3 investigates the toxicological effects of commercial, bio- and cit-coated silver nanoparticles and dissolved Ag via an acute aqueous bioassay approach in the exposed estuarine juvenile hard clams (*Mercenaria mercenaria*).

Chapter 4 summarizes the overall conclusions of the findings of research permed as part of this PhD dissertation.

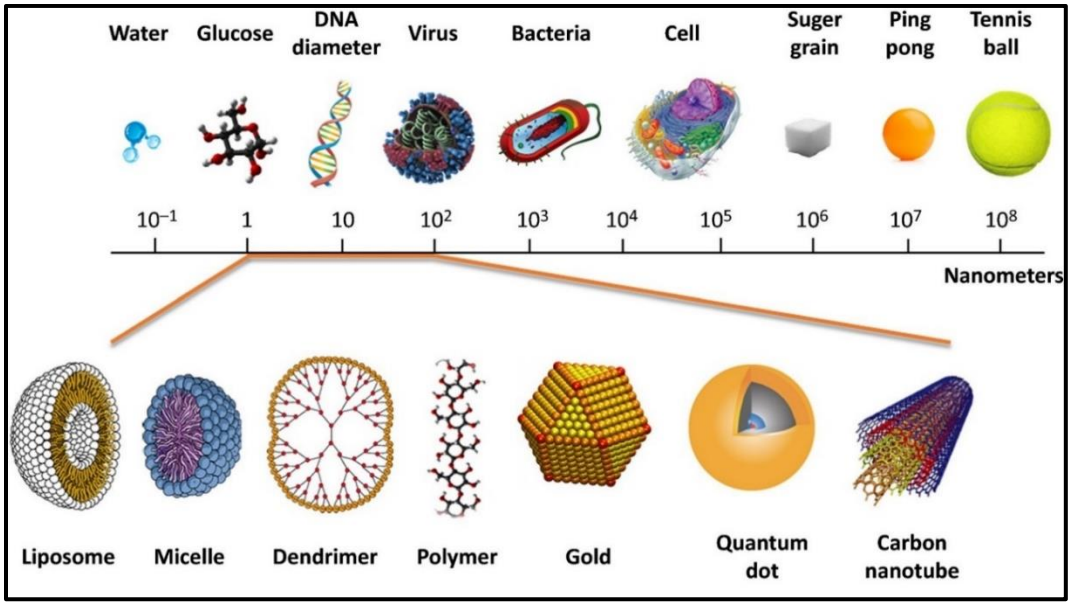

Figure 1.1 Schematic representation of nanoscale materials (1–100 nm) relative biological and common life objects (Wong et al. 2017).

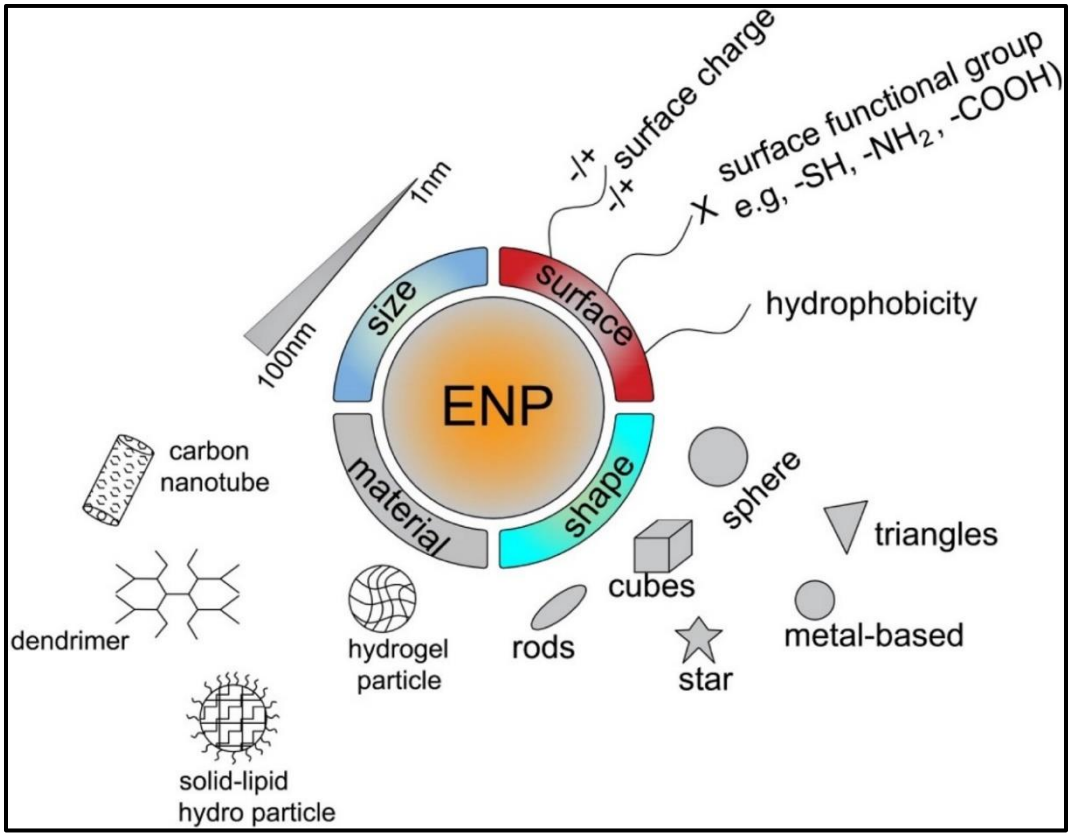

Figure 1.2 Schematic representation of the variability of the physicochemical properties of engineered nanomaterials (Turan et al. 2019).

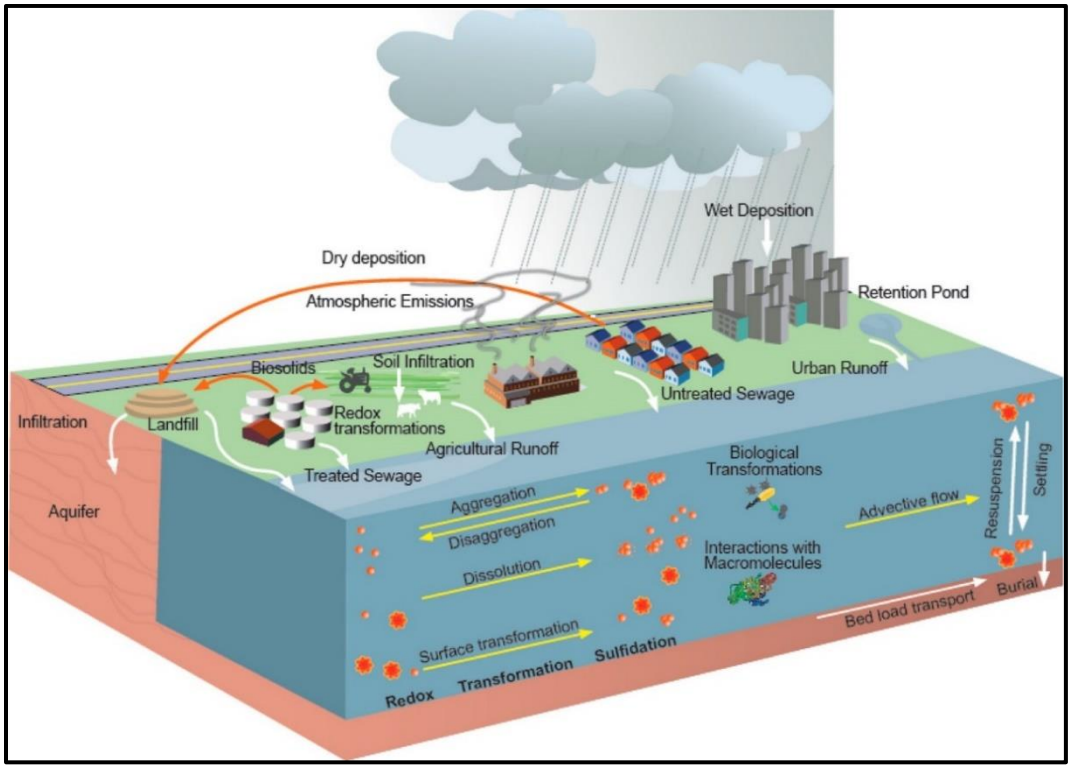

Figure 1.3 Schematic description of sources and flow of nanomaterials in the environment and the key processes are determined the fate and behavior of nanomaterials in aquatic environments (Dale et al.,2015).

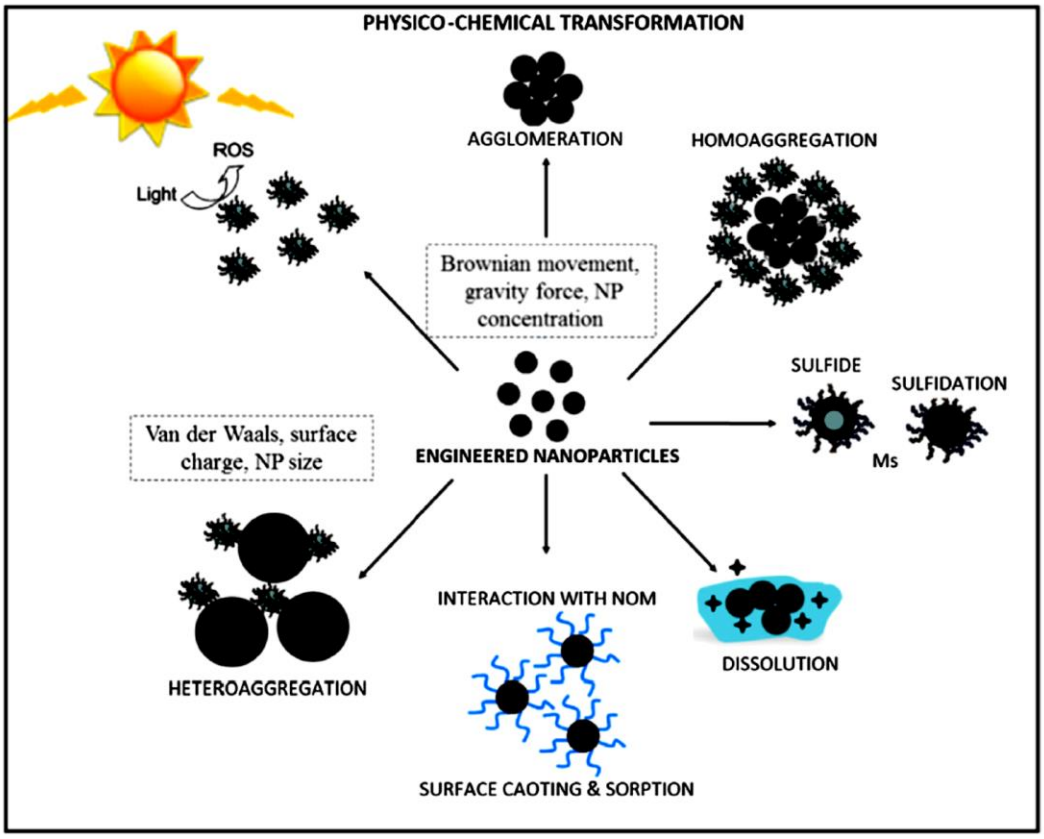

Figure 1.4 Physicochemical transformations include ENPs interaction with natural colloids (aggregation, sulfidation), photochemically mediated reaction generates the reactive oxygen (ROS), Natural organic matter (NOM) sorption on ENPs surface from (Lowry et al. 20; Abbas et al. 2020).

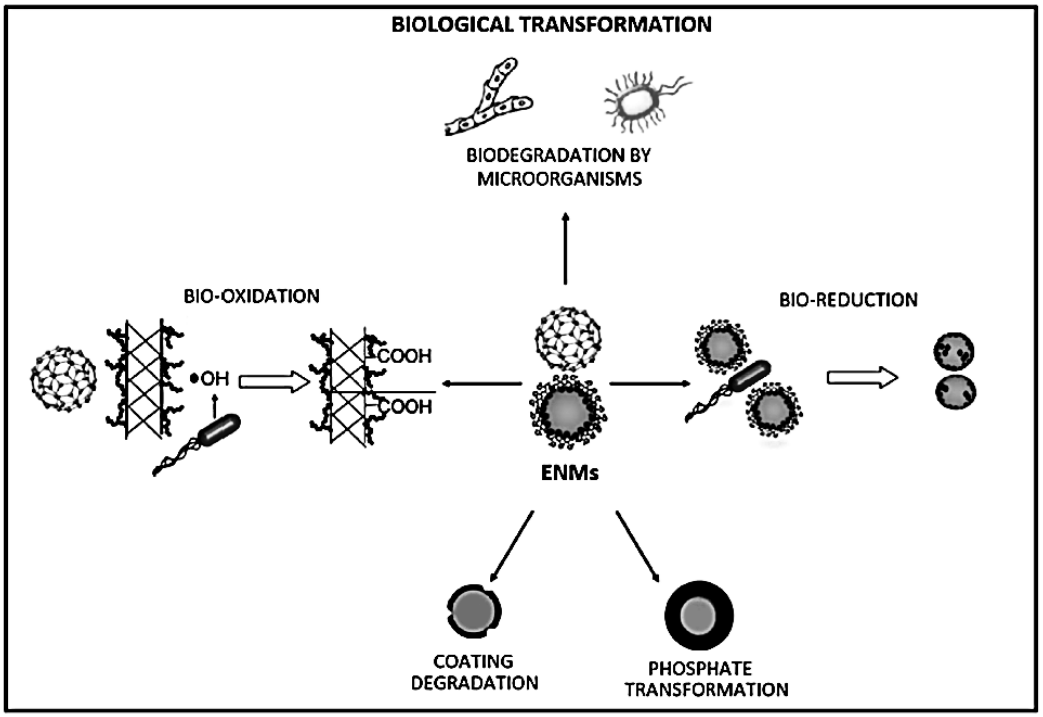

Figure 1.5 Biological medicated reactions degrade the ENPs surface coating, and microbial enzymes also govern the redox reactions (Lowry et al. 2012; Pachapur et al. 2016).

CHAPTER 2

SYNTHESIS AND CHARACTERIZATION OF SILVER NANOPARTICLES VIA CHEMICAL AND BIOLOGICAL ROUTS

ABSTRACT

Nanoparticles can be synthesized using different approaches, including physical, chemical, and biological approaches. This chapter investigates the synthesis and characterization of AgNPs through chemical and biological methods. The chemical approach (cit-AgNPs) is based on the reduction of ionic silver using sodium borohydride (NaBH4) as a reducing agent and trisodium citrate ($Na_3C_6H_5O_7$) as a reducing agent. The biological synthesis approach (bio-AgNPs) is based on the reduction of ionic silver using biomolecules extracted from the fungi *Aspergillus parasiticus* strain AFS10. The biomolecules also act as a capping agent. The physicochemical properties of the synthesized AgNPs were determined using UV-vis Spectrophotometer, dynamic light scattering (DLS), laser Doppler electrophoresis, inductively coupled plasma-atomic mass spectroscopy (ICP-MS), transmission electron microscopy (TEM), asymmetric flow-field flow fractionation (AF4-ICP-MS), and single-particle (SP-ICP-MS). Both synthesis approaches generated spherical AgNPs. The core and hydrodynamic diameters (9.72 ± 0.1 nm and 21.5 ± 0.1 nm) of the chemically synthesized AgNPs were slightly smaller than those (15.85 ± 0.8 nm and 38.6 ± 0.1 nm) of the biologically synthesized AgNPs. The chemical synthesis approach produced AgNPs with narrower size distributions (more monodispersed) than those generated through the biological synthesis approach. The magnitude of the zeta potential of the chemically synthesized AgNPs was higher than those of the biologically synthesized AgNPs. The environmental fate and effects of the chemically and biologically synthesized AgNPs are investigated in Chapters 3.

2.1 Introduction

The development of nanotechnology led to the creation of different types of nanomaterials (NMs), materials with at least one dimension of the order of 100 nm or less, where a nanometer is a billionth of a meter (10^{-9} m). The emerging growth of the nanotechnology industry also led to the development of numerous nano-enabled consumer products (Colvin, 2003; Maynard et al. 2006; Hartland et al. 2012). Due to their novel properties, nanomaterials, especially silver nanoparticles (AgNPs), are currently used in many applications such as pharmaceuticals, cosmetics, electronics, optical devices, environmental remediation, catalysis chemistry, and material sciences (Niemeyer 2010; Kim et al. 2016). In various stages of the production processes, applications, and during the disposal of the nano-wastes, nanoparticles might be released into aquatic environments. Since the demand escalates, the potentially released nanoparticles into the environment will also increase exponentially, and there will be added effects on organisms and ecosystems (Ringwood et al. 2010; Lapresta-Fernández et al. 2012). Even though several studies illustrated the adverse implications of AgNPs on human and environmental health, the mechanism of toxicity of AgNPs is still ambiguous.

Silver nanoparticles (AgNPs) are used in a wide range of applications, including pharmaceuticals, cosmetics, medical devices, food products, clothing, and water purification, among other uses (Choi et al. 2008).

Due to the novel properties and increased use of AgNPs in many consumer products, multiple synthesis protocols have been studied, which can be grouped into top-down and bottom-up methods (Ju-Nam and Lead 2008). The bottom-up

approach of the synthesis of AgNPs can be achieved using various approaches, including chemical, physical, and biological.

Chemical synthesis of nanoparticles in aqueous solutions necessitates the use of methods that allow for precise control over the shapes and sizes of nanoparticles, resulting in a combination of monodisperse nanoparticles with unique properties. The nature and concentrations of metal precursors, reducing agents, and stabilizing agents are crucial to controlling the synthesis of metal nanoparticles in an aqueous solution. The fabrication mechanism of colloidal solutions from the reduction of silver ions (Ag^+) consists of nucleation and growth phases. High activation energy is required in the nucleation step, whereas the growth step needs low activation energy. Various sizes and shapes of nanoparticles can be obtained by controlling the relative rates of these processes, which can be governed through the adjustment of the reaction parameters (temperature, pH, concentration, reducing ability, etc.) (Cushing et al. 2004; Burda et al. 2005; Evanoff and Chumanov 2005).

Given its chemical stability and low cost compared to the other available silver salts, silver nitrate is frequently used for AgNPs synthesis. Citrate (Pyatenko et al. 2007), borohydride(Evanoff and Chumanov 2005), ascorbate (Blanco-Andujar et al. 2010), and hydrogen gas (Moore 2006) are the most common reductants. One of the most potent reducing agents used is borohydride because it can form ultrafine particles with a faster reduction rate. Moreover, Sodium Borohydride ($NaBH_4$) also serves as a stabilizer of synthesized silver nanoparticles and prevents the aggregation processes during its decomposition (Moore, 2006). The

colloidal instability of AgNPs hampers the synthesis of high concentrations of AgNPs. The stabilizers include surfactants or ligands or polymers containing functional groups like polyethylene glycol, polyvinylpyrrolidone, poly-methacrylic acid, polymethyl methacrylate, and polymers such as poly (N-isopropyl acrylamide) and collagen (Chen et al. 2013).

Although chemical and physical processes of synthesis require a short period of time to synthesize a large number of nanoparticles yet, the problem with most of the chemical and physical methods of AgNPs production involves the use of toxic and hazardous chemicals, which may pose potential environmental and biological risks. Thus, the need for environmentally and economically feasible approaches to synthesize these nanoparticles leads to the increased interest in biological approaches that are free from the use of toxic chemicals as byproducts. Thus, there is an increasing demand for green nanotechnology (Singhal et al. 2011). Many biological procedures for both extracellular and intracellular nanoparticle synthesis have been reported to date using microorganisms, including bacteria, fungi, and plants (Mukherjee et al. 2001; Mohanpuria et al. 2008).

In biological methods, extracts from bio-organisms may act both as reducing and capping agents. Ag^+ ions are reduced by biomolecule combinations such as proteins, amino acids, enzymes, polysaccharides, and vitamins, which are environmentally benign compounds (Collera-Zúñiga et al., 2005). Biological synthetic approaches use various biological microorganisms such as bacteria

(Samadi et al. 2009), fungi (Bhainsa and D'Souza 2006), algae (El-Rafie et al. 2013), yeast (Jha et al. 2008), as well as plant extracts (Veerasamy et al. 2011).

Enzymatic and non-enzymatic reductions are potential mechanisms of biological synthesis. Nicotinamide adenine dinucleotide phosphate-dependent reductase (NADPH) can reduce Ag^+ to form AgNPs by enzymatic reduction, but the enzymatic reduction rate is often slow (between 24-120 hours) (Kumar et al., 2007). As for synthesized silver by the non-enzymatic reduction is like chemical reduction, but the reducers and stabilizers are derived from microorganisms or plant extracts. The non-enzymatic reduction is often completed within a few minutes and can accelerate the synthesis by dealing with extreme parameters, such as high pH or high temperature (Sintubin et al. 2009).

Biosynthesis of AgNPs is a bottom-up approach that mostly involves reduction/oxidation reactions. The three major components involved in synthesizing nanoparticles using biological methods are the solvent medium for synthesis, the environmentally friendly reducing agent, and a nontoxic stabilizing agent (Prabhu and Poulose, 2012). Hence, the use of fungal extracts to synthesize AgNPs becomes a feasible option. When compared with bacteria, fungi are known to secrete much higher amounts of bioactive substances, which directly translate to higher productivity of nanoparticles (Narayanan and Sakthivel, 2010). Also, the extracellular biosynthesis using fungi makes downstream processing much more accessible than bacteria (Mohanpuria et al. 2008). Moreover, biological synthesis using microbial cells makes it possible to generate AgNPs under a nontoxic silver nitrate concentration as they can continue to multiply (Mukherjee et al. 2001);

Nonetheless, a drawback of biological synthesis using bacteria is that the purification process could lead to the production of pathogenic bacteria and potentially give rise to contamination, which may be a basis for caution in medicinal uses (Sintubin et al. 2012).

Aim and objectives:

The overall aim of this chapter was to synthesize colloidally stable AgNPs of similar sizes using chemical and biological approaches. The specific objectives of this chapter are:

1. To synthesize AgNPs through a chemical route using sodium citrate as a capping agent and sodium borohydrides as a reducing agent.
2. To synthesize AgNPs through a biological route using fungal extracts as reducing and capping agents.
3. To fully characterize the physicochemical properties of the chemically and biologically synthesized AgNPs.

2.2 Methodology

2.2.1 Materials

Silver nitrate ($AgNO_3$) as a precursor (ACS grade, 99.9+%), sodium borohydride ≥98.0% ($NaBH_4$) as a reducing agent, and a commercial Ag-nanopowder (Nanopowder APS 20-40 nm, purity of ≥99.9% metals basis) were purchased by Alfa Aesar (Ward Hill, MA, USA). Trisodium citrate 99% ($Na_3C_6H_5O_7$) as a stabilizer and $NaNO_3$ supplied by VWR (West Chester, USA). Trace metal grade nitric acid (68-70% HNO_3) and FL-70 supplied by Fisher Scientific (Nazareth, USA) were used to acidify samples for ICP-MS analysis. Sodium azide was obtained by (Fisher Bioreagents™, India) as an antibacterial agent. A standard internal mix supplied by Perkin Elmer Pure Plus was used as the internal standard for IC-PMS analysis, and the ARISTAR PLUS silver (Ag) standard manufactured by British Drug House (BDH chemicals) was used to prepare standards for ICP-MS calibration.

Aspergillus parasiticus strain AFS10 - was used to generate extracellular extracts which were used as reducing and capping agents - was obtained from the Integrative Mycology Laboratory (IML) in the Department of Environmental Health Sciences (ENHS) within the Arnold School of Public Health. Sucrose and Yeast Extract supplied by VWR and BD Biosciences(Thermo Fisher), respectively.

Ultrapure water (resistivity = 18.2 MΩ.cm) was used in this study to prepare the suspension, reagents, media, and cleaning of the equipment provided by a Millipore Advantage System (Merck Millipore, Darmstadt, Germany).

2.2.2 Glassware preparation

Throughout this study, all new and used plastic- and glass-ware were acid-washed by a soaked overnight in 10% v/v $HNO_{3(aq)}$ and followed by washing with plenty of ultrapure water (UPW) were dried at room temperature before use. Most of the disposal equipment and plastic, such as test tubes, filter papers, scratched plastic cuvettes, etc., was used out of the box and discarded once used.

2.2.3 Synthesis processes

Chemical synthesis: Citrate-stabilized silver nanoparticles (cit-AgNPs) were synthesized using hydrothermal synthesis approaches under sterile conditions described in previously published protocol (MacCuspie 2011) with minor modification. All chemicals were prepared in ultrapure water (resistivity = 18.2 MΩ·cm). Concisely, AgNPs were prepared by the reduction of silver nitrate ($AgNO_3$) in trisodium citrate ($Na_3C_6H_5O_7$), and sodium borohydride ($NaBH_4$) is used as the reducing agent. Solutions of 1.69 mL of silver nitrate (58.8 mM) and 2.92 mL of trisodium citrate dihydrate (34 mM) were added to 400 mL of boiling water while vigorously stirring at 600 rpm during this process. To this solution, 2.00 mL of sodium borohydride (100 mM) was added into the mixture dropwise; the solution turned to yellow, indicating the formation of AgNPs. After 15 min of stirring, the reaction was allowed to cool for another 45 min on a hot plate and then left overnight at ambient temperature and kept in the dark at 4°C to the following procedures.

Biological synthesis: AgNPs were synthesized using the exudates produced by *Aspergillus parasiticus* strain AFS10 as reducing and capping agents. For preparation biomass to biosynthesis, the fungi were grown aerobically in yeast-extract-sucrose (YES), a liquid media containing 2% w/v yeast extract, 6% w/v sucrose, and the final pH were adjusted to 5.8. The flasks were inoculated by 10^7 spores per 100 mL of the growth medium, incubated on an orbital shaker at 29°C, and agitated at 150 rpm. The biomass was harvested after 48-h of growth by sieving through a Mira cloth, followed by extensive washing with autoclaved ultrapure water (UPW) to remove any medium component from the biomass. Typically, 20 g of biomass (fresh weight) was brought in contact with 200ml of ultrapure water for 72-h at 29°C in an Erlenmeyer flask and agitated in the same condition as described earlier. After the incubation, the cell filtrate was obtained by passing it through Mira cloth. For the synthesis of silver nanoparticles, $AgNO_3$, 10^{-3} M final concentration was mixed with cell filtrate in a 250 ml Erlenmeyer flask and agitated at 60°C in the dark. Control (without the silver ion, only biomass) was also run along with the experimental flask. The washing and cleaning procedure was followed above using ultrapure water instead of sodium citrate solution.

Ag-Nanopowder: Commercially available AgNPs powder was suspended in ultrapure water (18.2 MΩ·cm) at a concentration of 100 mg L^{-1}, followed by vigorous stirring (VWR® Advanced Hot Plate Stirrer, Henry Troemner, LLC) for 30 min at 1000 rpm at room temperature. In order to disaggregate AgNPs, the Ag-Nanopowder suspension was ultra-sonication for 3 hours in an ice bath (Branson 2800 ultrasonic cleaner). To constitute a homogeneous suspension, the sonicated

Ag-Nanopowder suspension was stirred for 24-h and then centrifuged for 5 min at 3500 rpm using a Thermo Scientific centrifuge (Sorvall Legend RT Plus, Inc.) to remove unaggregated AgNPs. The supernatant was collected and kept in darkness at 4°C until use.

2.2.4 Cleaning of AgNPs

Ultrafiltration is an appropriate way to separate AgNPs from dissolved Ag ions in aqueous media. Ultrafiltration was carried out under high pressure in the presence of an inert gas such as N_2 to force any remaining reactants to pass through a filter (Guo and Santschi 2007). In engineered NPs framework, Ultrafiltration techniques have a particular role in separating the dissolved phase metal from the NP metal suspension (for inorganic NPs), either due to the synthesis or from the dissolution of the NP over time (Ju-Nam and Lead, 2008). Clean and uncontaminated AgNPs suspensions in toxicology studies are highly significant to ensure that any observed effects are due to AgNPs alone without interferences from other substances. The clean-up process aimed to remove residual dissolved silver (Ag^+) and excess capping agents during synthesis processes. Diafiltration/ultrafiltration was carried out to clean up chemical and biological synthesized AgNPs under high pressure within the presence of N_2 gas to force the solvent to pass through a membrane pores of stirred-cell ultrafiltration (Amicon, 3-KDa regenerated cellulose membrane, Millipore). The material size in suspensions greater than 3-KDa has been retained above the membrane; ions, water, and other materials less than 3-KDa are excluded as filtrate. During this process, AgNPs suspension volume was reduced by half and then re-dispersed

by the addition of 0.25 mM sodium citrate solution for the chemically synthesized AgNPs and ultrapure water for biologically synthesized AgNPs; in order to avoid further growth, this process was repeated at least five times.

2.2.5 Filtration of AgNPs

Filtration was used to eliminate any large aggregates and agglomerates that may have formed during synthesis. This was accomplished utilizing a Millipore Inc. filtration flask and funnel, and the chemical and biological NP preparations were filtered through a 0.1 and 0.45 μm cellulose nitrate membrane (Millipore Inc.), respectively.

2.2.6 Physicochemical Characterization of AgNPs

Aliquots of the synthesized AgNPs were periodically characterized (e.g., size, shape, concentration, surface charge, etc.) using a multi-method approach.

2.2.6.1 Surface plasmon resonance (SPR)

Surface plasmon resonance- The reduction of Ag^{+} to Ag° was monitored using a dual-beam UV absorbance spectrometer (UV-vis) (Shimadzu UV-2600 spectrophotometer, Co., Kyoto, Japan) at a resolution of 1 nm from 200−800 nm wavelength range at room temperature. The samples were placed in cuvettes with an optical path length of 10 mm, requiring 1 mL to fill the light path of the UV–Vis spectrometer. Ultrapure water was used as the reference sample to correct the blank spectrum for all measurements.

2.2.6.2 Dynamic light scattering (DLS) and Zeta Potential (ζ)

Dynamic light scattering was used to determine particle size distribution (z-average) and surface charge (zeta potential) of the synthesized AgNPs suspensions using a Zetasizer (Nano-ZS, Malvern Instruments Ltd., MA, USA). The hydrodynamic size (d_H) and polydispersity index (PDI) were determined from the diffusion coefficient using the Stokes-Einstein equation, and the mean and standard deviation of five measurements was calculated. The zeta potential (ζ) was determined from the electrophoretic mobility of the particles, which was measured using the laser Doppler technique using Smoluchowski's assumption (Baalousha et al., 2012). Measurements were conducted in a 1cm optical path cell after an elapsed temperature equilibration, with precise temperature control (22 °C). The hydrodynamic size (d_H) and the zeta potential (ζ) were reported as the mean and standard deviation of five and ten replicates.

2.2.6.3 Inductively Coupled Plasma-Atomic Mass Spectroscopy (ICP-MS)

The concentration of the synthesized AgNPs was measured by inductively coupled plasma-atomic mass spectroscopy (ICP-MS). The samples were acidified in nitric acid (HNO_3) and then diluted 200-fold in 1% of HNO_3, followed by analysis via (NexION^{TM} 350 D, PerkinElmer Inc., Waltham, MA).

2.2.6.4 Transmission Electron Microscopy (TEM)

The core size and morphology of undiluted AgNPs were determined using a H-7800 transmission electron microscopy (TEM, Hitachi, Japan) with an acceleration voltage of 200 keV. For TEM analysis, nanoparticle stock

suspensions were pipetted onto carbon-coated 50 mesh Cu grids (S162-3, AGAR Scientific) and allowed to adsorb to the carbon coating for 15 min followed by rinsing with UPW to remove unadsorbed particles. Subsequently, the grids were left to dry for 48 h in a covered petri dish at room temperature. A series of images were selected to establish the mean core size of AgNPs by tracing single-particle contours using ImageJ software (Release 152a, National Institutes of Health, USA).

2.2.6.5 Asymmetric Flow-Field Flow Fractionation (AF4-ICP-MS)

AgNPs size distribution was determined by asymmetric flow-field flow fractionation (AF4, Wyatt Eclipse® DualTec™, Germany) coupled to ICP-MS (Perkin Elmer NexION350D). The AF4 was equipped with a 350 µm spacer and a 1-kDa OMEGA^{TM} polyether sulfonate membrane (Pall Corporation, NY, USA). The AF4 carrier solution consisted of 10 mM $NaNO_3$, 0.01% sodium azide as an antibacterial agent, and 0.0125% FL-70 in UPW. The sample injection volume was 5 µL, and the focus time was 10 min. Four polystyrene Nanosphere^{TM} size standards of 20, 40, 80, and 150 nm diameters (Nanosphere™, Thermo Scientific, USA) were used to calibrate particle size as a function of retention time. Dissolved Ag was used for the ICP-MS mass concentration calibration ranging from 0.1 to 100 µg L^{-1} before coupling AF4 to ICP-MS. Samples were introduced to the ICP-MS using a T-junction to monitor internal standards (ICP Internal Element Group Calibration Standard, BDH Chemicals, USA) for quality control and to acidify (1% HNO_3 after mixing with the sample) the samples just prior to introduction into the ICP-MS in order to avoid particle stability changes.

2.2.6.6 Single Particle (Sp-ICP-MS)

A Perkin Elmer NexION^{TM} 350D ICP-MS was used to perform single particle analysis (sp-ICP-MS) of AgNPs (Laborda et al. 2013; Montaño et al. 2016). Operating conditions were optimized to produce maximum Ag intensity by modifying the sample introduction rate and changing the nebulizer gas flow. ^{107}Ag was continuously monitored for detection, and Data were acquired at an RF power of 1600 W, a 50 µs dwell time, a 0 µs settling time, and a 60 s acquisition time. The length of dwell time contributed significantly to the quality of data, where 10 µs was optimal. Intensity data were recorded using the Syngistix Nano Application Module ICP-MS software and were exported to Excel (Microsoft) for data handling and processing. NIST^{TM} Au standard reference material was used to determine the transport efficiency. A rinse cycle consisting of 1 min with 1% aqua regia and 1 min with UPW was performed after each sample run to ensure cleansing of the sample introduction system between samples. All AgNPs' suspensions were measured in triplicate. Instrument calibration was achieved by analyzing a blank and four dissolved Ag solutions ranging from 0 to 20 µg L^{-1} with data collected in the SP mode. The ^{107}Ag intensity of Ag for each solution was then averaged from the entire length of the standards analysis (typical times). The NIST Au standard reference material was measured after each set as a QA/QC check.

2.3 Results and Discussion

2.3.1 Characterization of AgNPs

Suspension Color: In the case of chemical synthesis, at first sight, the color change of the colorless silver nitrate solution to yellow was a preliminary indication that AgNPs were formed (Figure 2.1). The cit-AgNPs suspension was generally golden yellow in color, which has been widely reported elsewhere (Pal et al. 1997).

In the case of biological synthesis of AgNPs, using cell-free extract (CFE) of *Aspergillus paratecuss* AFS10 in different volume ratios 50:1, 25:1, 10:1, 5:1, 1:1, 1:5, and 1:10 of the CFE and silver nitrate (10^{-3} M), the CFE exhibited a gradual change in color towards brown following CEF incubation with the $AgNO_3$ (Figure 2.1). This change in CFE color is an indication of the formation of AgNPs.

The yellow and brown color observed was due to the surface plasmon resonance in the AgNP. These observations confirmed the reduction of Ag^+ to Ag^0 by the organic compounds present in the fungal extract and thus the formation of AgNPs. The color density of different AgNP suspensions is consistent with the AgNP synthesis yield. The higher CFE:Ag^+ ratio results in a darker color and thus a higher synthesis yield. At higher CFE:Ag^+ ratios, high concentrations of capping and reducing agents are available to reduce Ag^+ ions results in increased synthesis yield. At low CFE:Ag^+ ratios, the low concentrations of reducing and capping agents in the CFE are consumed, and most Ag^+ ions remain are not reduced to Ag^0, resulting in low synthesis yield.

Surface Plasmon Resonance (SPR): UV-vis determined all samples' optical and structural properties, and the absorption spectra (λ 200−800 nm) are shown in (Figure 2.2). The absorption spectra of cit-AgNPs and bio-AgNPs showed absorption peaks in the entire visible region according to the previously published UV-vis spectra of AgNPs (Veerakumar et al. 2010; Mishra et al. 2013). Cit-AgNPs showed a single surface plasmon resonance peak at the value of 390 nm. UV-vis spectra of the bio-AgNPs showed absorbance peaks at 375–417 nm, depending on exact solution composition (Jana et al. 2001). The UV–vis spectra of bio-AgNPs formed using variety ratio extracts at 60°C display absorption, regardless of reaction time, between 440 nm and 428 nm (Figure 2.2). The characteristic peaks of AgNPs appeared at 410–440 nm on the UV–vis spectra, which is consistent with the frequency of the surface plasmon oscillations (Ocsoy et al. 2013*b*, *a*).

In a typical NP synthesis, reducing agents with high concentration results in smaller-sized NPs, which give a blue shift. Here, the increase in the concentration of fungal extract induces a shift towards a smaller wavelength of the surface plasmon resonance of AgNPs, indicating the formation of smaller AgNPs. The absorbance intensity of AgNPs in UV–vis spectra is directly proportional to the concentration of extract and reaction time, which refers to the increase in the yield of AgNPs production. Bio-AgNPs suspensions showed broad asymmetric peaks in general (Figure 2.2), unlike the sharp, clean peaks often seen with citrate-produced AgNPs. The broad UV-vis absorption peaks of bio-AgNPs are likely due to higher (poly)dispersity of bio-AgNPs and absorbance interference from cell-free extract (CFE).

UV-vis spectra were used to monitor the effectiveness of both contact time and CFE:Ag^+ ratio on AgNPs concentration in the reaction mixture at different time intervals with a change of color of the solution. The absorbance increased proportionally with increased CFE:Ag^+ ratios and increased synthesis time (Figure 2.2). The intensity of UV-vis absorption at 120-h increased with an increase CFE:Ag^+ ratios and then plateaued at CFE:Ag^+ of 10:1, indicating that the minimum amount of CFE extracts required to fully reduce the majority of Ag^+ under the experimental conditions (Figure 2.3).

Dynamic Light Scattering: The Hydrodynamic diameter (d_H) of Biosynthesized and Cit-AgNP measured by DLS was presented as size distribution by intensity. The size and polydispersity index (PDI) stability of AgNPs were monitored (Table 1). The PDI measurement of citrate and bio silver nanoparticles with different concentrations are presented in table 1 (1:1) Bio-AgNP samples have PDI value of 0.578, which shows as highly polydispersed NP suspension. The PDIs of AgNPs synthesized using CFE:Ag^+ ratios of (50:1), (25:1), and (10:1) were 0.204, 0.291 and 0.375, respectively, indicating the synthesize of less polydispersed AgNPs. On the other hand, the cit-AgNPs PDI value has given the value of 0.067, which is characteristic of highly monodispersed suspension. Thus, the chemical synthesis approach produced more monodispersed AgNP suspensions than those generated by biological synthesis.

The chemical synthesis allowed a faster reduction of Ag^+ into Ag° as it used $NaBH_4$ as a strong reducing agent. However, changing the stirring duration and the mass ratio of reactant did not alter the size of the synthesized AgNPs because

the reducing action of NaBH4 was extremely strong. Consequently, in general, cit-AgNPs were more monodisperse than biosynthesized AgNPs, and the lowest PDI (0.06) was achieved by adding the capping $NaBH_4$ in advance.

Particle size analysis was performed by the DLS for cit-AgNPs and different ratios of fungal extracts of bio-AgNPs (Figure 2.4 and 2.5). Most of the biologically synthesized AgNPs exhibited bimodal size distributions. Only bio AgNPs synthesized using CFE:Ag^+ ratios of 50:1 and 25:1 displayed near-monodispersed size distributions as indicated by the low PDI values of 0.204 and 0.291.

A nanoparticle system with PDI value < 0.1 is considered highly monodisperse, while PDI value > 0.4 is considered highly polydispersed, and those with PDI value in the range of 0.1 – 0.4 are considered moderately monodispersed distribution in the respective order (Bhattacharjee 2016). From the d_H measurement results, it was verified that the bio-AgNPs were the most polydispersed AgNPs. The gradual increase of the CFE ratio leads to a relatively slow reduction and nucleation rate, allowing the NP nucleation and growth process to occur simultaneously. If the nucleation and growth process could not be separated temporally, it would potentially lead to the generation of polydisperse particles (Sugimoto 1987; Patakfalvi et al. 2007) as was found with biosynthesized samples.

On the other hand, the chemical synthesis allowed a faster reduction of Ag^+ into Ag° as it used $NaBH_4$, a strong reducing agent. Varying the stir duration as well as the mass ratio of reactant, however, could not control the generated particle size as the reducing action of $NaBH_4$ was extremely strong. Thus, in general, cit-

AgNPs were more monodispersed than biosynthesized AgNPs, and the lowest PDI (0.06) was achieved by adding the capping $NaBH_4$ in advance.

Figure 2.5 shows the zeta potential (ζ) and Hydrodynamic diameter (d_H) of chemical and biological silver nanoparticles as a function of CFE:Ag^+ ratio. The zeta potential value indicates the nanoparticles' stability, which is formed in the solution (Agrawal and Patel 2011). The zeta potential of nanoparticles were (-42±1.05), (-38.7±1.13), (-35.8±1.79), (-27.2±2.48), (-24.5±2.78), (-25.6±3.12), (-25.2±2.62) and (-42.1±1.62) and (31.4±3.21) mV for the biosynthesized samples (50:1), (25:1), (10:1), (5:1), (1:1), (1:5), (1:10) and cit-AgNP and Ag-*n*-powder samples, respectively. The increases in zeta potential with increases CFE:Ag^+ ratios indicate increases in the surface coating of AgNPs with biomolecules which enhances a higher surface charge, which results in increased AgNP colloidal stability. The zeta potential of cit-AgNPs was similar to that obtained at the highest CFE:Ag^+ ratio of 50:1. Zeta potential is generally correlated with NPs stability where zeta potentials lower than -30mV or greater than +30mV are used as a rule of thumb to indicate NPs colloidal stability. That correlation, however, was only for electrostatically capped particles (DeLuca et al. 2006).

TEM. Representative TEM micrographs of the primary silver nanoparticles are shown in Figure 2.6. The average core size of the cit-, bio- (CFE to Ag+ of 50:1) and Ag-*n*-powder were ca 9.7±3.5, 15.9±6.0, and 87.4±19.7, respectively (Table 1). Both the cit-AgNPs and bio-AgNPs exhibited spherical shapes and a monodisperse nanoparticle size distribution predominantly without clusters or

aggregates, indicating greater stabilization of the coated AgNPs. On the contrary to Ag-*n*-powder revealed irregular shapes and the formation of AgNP aggregates.

Sp-ICPMS: Table (1) shows single-particle ICP-MS measurements . The mean sizes of AgNPs were (25.3±11), (26.8±7), (31.9±12), (29.3±8), 25.1±9), (23.4±8),)24.3±8), and (22.6±3) nm, which are corresponding for bio-AgNPs (50:1), (25:1), (10:1), (5:1), (1:1), (1:5), (1:10) and cit-AgNP samples, respectively (Figure 2.7).

F4-ICP-MS. The silver nanoparticles based-size distribution was determined by AF4-ICP-MS. AF4 fractograms for citrate and bio silver nanoparticles are presented in Figure 2.8. Bio-AgNPs synthesized using CFE:Ag+ ratios of 50:1, 25:1, and 10:1 display monomodal size distributions with small hydrodynamic diameters, whereas those synthesized, using CFE:Ag^{+} ratios of 5:1, 1:1, 1:5, and 1:10 exhibited bimodal size distributions a wide distribution of small and large hydrodynamic diameters. These results are in good agreement with the trend of the z-average hydrodynamic diameters and PDIs measured by DLS.

The mean sizes of AgNPs measured by the four different techniques (Table 1) are different and generally follow the order DLS > AF4-ICP-MS > sp-ICP-MS > TEM. This is because different analytical techniques provide different particle size measurements, as they are based on different principles.

DLS and AF4-ICP-MS measure NP hydrodynamic diameter (i.e., core size + diffuse layer) whereas TEM, and sp-ICP-MS measure particle core size. Thus, the NP sizes measured by DLS and AF4-ICP-MS are generally larger than those

measured by TEM, and sp-ICP-MS. TEM measures a projected surface area from which an equivalent circular diameter can be calculated assuming spherical particle shape.

DLS and AF4-ICP-MS measure NP diffusion coefficients, from which NM equivalent hydrodynamic diameter can be calculated using the Stokes-Einstein equation, assuming that the NPs are hard spheres. The higher hydrodynamic diameter obtained by DLS compared to AF4-ICP-MS is because DLS measures intensity-based particle size distribution (PSD) whereas AF4-ICP-MS coupled to UV-vis measures mass-based PSD.

DLS is the least accurate/representative size measurement for these NMs in polydisperse samples resulting from the presence of a small fraction of larger sizes of NMs that scatter more light than the small NMs that dominate the sample by number or mass concentration as AF4-ICP-MS data. The results suggest that DLS is of very limited use for accurate particle sizing of samples and provides accurate results only for highly monodisperse samples (i.e., PDI < 0.1). Any deviation in particle polydispersity will result in a large deviation of DLS from the true particle size (Baalousha and Lead 2012).

2.4 Conclusion

This chapter presents the synthesis and characterization of AgNPs via chemical and biological approaches. The chemical synthesis is based on reducing ionic silver using sodium borohydride in the presence of trisodium citrate as a capping agent. The Biological approach is based on the use of cell-free extracts of AFS10

as reducing and capping agents so convert ionic silver to metallic silver and to impart AgNP stability. The physicochemical characterization demonstrates the formation of spherical AgNPs with similar properties. The UV-vis absorbance underpins the conversion of Ag^{+} to Ag^{0} and the formation of AgNPs using the chemical and biological approaches. The chemical process generated AgNPs with a lower polydispersity compared to the biological synthesis approach as confirmed by the lower PDI values. . The biological synthesis is slower than the chemical synthesis and is more difficult to control. However, biological synthesis becomes faster with increased synthesis temperatures.

In the following chapter, chapter 3, Ag-*n*-powder, cit-AgNPs, and 50:1 ratio cit-AgNPs from these experiments were relied on to assess toxicity on juvenile hard clams and then underwent dissolution tests with natural seawater in the same conditions of the experiment.

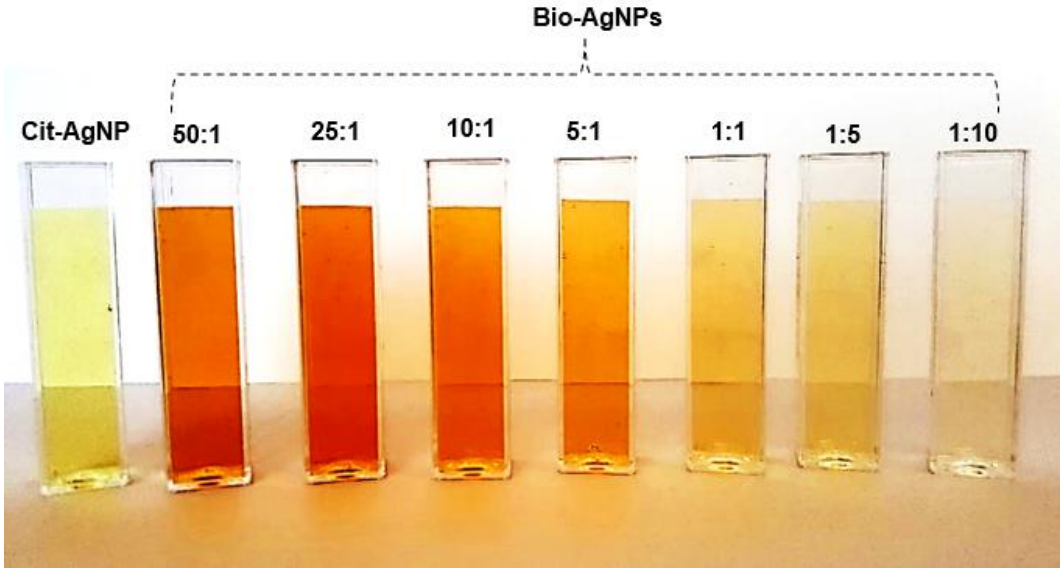

Figure 2.1 Photographs of the cit-AgNPs; the mixture of cell-free extracts and silver nitrate solution over 120 hours. The numbers indicate CFE:Ag^{+} ratios.

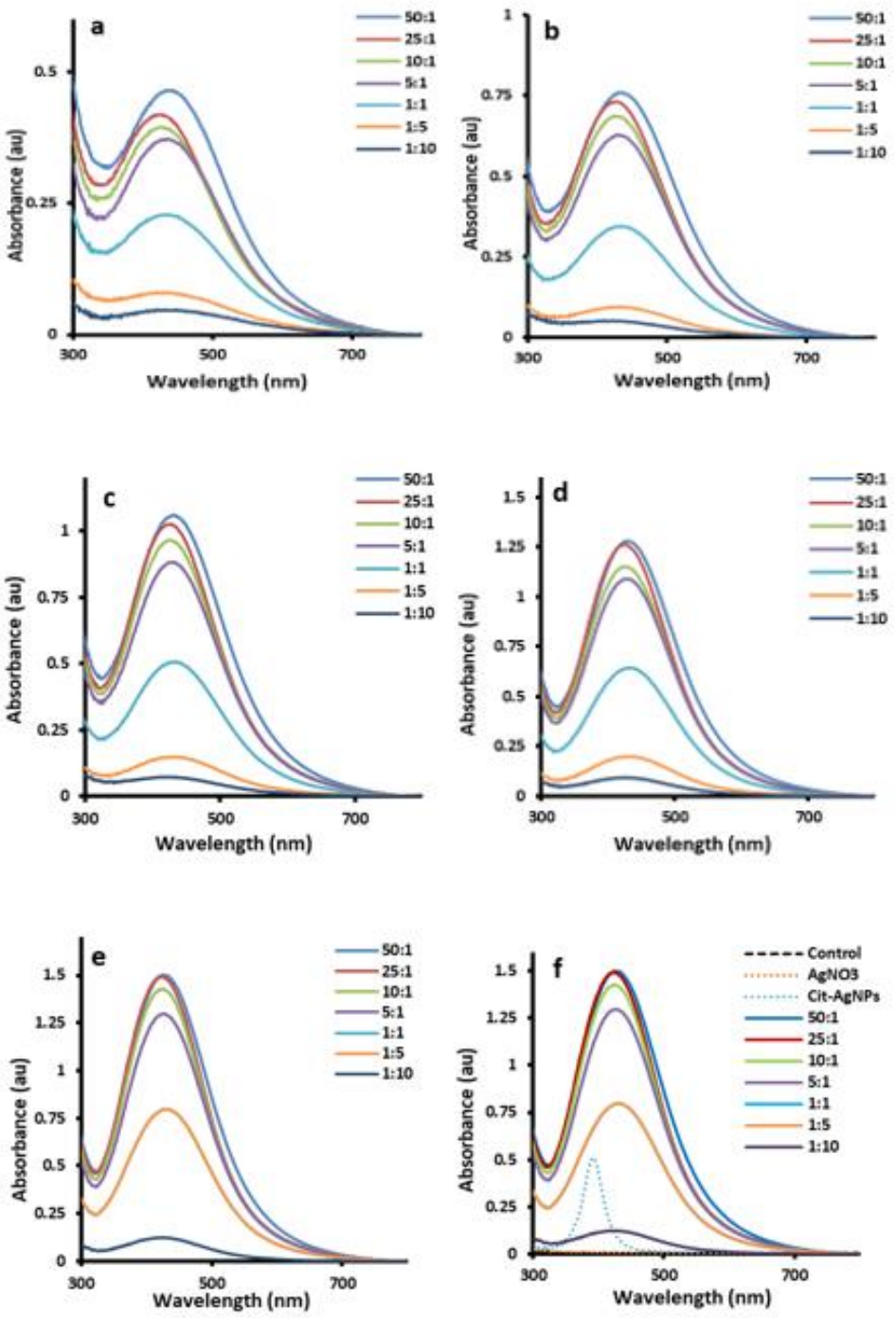

Figure 2.2 UV–vis cit-AgNPs and bio-reduction kinetics of the reaction of cell-free extract with aqueous $AgNO_3$ in different ratio (cell-free extract: Ag^+ ratios = 50:1,25:1, 10:1, 5:1, 1:1, 1:5 and 1:10) at time intervals. Reaction conditions: $[Ag^+] = 10^{-3}$ M, incubation temp. = 60C. a, b, c, d, and e represent incubation time intervals for mixture which are 24, 48, 72, 96, and 120-h respectively. Cit-AgNPs and 120-h bio-AgNPs shown by f.

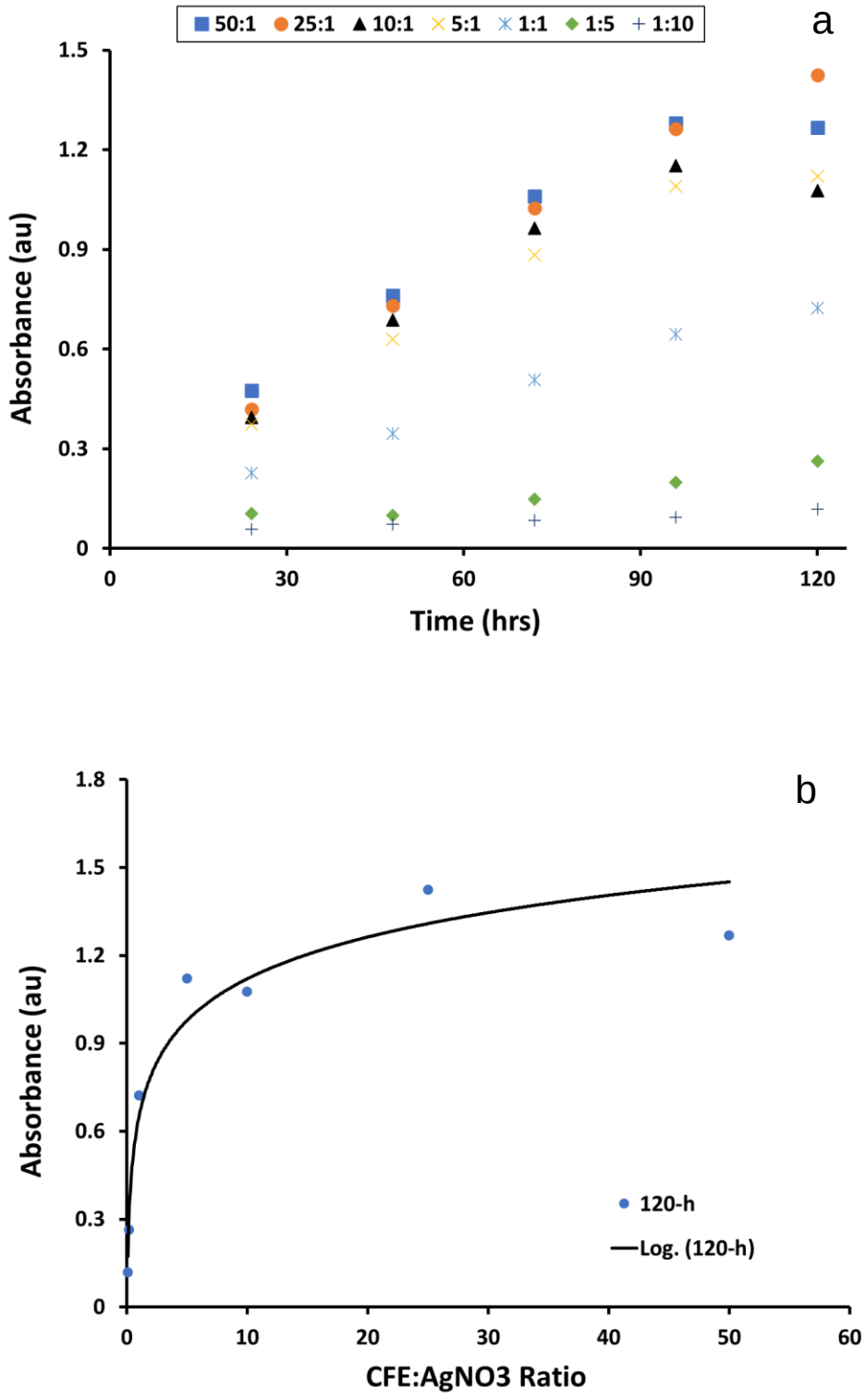

Figure 2.3 Absorbance of the biosynthesized AgNPs as a function of reaction time. (a) represents the linear relationship of absorbance with function time, (b) represents the logarithm relationship as function CFE:$AgNO_3$ of synthesized bio-AgNPs.

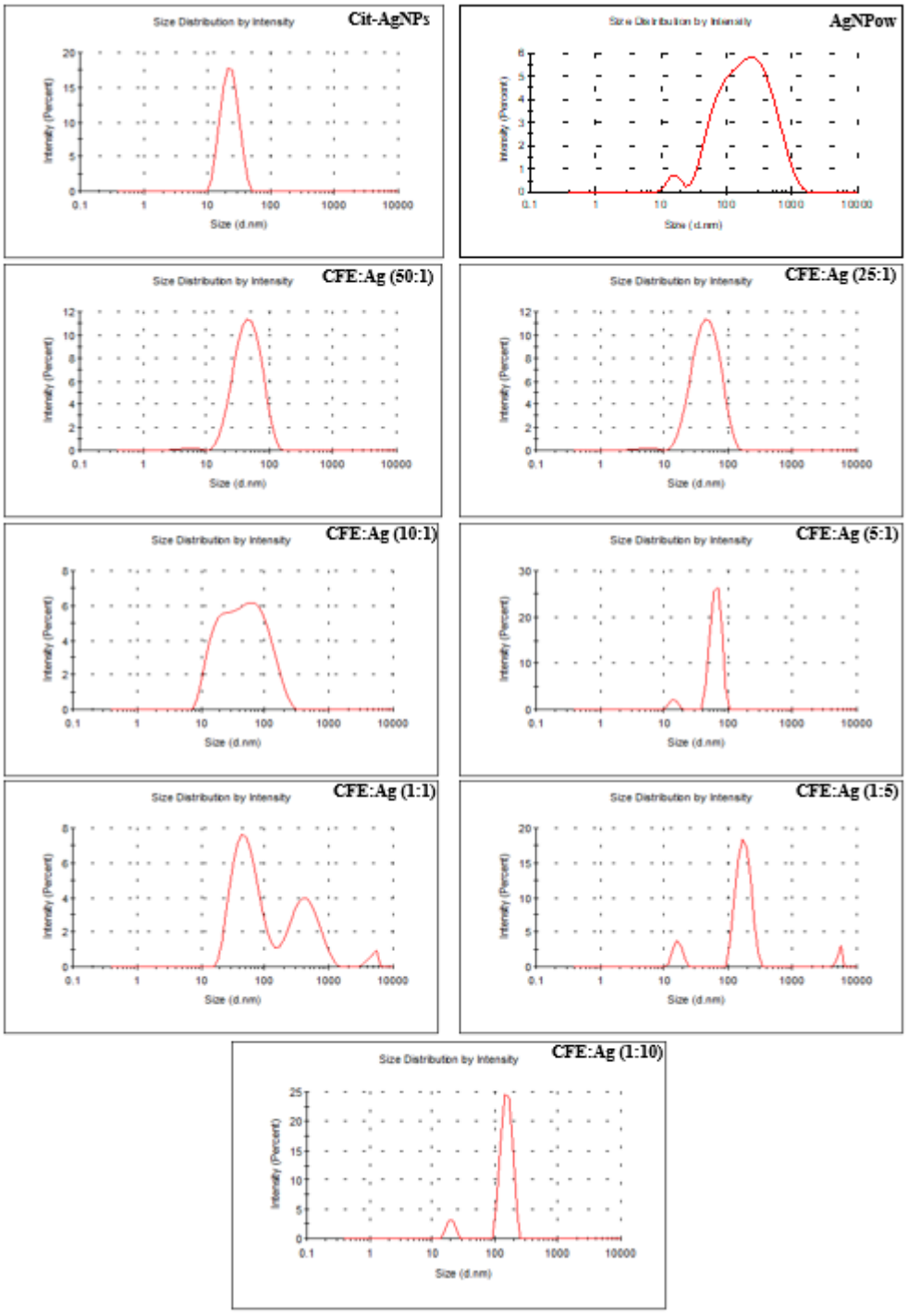

Figure 2.4 Size distribution by Intensity of AgNPs from chemical and biological processes measured by DLS.

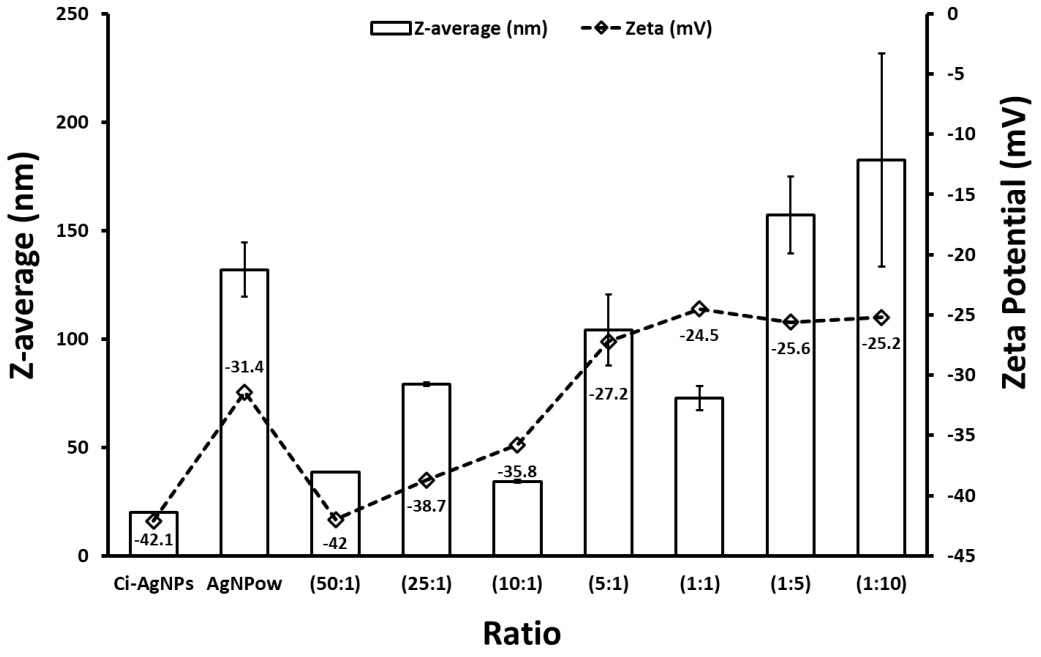

Figure 2.5 Zeta potential and Hydrodynamic diameter (d_H) from chemical and biological silver nanoparticles function as a cell-free extracts ratio. The ratios indicated in the figure are those of cell-free extract to Ag^+ ratios.

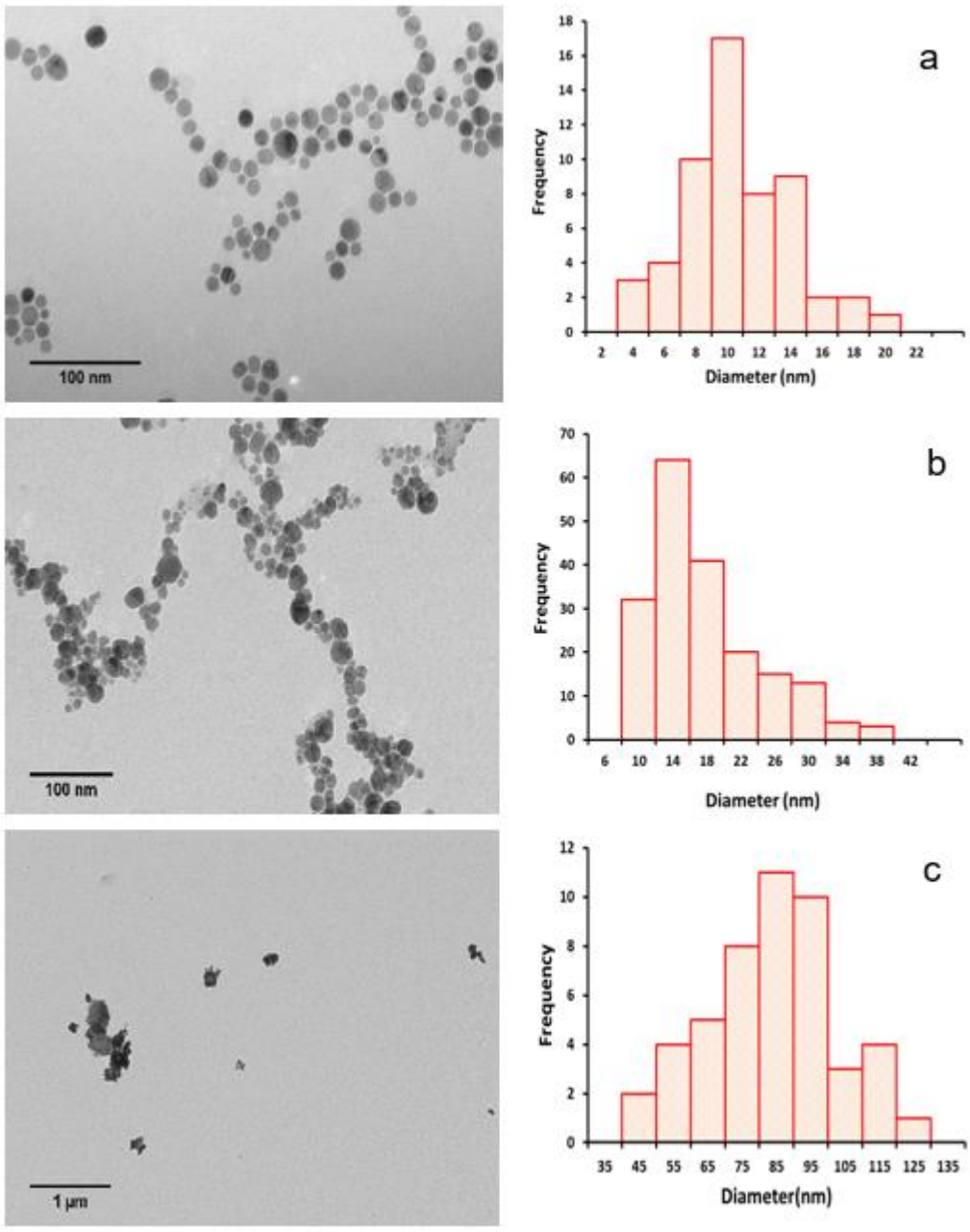

Figure 2.6 Transmission electron microscopy (TEM) micrographs of (a) cit-AgNP, (b) bio-AgNP (CFE:Ag+ of 50:1), and (c) Ag-*n*-powder.

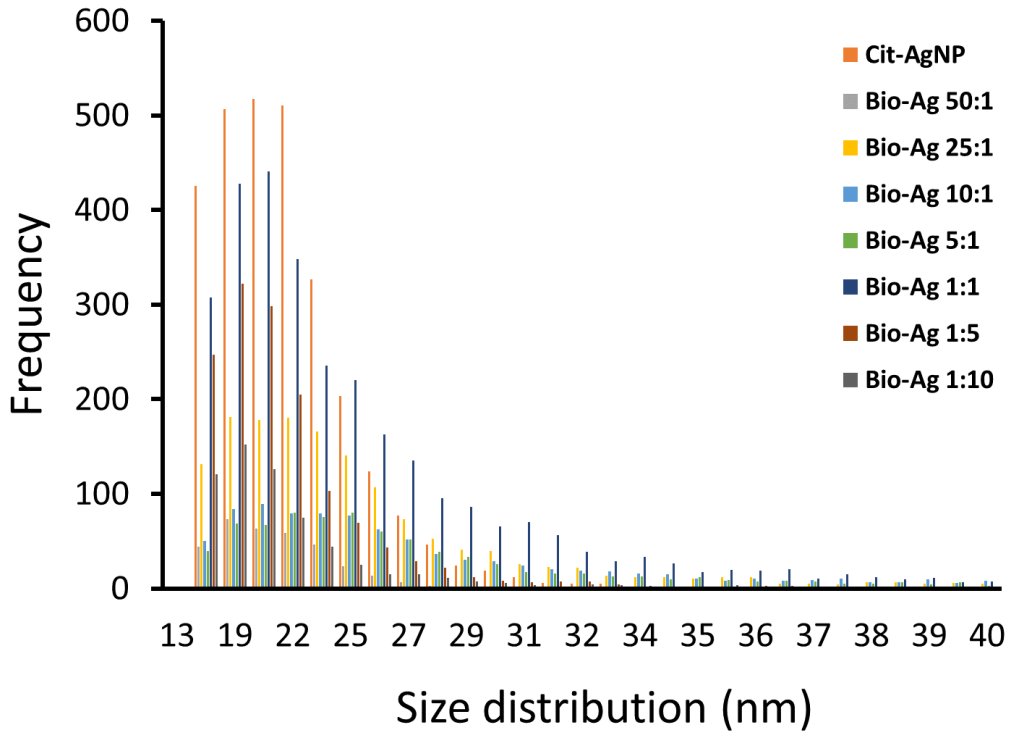

Figure 2.7 Number particle size distribution measured by single particle-inductively coupled plasma-mass spectrometer (sp-ICP-MS) of cit-AgNPs and bio-AgNPs of the reaction of cell-free extract with aqueous $AgNO_3$ in different ratio (50:1, 25:1, 10:1, 5:1, 1:1, 1:5 and 1:10) at 120 hours as time interval. Reaction conditions: [Ag+] = 10^{-3} M, incubation temp = 60 ˚C.

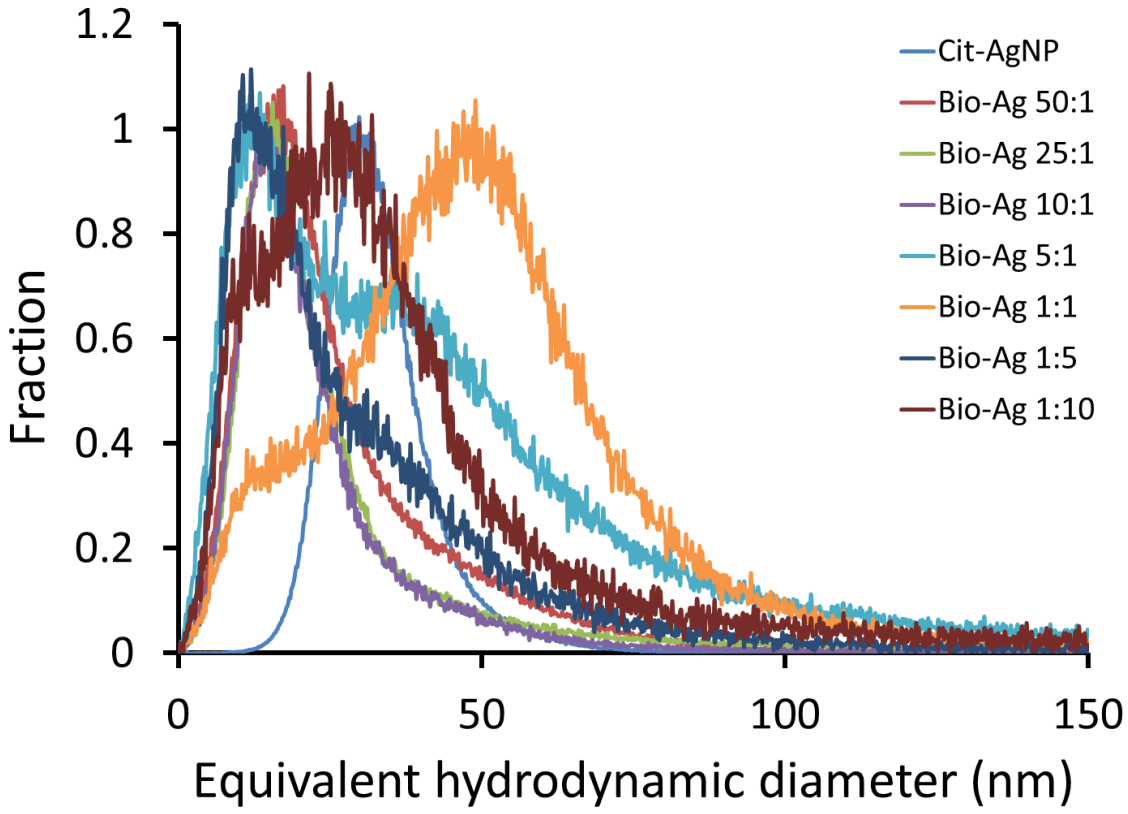

Figure 2.8 Nanoparticle equivalent hydrodynamic diameter cit-AgNPs and bio-AgNPs measured by flow-field flow fractionation with an inductively coupled plasma-mass spectrometer (AF4-ICP-MS).

Table 2.1 Summary of AgNPs sizes measured by different sizing techniques.

AgNPs	Z-average (nm) DLS	PDI	Hydrodynamic diameter FFF	Core size sp-ICP-MS	TEM
Cit-AgNPs	21.5 ± 0.1	0.06 ±0.0	32.9 ±0.1	22.6±0.04	9.72 ±0.1
Ag-*n*-powder	132 ± 2.0	0.49 ±0.0	ND	ND	74.11 ±0.8
CFE:$AgNO_3$ (50:1)	38.6 ±0.1	0.20 ±0.0	36.3 ±1.4	25.3 ±0.1	15.85 ±0.3
(25:1)	79.1 ±0.8	0.29 ±0.0	26.2 ±0.9	26.8 ±0.0	ND
(10:1)	34.4 ±0.6	0.38 ±0.1	32 ±0.3	31.9 ±0.1	ND
(5:1)	104.2 ±60.3	0.33 ±0.0	41.2 ±0.1	29.3 ±0.2	ND
(1:1)	72.8 ±5.6	0.58 ±0.1	49.8 ±1.1	25.1 ±0.2	ND
(1:5)	157.3 ±17.7	0.51 ±0.1	29.5 ±1.4	23.4 ±0.4	ND
(1:10)	182.4 ±49.2	0.45 ±0.1	36.0 ±0.7	24.3 ±0.1	ND

± represents the standard deviation of the measurement, not the standard deviation of true replicates.

CHAPTER 3

ACUTE BIOASSAY OF CHEMICAL AND BIOLOGICAL SYNTHESIZED SILVER NANOPARTICLES ON HARD CLAMS, *MERCENARIA MERCENARIA*

ABSTRACT

The uptake and effects of engineered nanoparticles (NPs) in aquatic biota constitute significant environmental and human health concerns because of the continuous development and production of ENMs. This chapter investigates the environmental behavior (i.e., aggregation and dissolution) and toxicity (i.e., mortality) of well-characterized commercially powder AgNPs (Ag-*n*-powder), chemically-synthesized AgNPs (cit-AgNPs), biologically-synthesized AgNPs (bio-AgNPs), and dissolved silver ($AgNO_3$) to Juvenile *M. mercenaria* (0.820 – 1.2 mm) at 24-h exposure. The hydrodynamic diameter of cit-AgNPs, bio-AgNPs, Ag-*n*-powder in stock suspensions, determined by dynamic light scattering ring, were 21.5 ± 0.1, 38.6 ± 0.1, and 132 ± 2.0 nm, respectively. All AgNPs formed aggregates in natural seawater. The dissolution of AgNPs in natural seawater (the toxicological test media) was measured by an inductively coupled plasma-mass spectrometer following ultrafiltration (3kDa). The dissolved Ag concentration increased with the increases in AgNP concentration over a range of environmentally relevant concentrations: 0.2, 0.35, 0.6, 1.0, 1.5, and 2.6 mg-Ag L^{-1}. Mortality (%) of juvenile clams decreased following the order $AgNO_3$ (24-h mean LC50 value of 0.24 mg L^{-1}, 95% confidence intervals: 0.22–0.27 mg L^{-1}) > cit- AgNPs (24-h LC50 of 0.7 mg L^{-1}, 95% confidence intervals: 0.645–0.87) > and bio-AgNPs (24-h LC50 of 1.05 mg L^{-1}, 95% confidence intervals: 0.90–1.36 mg L^{-1}) > powder-AgNPs (24-h LC50 of 2.44 mg L^{-1}, 95% confidence intervals: 1.81–2.43 mg L^{-1}). Dissolved Ag could not explain the toxicity of AgNPs, indicating that

the toxicity of AgNPs can be attributed to a combined effect of dissolved ions and the AgNPs.

3.1 Introduction

Engineered nanomaterials (ENMs) are ubiquitous and have become a part of our everyday lives. ENM's toxicology comparatively is a new and developing field. Due to unique and tunable ENMs properties, they have gained prominence in technological advancements and applications like in the form of cosmetics, biosensors, bioremediation, drug delivery systems, therapeutics, and aquaculture (Boxall et al. 2007; Jin and Ye 2007; Torkamani et al. 2010; Gong et al. 2011), and also including drinking water, air disinfection, food packaging and clothes (Foltynowicz et al. 2013; K et al. 2013; Zhang 2013). In the same context, silver nanoparticles (AgNPs) have increased in popularity due to their antimicrobial properties (Tian et al. 2007; Yoon et al. 2007). AgNPs are widely utilized in detergents and wound dressings that end during waste disposal in the environment (Asz et al. 2006). Given their increasing prevalence in most fields, questions regarding their impacts on the environment and health remain unanswered.

There is a lack of health standards and data on toxicology for the industrial applications of nanoparticles. Indeed, the unique properties that utilize nanoparticles are the same as those that can pose a risk to humans and environmental health. The potential environmental and toxicological properties of several forms of nanomaterials are still not well known. Consequently, there is a need to consider the risk assessment of nanoparticles along with their beneficial properties.

Among the likely route of discharge of nanomaterials into the environment, the release of commercial nanoparticles into natural waters through the discharge of treated municipal sewage attracts the most concern (Benn and Westerhoff 2008). The behavior and toxicity of engineered nanoparticles (ENPs) in seawater are likely very different than freshwater, even at high dilutions. For example, the vast input of natural colloids and suspended particulate matter have been shown to exhibit modified behaviors in estuarine systems (Aillon et al. 2009). In seawater, agglomeration, aggregation, and precipitation affect the behavior of ENPs (Stolpe and Hassellöv 2007). Aggregates may sink very slowly to the ocean floor unless they encounter significant changes in temperature, ionic strength, and natural organic matter (NOM). Besides, dissolution represents the most vital process determining the environmental fate of ENMs and for AgNPs mainly. Recent studies have endeavored to measure the dissolution of AgNPs in different water conditions. For instance, aqueous solutions with different pHs have found that lower pH can enhance the dissolution of AgNPs (Liu and Hurt 2010; Levard et al. 2012).

Classic marine invertebrate model organisms, such as bivalves, have only been recently investigated regarding bioavailability and toxicity based on the importance of invertebrates as sensitive and relevant organisms (Baun et al. 2008). In realistic environmental scenarios, the self-aggregation of ENPs into larger masses and incorporating ENPs into aggregate materials might increase the bioavailability and toxicity of aquatic organisms such as algae, phytoplankton, filter feeders and benthic deposit and detrital feeders. According to Navarro *et al*., 2008

the toxicity of inorganic ENPs, such as AgNP and ZnONP, appears to be related to solubility or the release of toxic metal ions (Ag^+ or Zn^+) from the ENPs instead of aggregation (Navarro et al. 2008*b*).

The ecoıogical behaviors of AgNPs, such as aggregation and dissolution in environmental media, are currently little known and understood. To measure and quantify dose-response relationships, it is essential to understand the essence of exposure and the physicochemical transformations of AgNPs during (eco)toxicology exposures. Aggregation and/or dissolution can significantly alter NP behavior (e.g., dosimetry, bioavailability, uptake, toxicity) and fate (e.g., pharmacokinetics and biodistribution) (Fabrega et al. 2011; Moore et al. 2015).

In order to investigate putative ecological impairments caused by AgNPs, it is necessary to select species that have an essential role in the structure and functioning of ecosystems and are recognized as useful models for biomonitoring purposes. In this way, marine invertebrates such as hard clam *Mercenaria mercenaria* suitable candidate. The hard clam *M. mercenaria* is a common inhabitant of estuarine sediments and a critical United States fishery species. The hard clam, *M. mercenaria*, is a marine filter-feeding, infaunal mollusk (Dillon and Manzi 1989). A juvenile clam toxicity bioassays have illustrated the sensitivity of this species compared to other commonly used test organisms (Chung 1999). Since bivalves in estuarine systems play a significant role in the ecological and economic aspects, juvenile clams are a vital representative test species.

The aims of this contribution is to evaluate the behavior, and toxicological effects of commercially available powder AgNPs (Ag-*n*-powder), biologically

synthesized AgNPs (bio-AgNPs), and chemically synthesized AgNPs (cit-AgNPs) and dissolved Ag using an acute aqueous bioassay approach in exposing the estuarine juvenile hard clams (*Mercenaria mercenaria*).

3.2 Methodology

3.2.1 Synthesis, Purification, and Characterization of AgNPs

Suspension of silver nanoparticles (cit-AgNPs, bio-AgNPs, and Ag-*n*-powder) was prepared and analyzed through a multi-approach for their average diameter, PDI, colloidal stability, absorbance spectra, and metals concentrations have been presented previously (see chapter 2).

3.2.2 Natural seawater

All seawater used for holding and exposure clams was collected from Belle W. Baruch Institute for Marine and Coastal Sciences, University of South Carolina.

3.2.3 Artificial seawater

Artificial Seawater (ASW) was prepared in volumes sufficient to last through each experiment by adding Instant Ocean Crystal Seas® bioassay grade sea to ultrapure water (UPW) until a salinity of 28.5–30.5 ppt was measured. This ASW was continuously mixed for at least one week before use by plastic barrel air that was passed through a sterile 0.45 mm filter. Minor salinity adjustments were made as needed.

3.2.4 Algae culture

3.2.4.1 Microalgal strain

Isochrysis galbana T-iso is a free-living marine unicellular phytoflagellate of the order Chrysomonadales. Like other members of this order, it is rich in polyunsaturated fatty acids (Wood 1974), which are of nutritional value for marine fish larvae (Scott and Middleton 1979) and juvenile stages of mollusks (Rhodes and Landers 1974).

The marine microalga *Isochrysis galbana* T-iso specimen (UTEX LB 987) was provided by Culture Collection of Algae, Department of Botany, The University of Texas at Austin (UTEX). *Isochrysis galbana* can be cultivated in a standard F/2 (Guillard's) medium. In this work, the culture medium used for cultivation was a prepared solution of F/2 provided by (Guillard 1975). This medium is composed of solutions, whose composition is shown in Table 3.1.

3.2.4.2 Stock solutions

All stocks (nutrients, trace elements, and vitamins) separately began with 950 mL of dH_2O, added the components, and brought the final volume to 1 liter with autoclaved ultrapure water (UPW).

3.2.4.3 Medium

To prepare media of *Isochrysis galbana* T-iso, began with 950 mL of autoclaved filtered natural seawater and added the following components. The trace element and vitamin solutions are provided below. Bring the final volume to 1 L with autoclaved filtered natural seawater.

3.2.5 Inoculation

Microalgae, *Isochrysis galbana,* were cultured in 500 mL sterilized flasks containing 300 mL media previously sterilized in an autoclave at 120°C for 20 min, and 10% (v/v) algal inoculum. Until the advanced stationary phase, flasks were maintained on an orbital shaker at 100 rpm at 24°C and illuminated 16 hours on and 8 hours off by white cool fluorescent lamps. The flasks were not aerated, and additional agitation of the culture media was conducted by shaking the flasks twice daily to avoid the sedimentation of algal cells.

The transfer was made into 2 L-class bottles, 5 to 7 days later, to culture a microalgal population sufficient for the subsequent experiments. Once cultures were inoculated, put them on the table and attached the airline by turned the air on until moderate bubbling was going. Algae were concentrated on a Beckman model Allegra X-12R centrifuge at 3500 rpm for 20 minutes for feeding.

3.2.6 Acute clam *Mercenaria mercenaria* toxicity test

This method evaluates the sensitivity of the juvenile clam, *M. mercenaria,* in aqueous bioassays to three model AgNPs (Ag-*n*-powder, cit-AgNPs, and bio-AgNPs). The endpoint measured was mortality.

3.2.6.1 Collection and Holding of Hard Clams

Test organism – *Mercenaria mercenaria*, an estuarine bivalve. Juvenile clams of approximately (0.820 – 1.2 mm) in size were attained from Bay Shellfish Inc., located on Terra Ceia, Florida. Animals were shipped overnight in mesh

netting from the clam farm. Upon arrival at the laboratory, opened the mesh and put the clams in a glass finger bowl (approx. 1.5 L). Rinsed the clams with fresh 20-ppt seawater at least 3x to wash off any debris.

The 0.820 – 1.2 mm size class was retained on a 790-µm sieve, ranged 790–1280µm, and averaged 1000-µm. The smaller and bigger clams are kept in a separate bowl. The juvenile clams were then acclimated for 7 days prior to testing in 500-mL precleaned glass jars at 20°C, 30% salinity, and a 12-h light:12-h dark cycle. An air-stone was attached to an airline for gentle aeration and inserted into the jar. To minimize ammonia concentration, partial water changes (approximately 3/4 of the total volume) were conducted daily. *Isochrysis galbana* (average count of 6-8 million cells/mL), which is grown reproduced in the lab, was daily added as food

3.2.6.2 Reference toxicant bioassay experiment

Sodium dodecyl sulfate (SDS) was used as the reference toxicant. Reference toxicant tests were conducted to assure that each lot of clams used in the different assays was healthy. According to (Chung, 1999) assays were performed using concentrations of 1.94, 3.24, 5.4, 9.0, 15.0, and 25.0 mg L^{-1} SDS. Added an appropriate amount of SDS and DI water into beakers for each concentration, and then ten clams were placed to each concentration and control. An Olympus SZH10 Microscope (Olympus optical, Ltd. Japan) under 7.0× magnification was used to determine clam mortality by visible inspection. Criteria of mortality were determined gaping of valves and lack of locomotion which was exhibited following placement in the petri dish by tapping the petri dish to move

clams around that remained closed for at least five minutes. The population of animals used for the aqueous bioassay was considered healthy, and testing proceeds when the SDS LC50 value for a new lot of clams fell within two standard deviations of the averaged LC50 value.

3.2.6.3 Aqueous bioassay test

Range finding tests using a series of test AgNPs concentrations were initially tested. After a range-finding test, a definitive, narrow range of test nanoparticle concentrations was performed to delineate the dose-response curve. 24-h acute toxicity (LC50) tests of AgNPs on juvenile clams, standard length 0.98±0.3 mm, were carried out in static non-renewal tests. 10 Clams were exposed in 600-mL glass beakers with a test volume of 300-mL at 20-ppt salinity (5-µm-filtered seawater), 25°C, and a 16-h light: 8-h dark cycle. With five replicates, the six-silver nanoparticle nominal exposure concentrations were as follows: control, 0.2, 0.35, 0.6, 1.0, 1.5, and 2.6 mg-Ag L^{-1}.

Similarly, a 24-h acute toxicity (LC50) test of silver was conducted with clams of the average length of 1.0 ± 0.18 mm in order to compare the toxicity of silver nanoparticles with silver ions. The nominal exposure concentrations were 0.18, 0.22, 0.26, 0.3, 0.34, and 0.38 mg silver ions L^{-1} run as silver nitrate ($AgNO_3$). All exposure tests, an unexposed control group were determined from exposure studies. Water quality parameters were measured using YSI professional plus (YSI Incorporated, OH, USA). Post-exposure, water quality parameter ranges (Oxygen saturation ≥ 78%, temperature 22-23°C, salinity 20.09±0.1 ppt, and pH 8±0.15) were recorded in one replicate of the test concentration and the other of the control.

All replicates were not fed during the acute 24-h test periods. At the end of the exposure period, Juvenile clams were sieved from the testing chambers and counted under a dissecting scope to determine mortality. Percentage mortality was calculated by following the formulae:

$$\%\ \boldsymbol{Mortality} = \frac{number\ of\ dead\ M.mercenaria}{intial\ number\ of\ live\ M.mercenaria} * 100$$

The test was terminated 24-h hours after initiation, depending on the initial goal of the experiment. Clam mortality for the aqueous bioassay was assessed in the same manner as the reference test. The assays were rejected only if the control mortality was >10%. The data were then analyzed using appropriate statistics, and an LC50 was calculated.

3.2.7 Dissolution of AgNPs in seawater

It is significant to assess the quantity of Ag ionic release from the cit-AgNPs, bio-AgNPs, Ag-*n*-powder, and $AgNO_3$ suspensions in the media exposure tests. Following separation by ultracentrifugation, dissolved Ag concentrations in the test media-20 ppt seawater were measured by ICP-MS. Thus, a 4 mL aliquot of exposure medium from the different assays was taken at different time points at zero and 24-h depending on the test organism's exposure duration. Dissolved Ag ion release form AgNPs species were isolated using a centrifuge and filtering through 3KDa centrifugal ultrafiltration units (3KDa regenerated cellulose

membranes, Amicon Ultra-4) for 20 min 4000 rpm using an Eppendorf 5810R centrifuge. The total silver concentration of the exposure suspensions and dissolved Ag content were determined by Inductively Coupled Plasma Mass Spectrometry (ICP-MS) (NexION™ 350D, PerkinElmer Inc., Massachusetts, USA), following sample digestion with 10% HNO_3 using concentrated acid (70% HNO_3) and then diluted 200-fold in 1% of HNO_3 before the analysis so as to avert the salt formation and diminish matrix effects. The samples of all Ag particles, additionally, were examined via ICP-MS with the presence of indium (In_{115}) (analytical grade, BDH, VWR International LLC, PA) as an internal standard to correct non-spectral interferences during analysis(Vanhaecke et al. 1992).

3.2.8 Monitoring of AgNPs dissolution in natural seawater

In seawater, it is well known that AgNPs will release substantial amounts of silver ions (Ag+) to the surrounding suspension when some factors break up the colloid structures of AgNPs (e.g., salinity, Cl^{-}, S^{-2}, DOM, …. etc.). ICP-MS was used to determine the dissolution of AgNPs in natural seawater. AgNP dispersions (n = 3) of 200 µg L^{-1} (representing the less of determined LC50 concentration; see below) were incubated in 500 ml SW for 1, 24, 48, 72, and 96 hours under the same experimental conditions of toxicity (temp, pH, and light:dark). A 4 mL aliquot of AgNPs suspensions was withdrawn at different time points, hereafter mixing and gently agitated in seawater. Samples were processed before analysis as described above.

3.2.9 Statistical analysis

To statistically assess the Median Lethal Concentration (LC50) values (mg/L for aqueous) and their respective 95% confidence interval were analyzed for each bioassay using the Trimmed Spearman–Karber method (Hamilton et al., 1977). The mortality data analysis of variance (ANOVA) with Dunnett's procedure for comparison to determine significant differences ($p<0.05$) from the control response (Zar 1996) was achieved to determine the percentage of mortality. All statistical analyses were performed with SAS version 9.4 software (SAS® Institute, Cary, NC).

3.3 Results and Discussion

3.3.1 Natural seawater quality

Water quality parameters (dissolved oxygen, pH, salinity, temperature) were measured daily for control and treatments for all the toxicity tests. These parameters were not significantly different among any of the exposures (Table 3.2).

3.3.2 Measured Exposure Test concentrations

During the acute exposure, the measured total silver concentrations in the test suspensions were determined at time-zero and 24-hour test periods. At time-zero, the measured total silver concentrations in $AgNO_3$ exposure were ≥ 92% of nominal target concentrations (0.18, 0.22, 0.26, 0.30, 0.34, and 0.38 mg Ag L^{-1}) (table 3.3a). The measured total Ag concentrations in cit-, bio- AgNPs, and Ag-*n*-

powder were ≥ 89, ≥ 87, ≥ 90 of nominal concentration targets (0.20, 0.35, 0.60, 1.00, 1.50, and 2.60 mg Ag L^{-1}), respectively. The measured total Ag concentrations in the AgNP suspension and $AgNO_3$ solution at the start of the exposure were within the experimental/analytical error (e.g., <15 %) (table 3.3b). Therefore, all subsequent results are discussed as a function of the nominal Ag concentrations. Total Ag concentration in AgNP suspensions decreased at 24 h compared to those measured at 0 h, which can be attributed to the aggregation and sedimentation of AgNPs in seawater. The decrease in total Ag concentration was highest in Ag-*n*-powder, which can be attributed to the lower colloidal stability of powder AgNPs compared to cit-AgNPs and bio-AgNPs.

Greater than 88% of the $AgNO_3$-spiked samples were observed in the water column after 24-h spiking. However, some of the AgNPs behaved entirely differently. The measured total Ag concentrations were ≥77 ≥ 82 ≥ 63 of cit-, bio-AgNPs, and Ag-*n*-powder, respectively. Most of the measured total Ag concentrations displayed deviations are uneven from their nominal concentrations and measured total Ag concentrations at time-zero. Total silver concentration loss over time might be due to many reasons including **i**) sorption to the container walls, **ii**) aggregation and sedimentation, and **iii**) uptake by the organisms.

Seemingly, the total concentration of cit-AgNPs and Ag-*n*-powder decreased over time. The decrease might be more significant for the higher concentrations. Then, the Ag content in the water was higher in the $AgNO_3$ exposures than for either cit-AgNPs or Ag-*n*-powder exposures, which is

evidenced by ending up that aggregation and sedimentation are the cause of loss in the case of cit-AgNPs and Ag-*n*-powder.

The total Ag^+ concentrations determined in most AgNPs exposures decreased within the 24-h of exposure, whereas the Ag concentration in the Ag^+ exposures remained almost constant. This indicates, alongside the results of the dispersion characterizations, that AgNPs have been aggregated and sedimented over time. AgNPs are, therefore, more likely to be removed from the water column and thus less bioavailable compared to Ag^+, which may, at least partly, explain the lower toxicity in static exposures.

3.3.3 Ag ionic release behavior in the bioassay environment

To assess the impact of dissolved Ag and the observed AgNPs toxicity, Clams/silver nanoparticle combinations exhibiting substantial toxicity were further investigated. At the beginning and end of the exposure, spiked water samples were withdrawn and analyzed as described above to calculate total and dissolved silver concentrations in the aqueous bioassay media (Figure 3.1). The majority of Ag (> 96%) in $AgNO_3$ occurred as dissolved Ag. The concentration of dissolved Ag decreased following the order Ag-n-powder (≥ 40%) > cit-AgNPs (≥17 %) > bio-AgNPs (≥ 9%). The higher dissolution of powder AgNPs may be attributed to the fact that these AgNPs are not coated by a capping agent. On the other hand, cit-AgNPs are coated by citrate molecules may provide some protection for AgNP against dissolution. Bio-AgNPs are coated with biomolecules which 1) are generally larger than citrate molecules and thus form a thicker surface coating on

the surface of AgNPs, which may provide higher protection against dissolution, and 2) biomolecules may act as a reducing agent that counteracts the oxidative dissolution of AgNPs.

It should be borne in mind that Ag^{+} ions ($AgNO_3$ as dissolved as in the current study) also have limited stability in seawater and will rapidly form Ag-Cl complexes (e.g., $AgCl^{-2}$, $AgCl_3^{-2}$, $AgCl_4^{-3}$), even though those may be bioavailable (Farkas et al. 2020). Moreover, results of dissolution studies show the AgNP-exposure were present in dissolved form, or as unprecipitated AgCl complexes, which remained quasi-stable in seawater during 24-h in particular with (12 %) and (≥ 6%) of the cit-, and bio-AgNPs, respectively (Figure 3.1).

Dissolved Ag from AgNPs exposure is likely to have contributed to the observed toxicity, especially in the static acute exposure study, documented in other studies (Navarro et al. 2008*b*; Angel et al. 2013; Lee et al. 2018). The establishment of LC50 concentrations and toxicity comparisons between AgNP and Ag^{+} remains challenging due to complex metal behavior in seawater, including aggregation, dissolution, and complexation (Figure 3.5).

3.3.4 AgNPs aggregation in seawater

Increasing the salinity of the aqueous solutions resulted in the accelerated aggregation of AgNPs Ag nanoparticles (Ag-*n*-powder, cit-AgNPs, and bio-AgNPs) and as evidenced by increasing NP hydrodynamic diameters. Changes in size were monitored by the growth of AgNPs z-average dynamic light scattering (DLS) while they have deployed in 20 ppt the natural seawater at an interval of 1, 6, 24,

48, 72, and 96-h at 23±0.5 °C. All aggregation experiments were conducted in triplicates. The DLS measurements increased with time due to growing aggregate sizes (Figure 3.2). There were differences regarding sizes between AgNPs; the sequence of relative aggregation sizes were Ag-*n*-powder > cit-AgNPs > or ~ bio-AgNPs.

As expected, we observed smaller aggregates of cit and bio AgNPs compared to larger aggregates of Ag-*n*-powder. Aggregation in Ag-*n*-powder took place early and remained relatively continuous over 96-h.

Badawy et al. 2010 state that cit-AgNPs are stabilized by electrostatic repulsion. PVP-AgNPs are stabilized by steric repulsion, with ionic strength and electrolyte type (e.g., $NaNO_3$, NaCl), not affect the aggregation of the AgNP-PVP (Badawy et al. 2010). In this study, cit-AgNPs and bio-AgNPs aggregated as exposure time increased, suggesting that both particle electrostatic repulsive forces and steric repulsive interactions can be overwhelmed by an increase in ionic strength (i.e., a seawater effect). Under the same conditions, bio-AgNPS were more stable than cit-AgNPs in seawater. It is worth notable that bio-AgNps were found in some disaggregation at 96-h. This behavior can be attributed to multiple factors. The disaggregation might be triggered by the enhanced surface charge, abundance, coating, ionic strength, and NOM substances in the natural aquatic environment. The increase in surface charge induces an increase in the degree of repulsion within the aggregate matrix and thus aggregate disaggregation (Baalousha 2009). A study has been shown that polymers (Polyvinylpyridine) can disaggregate latex particle (885 nm) aggregates (Ouali and Pefferkorn 1994).

3.3.5 AgNPs dissolution in seawater

Nanoparticle toxicity could be attributed to dissolved Ag released from NPs, AgNPs themselves, or both (Griffitt et al. 2008; Navarro et al. 2008*b*; Fabrega et al. 2009). Thus, to better understand the stability of AgNPs and potential drivers of AgNPs suspension toxicity, the dissolution of AgNPs was examined in 20 ppt seawater over a 96-h period (Figure 3.3). No complete dissolution of silver nanoparticles was observed in all cases. According to the One-Way variable ANOVA statistical analysis performed in SAS® version 9.4 software (SAS Institute, Cary, NC, USA), the concentration of dissolved silver was relatively high and significantly different (*p-value* < 0.05) between the three types of nanoparticles.

The results showed that the dissolution behavior of AgNPs increase in the order of cit-AgNPs > bio-AgNPs > Ag-*n*-powder. The cit-AgNPs dissolved faster and to a higher extent than other bio-AgNPs and Ag-*n*-powder. More than 10 and 40% of the total spiked cit-AgNPs in the water from one to 24-h after spiking as closer with previous observations (Nair et al. 2013). A similar trend was observed in the $AgNO_3$-spiked samples as aforementioned (Figure 3.1 (dissolve)), yet the bio-AgNPs and Ag-*n*-powder behaved quite differently. Dissolution of AgNPs was insignificant at early time points, and even at 24-h, 18%, and 10% of the bio-AgNPs and Ag-*n*-powder dissolved in the seawater, respectively.

These findings can be used to underpin the factors that may cause or determine AgNP toxicity. The difference in dissolution processes of Ag-*n*-powder, cit-AgNPs, and bio-AgNPs was attributed to differences in surface chemistry, size,

aggregation state of NP, and ionic strength in environmental media. The cit-AgNPs showed the highest dissolution with regard to the other two AgNPs (bio-AgNPs dissolution was lower than that of Ag-*n*-powder).

Liu et al., 2010 have observed that citrate groups capped Ag NPs in de-ionized water, with the Ag ion migration, which has been prevented because of electrostatic interaction between Ag ions and the capping agents (Liu et al. 2010). Nonetheless, the possibility of electrostatic interaction between negatively charged Ag chloride complexes formed in seawater has been rejected due to seawater pH values ~ 8.00 and the resulting weakening of electrostatic interactions in high ionic strength solutions (Badawy et al. 2010), as in the current study.

On the other side, in literature, higher dissolution behaviors correlate to smaller NP sizes. Smaller-sized NPs have a greater surface area for the interactions with the surrounding media; therefore, this might explain the higher dissolution of cit-AgNPs compared to larger NPs dissolve at slower rates and become smaller over time.

The biological coating of NPs can be similar to proteins or their subunits: linear high molecular weight polymers built from chains of amino acids with numerous amino groups available for reaction with metallic ions.

In this particular case, the biological coating can be assumed very stably and cannot be displaced away from the surface of the nanoparticles by competing for organic species. Considering strong repulsive forces generated by functional groups distributed along polymer chains, it can be hypothesized that bio-AgNPs

are not subject to a critical aggregation even in seawater because of strong steric and electrostatic stabilization of the biological coating polymer chains. This hypothesis is somewhat consistent with its curve in figure (Figure 3.3), where the dissolution process of bio-AgNPs started from 1-h, gradually increased, then reached a plateau from 24-h towards 96-h. It is demonstrated the dissolution of bio-AgNPs underwent an equilibrium state with 20% dissolved [Ag] within 96-h although the high concentration of Cl^- in SW, which acts as a sink for Ag^+ ions released from AgNPs following the oxidative dissolution and the formation of $AgCl_2^-$ and $AgCl_3^{2-}$ complexes (Byrne 2002). Furthermore, the bio coating may prevent the migration of released Ag ions due to its amino groups chelating released Ag ions (Ghoul et al. 2003).

Ag-*n*-powder (bare) behavior has been observed as less dissolution than others in SW. A lack of dissolution of Ag-*n*-powder in low ionic strength waters was expected from previous work as chloride concentration in river water is considered too low to drive the formation of silver chloro-complexes (Liu and Hurt 2010; Li et al. 2012; Dobias and Bernier-Latmani 2013). However, dissolution of Ag-*n*-powder (bare) should have been observed in SW due to high ionic strength and high chloride concentration, well above the dissolution threshold reported by Li and Lenhart (Li and Lenhart 2012).

The reasons that Ag-*n*-powder did not dissolve in seawater are not clear, as AgNP should not be persistent in realistic environmental compartments containing dissolved oxygen (Liu and Hurt 2010). An influence of Ag concentration on dissolution kinetics may be suggested. Still, the relatively large size of Ag-*n*-

powder (138 ± 5 nm, review ch. 2) may have played a determining role in this lack of dissolution (Zhang et al. 2011).

It is well understood the seawater can lead to the formation of nanoparticle aggregates via electrostatic interactions, thereby reducing the surface area-to-volume ratio of nanoparticles, thus reducing chances of reactivity and dissolution (Alkilany and Murphy 2010). This is in good agreement with the Values presented for the aggregation state of Ag under the same conditions as discussed above (**Figure 3.2**). In addition, it may reduce the surface area of the particles by minimizing their interaction with the biological ions in the surrounding media, therefore inhibiting nanoparticle dissolution. These factors explain the low dissolution of Ag-*n*-powder.

3.3.6 Reference toxicity bioassays

No mortality or visible disease was observed in clams during exposure for 24-h LC50s with the SDS reference toxicant ranged from 6.74 to 9.27 mg L^{-1}. All the reference toxicant tests for the assays using *M. mercenaria* provided LC50 estimates that met the acceptance criteria (Table 3.4).

3.3.7 Acute aqueous bioassay

Both the rangefinder and definitive aqueous acute assay were performed with the 0.82 – 1.2 mm size class. All results were calculated based on nominal concentrations. Clam survival in controls was 96% for all aqueous contaminant

assays. The 24-h toxicity test results showed that all silver nanoparticles tested were toxic to juvenile *M. mercenaria* (Table 3.5).

Survival after exposure to contaminated and uncontaminated (control) waters is the primary toxicity test criterion. None of the control clams died showed that handling techniques and holding facilities were acceptable for conducting such experiments, as required by the standard EPA / COE protocol where the mean survival should be 90%.

Mortality of test animals was positively correlated with increasing concentration and type of toxicants as well as increasing exposure period. As may be expected, the higher the toxicant concentration, the higher is mortality. Comparison of aqueous AgNPs LC50 values obtained in this study with marine mollusks and invertebrates were observed in relation to silver nanoparticles toxicity (Table 3.6).

After the rangefinder assay, the definitive 24-h acute assay was executed with control and the following nominal toxicants concentrations: 0.18, 0.22, 0.26, 0.30, 0.34 and 0.38 mg L^{-1} $AgNO_3$ and 0.2, 0.35, 0.6, 1.0, 1.5, and 2.6 mg L^{-1} AgNPs. Prior to 24-h of exposure, Mortality in the acute aqueous assays followed a dose-dependent response (Table 3.5). In general, Mortality (%) of juvenile clams as a function of the concentration of $AgNO_3$ exhibited consistently higher clams' mortality than all AgNPs for a 24-h mean LC50 value of 0.24 mg L^{-1} (95% confidence intervals: 0.22-0.27 mg L^{-1}) (Figure 3.4). Ag-*n*-powder displayed higher toxicity than cit-, and bio- synthesized AgNPs with a 24-h LC50 of 0.75 mg L^{-1} (95% confidence intervals: 0.645–0.87), 1.12 mg L^{-1} (95% confidence intervals: 0.90–

1.36 mg L^{-1}), and 2.14 mg L^{-1} (95% confidence intervals:1.81–2.43 mg L^{-1}), respectively (Figure 3.5).

The present study results demonstrate that nanoparticles are capable of causing acute toxicity in this aquatic species; however, toxicity differs significantly with the particle composition and the species tested. The toxicity of nanometals does not appear to be a generic response to exposure to nanosized particles; instead, it seems that particular nanometals have an intrinsic property that confers toxicity.

Of the three silvers tested, $AgNO_3$ displayed the highest toxicity to juvenile clams with a 24-h LC50, indicating the high toxicity of silver. The high toxicity might have resulted from the dissociation of silver nitrate in the water resulting in ionic silver (Ag^+) form, the main toxic form of silver to clams. An aquatic environment contaminates by metals is a serious threat to the aquatic. Metals and their salts are simple inorganic compounds, and the toxicity is based on their physicochemical properties (Morgan et al. 2004). It is well-documented that $AgNO_3$ exposure in the presence of the same conditions with different aquatic animals can appear $AgNO_3$ to be the most toxic form of silver nanoparticles (Table 3.5).

AgNPs: The differences in toxicity observed for the various chemical and biological synthesis could be partially explained by their different dissolution in the exposure medium. Indeed, the content of dissolved silver ions analysis revealed that cit-AgNPs dissolved more in exposure medium than Ag-*n*-powder and bio-AgNPs. These results are in accordance with those reported previously after exposing *D. magna* to the same particles (Georgantzopoulou 2015).

Nevertheless, the observed effects could not be attributed to the effects of Ag ions only as the observed effects for AgNPs were lower than those observed for $AgNO_3$ with comparable dissolved Ag concentrations in natural seawater. The differences in effects could be explained by different factors such as the size, surface charge, and specific molecules present on the surface of AgNPs. As previously described, bio-AgNPs were synthesized using the fungal extract. Therefore, biomolecules (e.g., proteins, enzymes, and sugars) are present on their surface (Balachandran et al. 2013; Georgantzopoulou et al. 2013). Also, it can be hypothesized that AgNPs have a different or an additional uptake route compared to $AgNO_3$ may readily release the ions in the cells after uptake (Georgantzopoulou 2015).

These findings also indicate that it is unlikely that silver nanoparticle toxicity is caused by particle dissolution in juvenile clams (Figure 3.6). The soluble concentrations of bio-AgNPs present were well below the 24-h LC50s for the soluble nanoparticles. In other words, silver dissolution was, again, much lower than concentrations required to produce acutely lethal effects (Figure 3.6). At the same time, the dissolution of cit-AgNPs appears to produce sufficient soluble ions to account for 5 to 10% of the observed mortality (Figure 3.6). In contrast, Ag-*n*-powder was predominantly present in the clam exposures' dissolved form and reached approximately 40% of the soluble silver at 24-h. Still, concentrations of LC50 were around 9% from soluble Ag-*n*-powder.

The function of dissolution in nanomaterials toxicity also differs according to the composition of the particles and species. The dissolution of silver forms is

relatively low and mortality observations may not be attributed solely to the solubilization of particles during exposures (Figure 3.6).

Nanoparticle forms were less toxic than soluble forms of metal based on the mass of metal added to each exposure. Nanomaterials in aqueous suspensions are dynamic systems undergoing simultaneous dissolution, aggregation, and sedimentation (Brant et al. 2005; Murdock et al. 2008). Figure 3.1, therefore, shows approximately 10 to 40% of the initial mass of silver nanoparticles added to exposure may be lost through aggregation and sedimentation during a 24-h exposure. The amount of material in the media is likely lost by the bioaccumulation in the body of the species of organism present via uptake processes. Because of, perhaps, differences in organic matter excreted by various organisms, these results in constantly changing exposure parameters that differ between test systems and calculate appropriate dose metrics for aquatic exposures difficult.

In the experiment with *Oryzias latipes*, bare-AgNPs were more toxic than PVP-coated AgNPs (Wu et al. 2010). In another study with AgNPs of similar sizes coated with either citrate, PVP, or Gum Arabic (GA), all had significantly different growth inhibitory effects. The GA-AgNPs were more toxic than the PVP-AgNPs. In contrast, the PVP-AgNPs were more toxic than the citrate-AgNPs (Yang et al. 2012).

In this study, it was found that bio-AgNPs had different effects compared with Ag-*n*-powder and cit-AgNPs in acute toxicity (Figure 3.5) and different fates of silver as reflected in dissolution (Figure 3.3) and dissolved silver released by dissolution over 24-h (Figure 3.6). Ag-*n*-powder was reported to dissolve quickly

and were more likely to attach within the wall and settle onto the sediment, thereby enhancing the risk to bivalve organisms. Unlike the Ag-*n*-powder particles, stable AgNPs, such as bio- and cit-AgNPs, are likely to remain in the water column and increase potential toxicity to bivalve organisms (Kwok et al. 2012).

The results of the total content of Ag and the release of ions also suggest that there were bio-AgNPs as particles rather than ions in the seawater. In the absence of aggregation, the adverse effects of AgNPs on aquatic species are thought to be maximized because of increased residence times in the water, leading to increased bioavailability (Navarro et al. 2008*a*; Fabrega et al. 2011).

Table 3.1 Composition of Stock Solutions and Prepared medium of F/2 medium.

Stock Solutions (Deionized water)		
	Material	*Grams /1L*
Nutrients	$NaNO_3$ (Sodium Nitrate)	75
	NaH_2PO_4 (Monosodium Phosphate)	5
	$NaSiO_3$ (Sodium Silicate--liquid)	30
Trace elements stock	$CuSO_4$ (Copper II Sulfate)	9.8
	$ZnSO_4$ (Zinc Sulfate)	22
	$CoCl_2$ (Cobalt II Chloride)	10
	$MnCl_2$ (Manganese II Chloride)	180
	Na_2MoO_4 (Sodium Molybdate)	6.3
Vitamin Stocks	Vitamin H (Biotin)	0.1
	Vitamin B_{12} (Cyanocobalamin)	1
	Vitamin B_1 (Thiamine HCl)	0.2
Prepared medium (Seawater)		
	Solutions	*Quantity*
Stock solutions	Nutrients	1.0 ml
	Trace Metal Stocks	1.0 ml
	Vitamin mix stock solution	0.5 ml

Table 3.2 Average water quality parameters with standard error for the juvenile *Mercenaria mercenaria* toxicity tests.

Silver Forms	DO (mg L^{-1})	pH	Temp. (°C)	Salinity (ppt)
$AgNO_3$	7.11 ± 0.14	7.71 ± 0.18	24.06 ± 0.08	20.06 ± 0.06
Cit-AgNPs	6.92 ± 0.15	7.90 ± 0.08	23.74 ± 0.44	20.72 ± 0.28
Bio-AgNPs	6.88 ± 0.17	7.79 ± 0.14	23.56 ± 0.22	20.31 ± 0.04
Ag-*n*-powder	6.91 ± 0.1	7.81 ± 0.11	23.98 ± 0.07	20.09 ± 0.12

Table 3.3 Nominal and actual concentrations of silver during toxicity testing

(a) $AgNO_3$

Nominal $AgNO_3$ (mg/L)	0.18	0.22	0.26	0.30	0.34	0.38
Measured total Ag at time-zero (mg/L)	0.18±6	0.22±5	0.26±1.5	0.29±1.9	0.35±11	0.38±2.4
Measured total Ag after 24-h (mg/L)	0.16±5.1	0.17±5.5	0.22±5.8	0.28±4.9	0.27±4.5	0.33±5.8

(b) AgNPs Forms

Nominal AgNPs (mg/L)	Measured total Ag at time-zero (mg/L)			Measured total Ag after 24-h (mg/L)		
	cit-AgNP	bio-AgNPs	Ag-*n*-powder	cit-AgNP	bio-AgNPs	Ag-*n*-powder
0.20	0.19±3.2	0.19±2.8	0.20±3.3	0.14±2.8	0.15±3.5	0.11±3.7
0.35	0.34±1.3	0.34±4.4	0.34±3.3	0.25±3.7	0.33±5.0	0.22±5.4
0.60	0.59±7.4	0.57±6.7	0.59±7.4	0.49±5.9	0.50±8.1	0.40±6.8
1.00	0.99±5.9	0.98±10.9	0.97±8.3	0.84±8.8	0.90±10.3	0.70±17
1.50	1.47±2.2	1.49±18.7	1.49±12.6	1.18±6.5	1.24±8.5	0.92±18
2.60	2.55±8.5	2.57±15.1	2.56±28	2.11±11.6	2.05±17.0	1.70±15

* $P < 0.05$, time-zero-h versus 24-h by single-factor ANOVA. Data are presented as mean ±standard deviation

Table 3.4 Results of the SDS exposures.

	Table 3.5	**CI: 95%**	**CI: 95%**
	6.97	5.17	8.77
	7.91	6.10	9.71
	8.25	6.45	10.05
	7.79	5.99	9.62
	9.14	7.33	10.94
	9.59	7.79	11.39
Mean (acceptance range)	**8.28**	**6.48**	**10.07**

Table 3.6 LC50 values with 95% confidence intervals for juvenile clams exposed to $AgNO_3$ and Ag-*n*-powders, cit-AgNPs, and bio-AgNPs for 24-h.

Silver forms	Range of Conc. (mg. L^{-1})	LC50 24-h (mg. L^{-1})	95% CIs (mg. L^{-1})
$AgNO_3$	0.18 – 0.38	0.24	0.22 – 0.27
Ag-*n*-powder	0.20 – 2.60	0.70	0.64 – 0.87
Cit-AgNPs	0.20 – 2.60	1.05	0.90 –1.36
Bio-AgNPs	0.20 – 2.60	2.44	1.81 – 2.43

Table 3.7 Comparative toxicity estimates (LC50) were reported in the literature for M. mercenaria and other invertebrate species to AgNPs in aqueous exposures.

Species	Toxicant	Organisms	Duration (h)	Life stage	LC50 (mg/L)	Reference
M. mercenaria	AgNO3	Hard clam	24	juvenile	0.24	Current study
	Ag-*n*-powder				0.70	
	Cit-AgNPs				1.05	
	Bio-AgNPs				2.44	
Danio rerio	Bio-AgNPs	Zebrafish	96	adult	0.1422	(Krishnaraj et al.
Artemia nauplii	commercial AgNPs	Brine Shrimp	24	nauplii	0.001	(Arulvasu et al. 2014)
Gammarus fossarum	AgNO3	Amphipoda	96	juveniles	0.001	(Funck et al. 2013)
				ovigerous females	0.0019	
				adult males	0.0022	
Danio rerio	AgNO3	Zebrafish	48		0.025	(Bilberg et al. 2012)
	pvp-AgNPs				0.084	
Amphiascus tenuiremis	AgNO3	copepod	96	adult	0.064	(Sikder et al. 2018)
	PVP-AgNPs				0.095	
Oryzias latipes	Cit-AgNPs	medaka	96	juvenile	1.8	(Sohn et al. 2015)
	AgNWs				4.18	
Oreochromis niloticus	Ag nano powder	Nile tilapia	96		19.5	(Afifi et al. 2016)
Tilapia zillii		redbelly tilapia			20	
Oncorhynchus mykiss	AgNPs	Rainbow trout	96	embryos	0.25	(Johari et al. 2013)
				larvae	0.71	
				juvenile	2.16	
Calanus finmarchicus	PVP-AgNPs	copepod	96		0.403	(Farkas et al. 2020)
	AgNO3				0.147	
Gammarus fossarum	AgNO3	Amphipod	72	adult males	0.039	(Mehennaoui et al. 2016)
	Bare AgNPs				0.835	
	Bio-AgNPs				> 0.1	

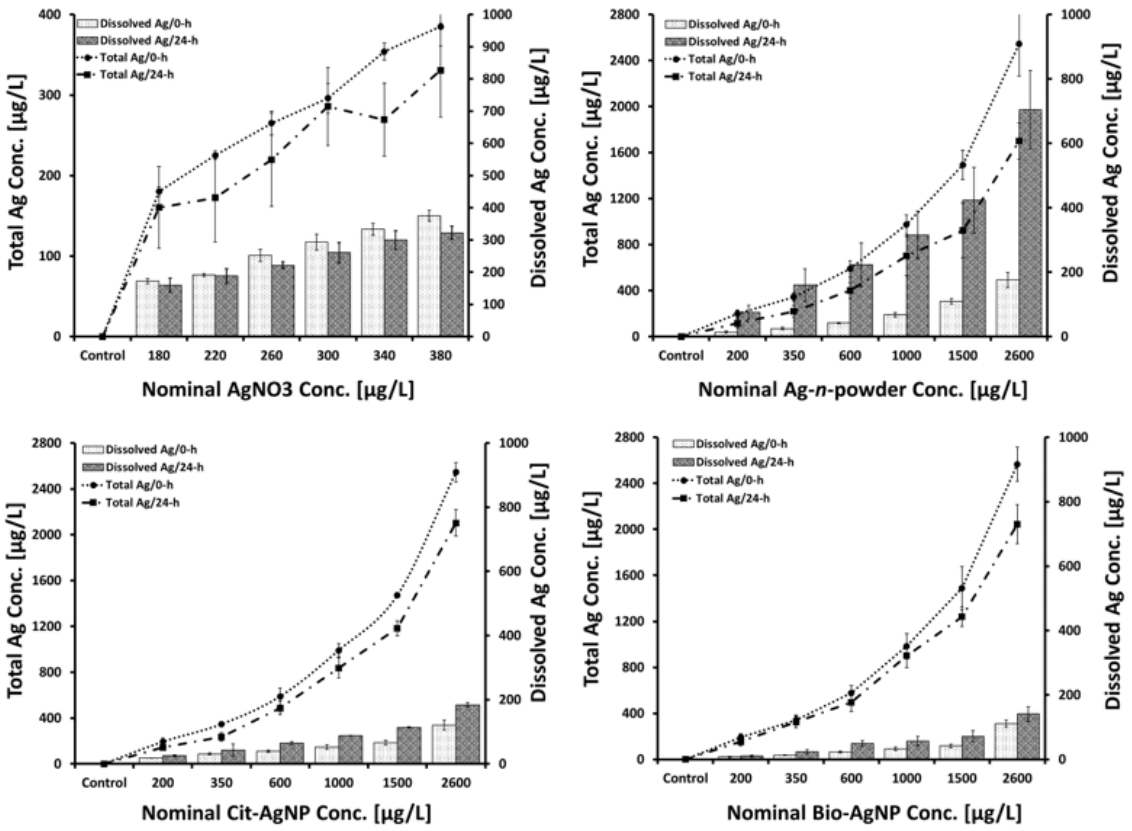

Figure 3.1 Total and dissolved silver concentration during zero and 24-h exposures of juvenile clams to silver nanoparticles at the median lethal concentration (LC50). The initial concentrations of particles, the concentration of total and soluble metal in the exposure media after 24-h are plotted for each combination. Bars represent the mean ± standard deviation.

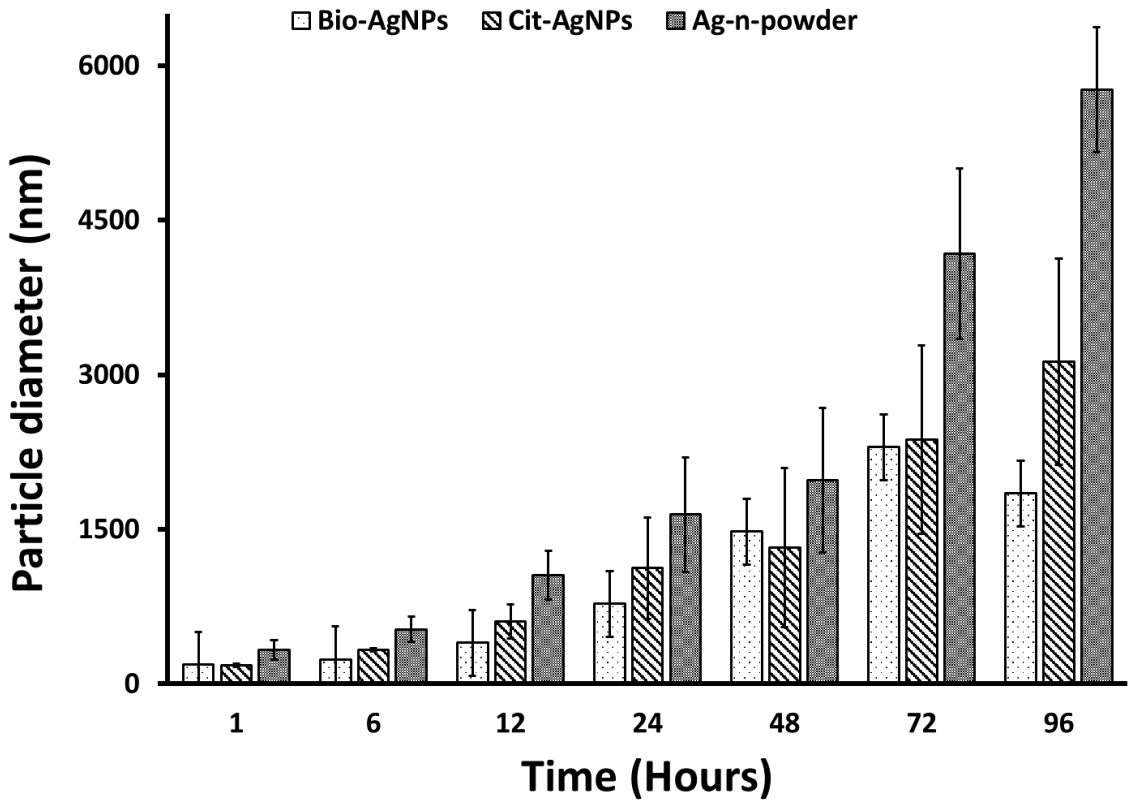

Figure 3.2 Time-dependent hydrodynamic diameter (nm) of 200 ug/L cit-AgNPs, bio-AgNPs, and Ag-*n*-powder in seawater as a function of time. The analysis was carried out on 1, 24, 48, 72, and 96 hours.

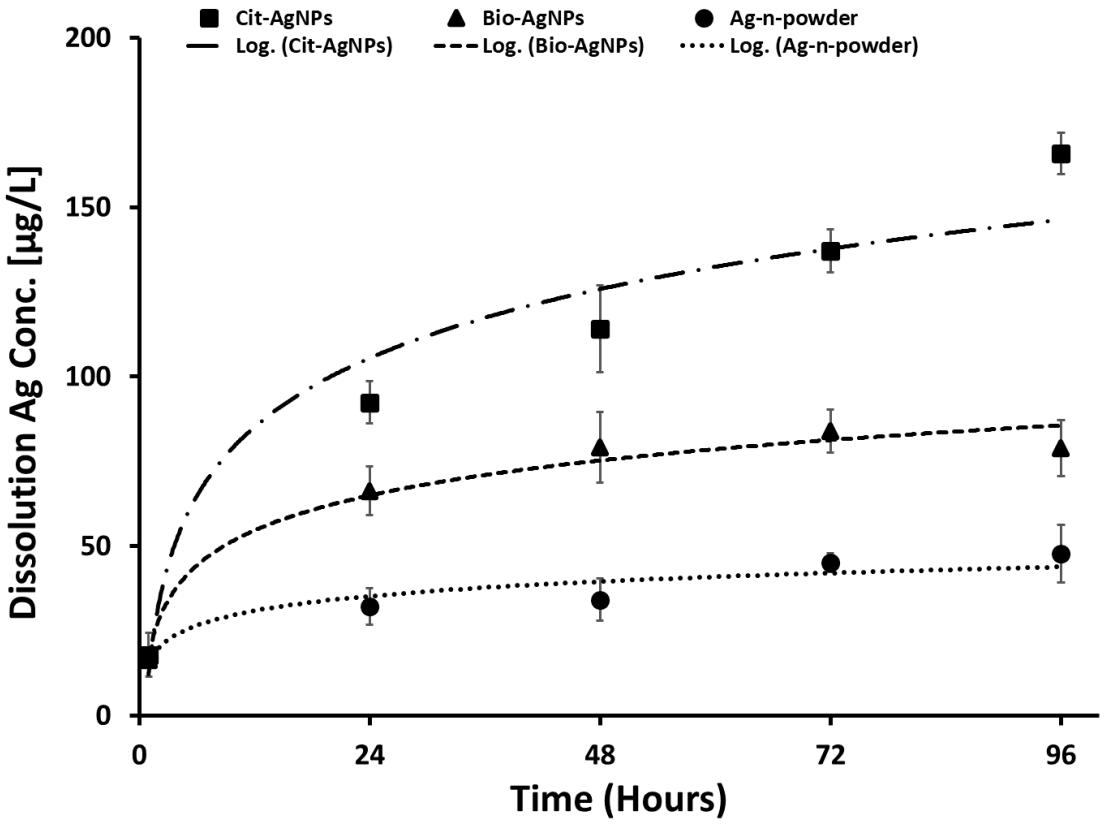

Figure 3.3 . ICP-MS of silver (Ag) dissolution in natural seawater after spiking 200 ug/L of silver Ag-*n*-powder, cit-AgNPs, and bio-AgNPs as a function of time. The analysis was performed on 1, 24, 48, 72, and 96 hours. The figure shows the measured values (cit-AgNPs [■], bio-AgNPs [▲], and Ag-*n*-powder [●]), the model fit (dotted lines), 95% interval around the model fit (error bars).

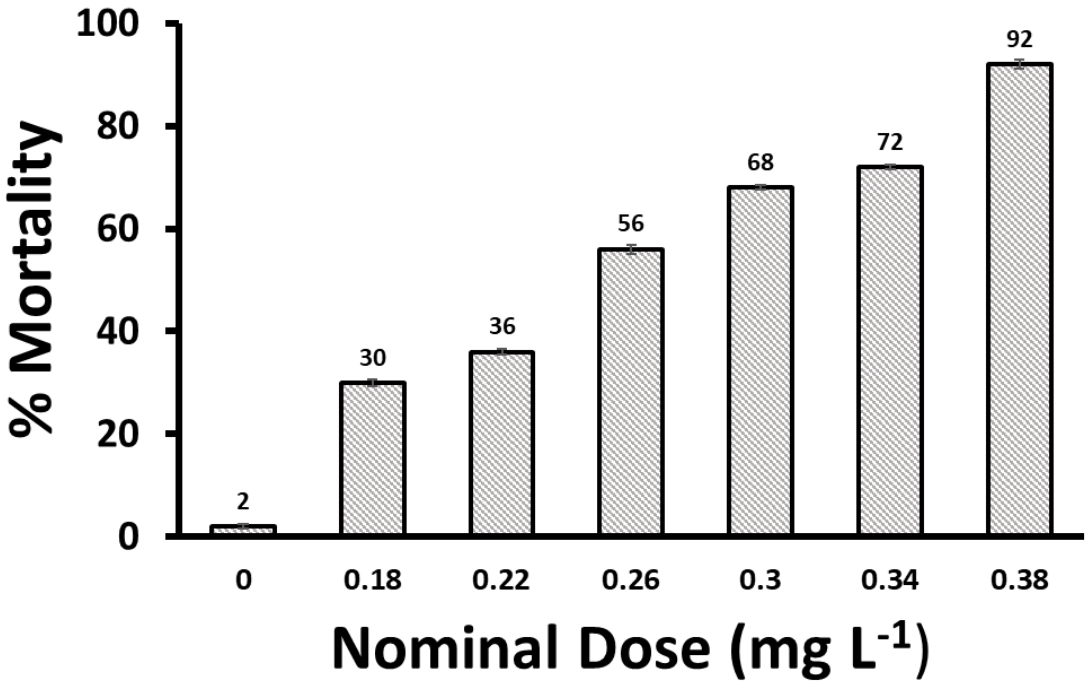

Figure 3.4 Mortality (%) of juvenile clams as a function of the concentration of $AgNO_3$ for 24-h acute aqueous exposure.

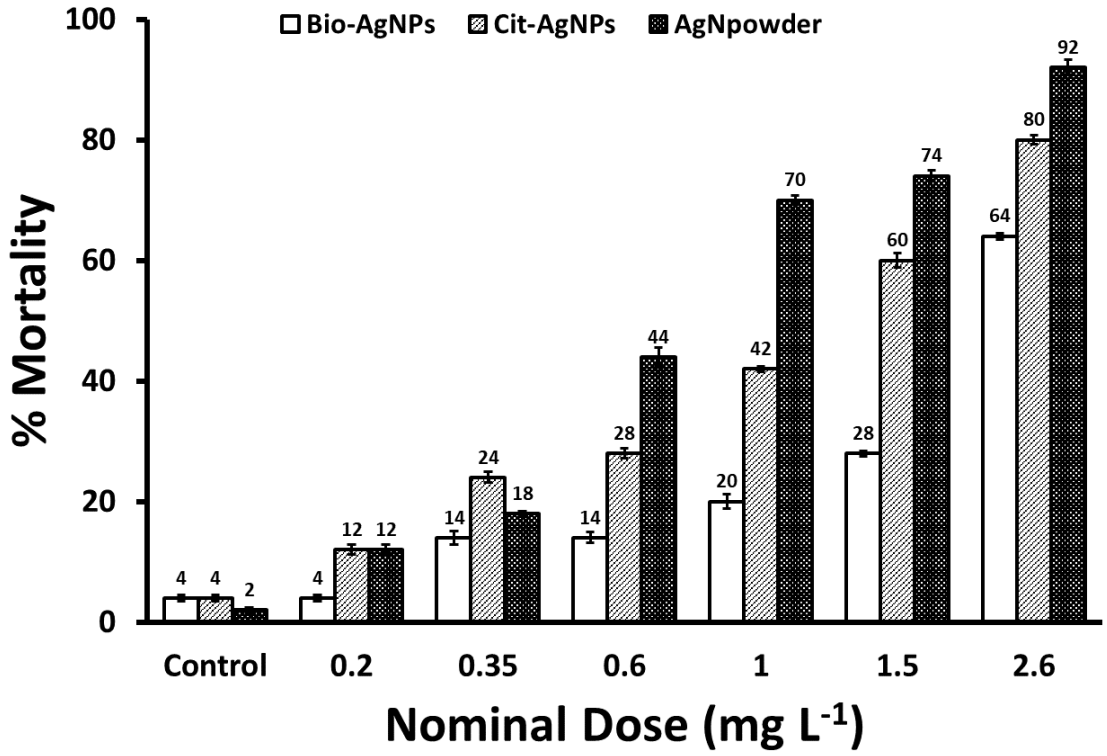

Figure 3.5 Mortality (%) of juvenile clams as a function of the concentration of cit-AgNPs, Biosynthesized AgNPs and Ag-*n*-powder for 24-h acute aqueous exposure.

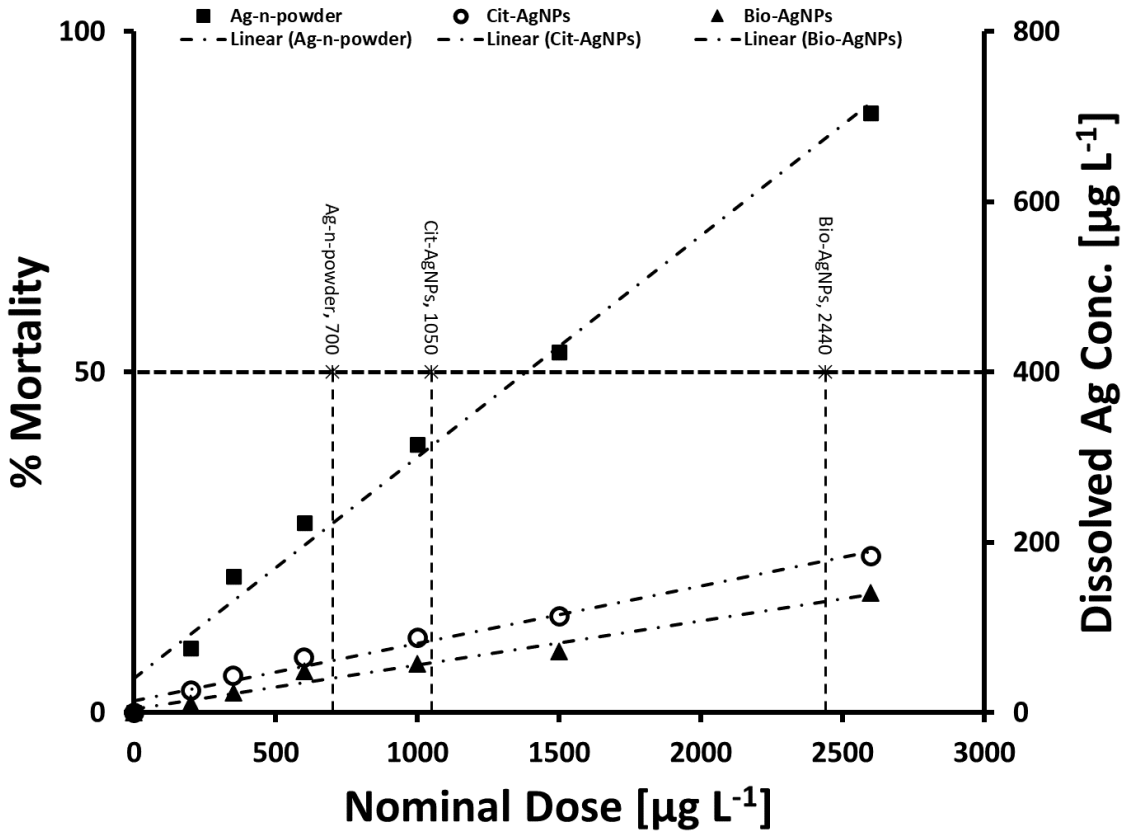

Figure 3.6 The toxicity Mortality percentage curves for species of soluble silver nanoparticulate. Data in this figure illustrate the toxicity of nanoparticulate silver groups in Juvenile clams, as well as the contribution of dissolution to nanoparticulate toxicity. The dissolved nanoparticles' mortality curves are plotted along with dissolved silver released by dissolution over 24-h. (Short dashed lines) represent calculated median lethal concentrations (LC50s) for dissolved concentrations released from nanoparticles. (The dotted, sphere, and filled blue area) represent the dissolving of Ag-*n*-powder, cit- and bio-silver nanoparticles, respectively.

CHAPTER 4

CONCLUSIONS

The synthesis and characterization of AgNPs were successful via chemical and biological approaches. The chemical synthesis is based on reducing ionic silver using sodium borohydride in the presence of trisodium citrate as a capping agent. The Biological approach is based on the use of cell-free extracts of AFS10 as reducing and capping agents, and then convert ionic silver to metallic silver and impart AgNP stability. The physicochemical characterization demonstrates the formation of spherical AgNPs with similar properties. The UV-vis absorbance underpins the conversion of Ag^{+} to Ag^{0} and the formation of AgNPs using the chemical and biological approaches. The chemical process generated AgNPs with a lower polydispersity compared to the biological synthesis approach, as confirmed by the lower PDI values. The biological synthesis is slower than the chemical synthesis and is more difficult to control and. However, biological synthesis becomes faster with increased synthesis temperatures.

Also, throughout this study, it has been proved that environmental conditions may influence the toxicity that is supposed to be caused by silver nanoparticles (AgNP). It was also quite clear that this nanotoxicity was coating-dependent and size-dependent, and length-of-exposure-dependent. Significant differences compared the fate and toxicity of chemically- and biologically synthesized AgNPs alongside silver nanopowder (Ag-*n*-powder) and silver nitrate ($AgNO_3$) to juvenile hard clams (*Mercenaria mercenaria*). These results indicate the importance of assessing the AgNPs interactions in natural seawater. Factors such as pH, AgNPs concentration, size, and salinity, may induce dissolution and aggregation of AgNPs, influencing the marine organisms. All AgNPs formed

aggregates in seawater, and the size of these aggregates decreased following the order Ag-*n*-powder > cit-AgNPs > bio-AgNPs. Additionally, all AgNPs have undergone dissolution in seawater, and the concentration of dissolved Ag decreased following the order cit-AgNps > Ag-*n*-powder > bio-AgNPs. This study demonstrated that both dissolved and particulate Ag induces toxicity to the juvenile clam, *M. mercenaria*. The toxicity of Ag to the juvenile hard clams (*Mercenaria mercenaria*) decreased following the order $AgNO_3$ > Ag-*n*-powder > cit-AgNps > bio-AgNPs. The toxicity of AgNP suspensions could not be fully explained by the dissolved Ag concentrations and thus is attributed to both dissolved Ag and particulate Ag.

Overall, the environmental release of AgNPs from consumer products, sewage outfalls, etc., would still pose some risk to marine ecosystems through a rapid and complete dissolution of AgNPs in seawater. Therefore, it is necessary to evaluate the potential role of different types of nanoparticles in relevant environmental exposures.

REFERENCES

Abbas, Q., Yousaf, B., Ullah, H., Ali, M.U., Ok, Y.S. and Rinklebe, J. 2020. Environmental transformation and nano-toxicity of engineered nano-particles (ENPs) in aquatic and terrestrial organisms. *Critical Reviews in Environmental Science and Technology* 50 (23): 2523–2581.

Adams, L.K., Lyon, D.Y. and Alvarez, P.J.J. 2006. Comparative eco-toxicity of nanoscale TiO2, SiO2, and ZnO water suspensions. *Water Research* 40 (19): 3527–3532.

Afifi, M., Saddick, S. and Abu Zinada, O.A. 2016. Toxicity of silver nanoparticles on the brain of Oreochromis niloticus and Tilapia zillii. *Saudi Journal of Biological Sciences* 23 (6): 754–760.

Aggarwal, P., Hall, J.B., McLeland, C.B., Dobrovolskaia, M.A. and McNeil, S.E. 2009. Nanoparticle interaction with plasma proteins as it relates to particle biodistribution, biocompatibility and therapeutic efficacy. *Advanced Drug Delivery Reviews* 61 (6): 428–437.

Agrawal, Y. and Patel, V. 2011. Nanosuspension: An approach to enhance solubility of drugs. *Journal of Advanced Pharmaceutical Technology & Research* 2 (2): 81.

Aillon, K.L., Xie, Y., El-Gendy, N., Berkland, C.J. and Forrest, M.L. 2009. Effects of nanomaterial physicochemical properties on in vivo toxicity. *Advanced Drug Delivery Reviews* 61 (6): 457–466.

Ajayan, P.M. 2003. Bulk Metal and Ceramics Nanocomposites. *Nanocomposite Science and Technology*: 1–75.

Alkilany, A.M. and Murphy, C.J. 2010. Toxicity and cellular uptake of gold nanoparticles: What we have learned so far? *Journal of Nanoparticle Research* 12 (7): 2313–2333.

Angel, B.M., Batley, G.E., Jarolimek, C. V. and Rogers, N.J. 2013. The impact of size on the fate and toxicity of nanoparticulate silver in aquatic systems. *Chemosphere* 93 (2): 359–365.

Arce Funck, J., Danger, M., Gismondi, E., Cossu-Leguille, C., Guérold, F. and Felten, V. 2013. Behavioural and physiological responses of Gammarus fossarum (Crustacea Amphipoda) exposed to silver. *Aquatic Toxicology* 142–143: 73–84.

Arulvasu, C., Jennifer, S.M., Prabhu, D. and Chandhirasekar, D. 2014. Toxicity effect of silver nanoparticles in brine shrimp artemia. *The Scientific World Journal* 2014.

Asgharian, B. and Price, O.T. 2007. Deposition of Ultrafine (NANO) Particles in the Human Lung. *Inhalation Toxicology* 19 (13): 1045–1054.

Asz, J., Asz, D., Moushey, R., Seigel, J., Mallory, S.B. and Foglia, R.P. 2006. Treatment of toxic epidermal necrolysis in a pediatric patient with a nanocrystalline silver dressing. *Journal of Pediatric Surgery* 41 (12): e9.

Baalousha, M. 2009. Aggregation and disaggregation of iron oxide nanoparticles: Influence of particle concentration, pH and natural organic matter. 407 (6): 2093–2101.

Baalousha, M., Ju-Nam, Y., Cole, P.A., Hriljac, J.A., Jones, I.P., Tyler, C.R., Stone, V., Fernandes, T.F., Jepson, M.A. and Lead, J.R. 2012. Characterization of cerium oxide nanoparticles-Part 2: Nonsize measurements. *Environmental Toxicology and Chemistry* 31 (5): 994–1003.

Baalousha, M. and Lead, J.R. 2007. Characterization of natural aquatic colloids (<5 nm) by flow-field flow fractionation and atomic force microscopy. *Environmental Science and Technology* 41 (4): 1111–1117.

Baalousha, M. and Lead, J.R. 2012. Rationalizing nanomaterial sizes measured by AFM, FlFFF and DLS: sample preparation, polydispersity and particle structure. *Environmental Science Technology*.

Badawy, a. M.E., Luxton, T.P., Silva, R.G., Scheckel, K.G., Suidan, M.T., Tolaymat, T.M., El Badawy, A.M., Luxton, T.P., Silva, R.G., Scheckel, K.G., Suidan, M.T., Tolaymat, T.M., Badawy, a. M.E., Luxton, T.P., Silva, R.G., Scheckel, K.G., Suidan, M.T. and Tolaymat, T.M. 2010. Impact of environmental conditions (pH, ionic strength,and electrolyte type) on the surface charge and aggregation of silver nanoparticle suspensions. *Environmental Science & Technology* 44 (4): 1260–1266.

Balachandran, Y.L., Girija, S., Selvakumar, R., Tongpim, S., Gutleb, A.C. and Suriyanarayanan, S. 2013. Differently Environment Stable Bio-Silver Nanoparticles: Study on Their Optical Enhancing and Antibacterial Properties. *PLoS ONE* 8 (10): 77043.

Baun, A., Hartmann, N.B., Grieger, K. and Kusk, K.O. 2008. Ecotoxicity of engineered nanoparticles to aquatic invertebrates: A brief review and recommendations for future toxicity testing. *Ecotoxicology* 17 (5): 387–395.

Benn, T.M. and Westerhoff, P. 2008. Nanoparticle silver released into water from commercially available sock fabrics. *Environmental Science and Technology* 42 (11): 4133–4139.

Bhainsa, K.C. and D'Souza, S.F. 2006. Extracellular biosynthesis of silver nanoparticles using the fungus Aspergillus fumigatus. *Colloids and Surfaces*

B: Biointerfaces 47 (2): 160–164.

Bhattacharjee, S. 2016. DLS and zeta potential - What they are and what they are not? *Journal of Controlled Release* 235: 337–351.

Bilberg, K., Hovgaard, M.B., Besenbacher, F. and Baatrup, E. 2012. In vivo toxicity of silver nanoparticles and silver ions in zebrafish (Danio rerio). *Journal of Toxicology* 2012.

Blanco-Andujar, C., Tung, L.D. and Thanh, N.T.K. 2010. Synthesis of nanoparticles for biomedical applications. *Annual Reports on the Progress of Chemistry - Section A* 106 (0): 553–568.

Boverhof, D.R., Bramante, C.M., Butala, J.H., Clancy, S.F., Lafranconi, W.M., West, J. and Gordon, S.C. 2015. Comparative assessment of nanomaterial definitions and safety evaluation considerations. *Regulatory Toxicology and Pharmacology* 73 (1): 137–150.

Boxall, A.B.A., Chaudhry, Q., Sinclair, C., Jones, A., Aitken, R., Jefferson, B. and Watts, C. 2007. Current and future predicted environmental exposure to engineered nanoparticles. *Central Science Laboratory, Department of the Environment and Rural Affairs, London, UK* 89.

Brant, J., Lecoanet, H. and Wiesner, M.R. 2005. Aggregation and deposition characteristics of fullerene nanoparticles in aqueous systems. *Journal of Nanoparticle Research* 7 (4–5): 545–553.

British Standards Institution. 2007. Terminology for nanomaterials. PAS 136:2007. *Text*: 16.

Buffle, J., Wilkinson, K.J., Stoll, S., Filella, M. and Zhang, J. 1998. A generalized description of aquatic colloidal interactions: The three- culloidal component approach. *Environmental Science and Technology* 32 (19): 2887–2899.

Burda, C., Chen, X., Narayanan, R. and El-Sayed, M.A. 2005. Chemistry and properties of nanocrystals of different shapes. *Chemical Reviews* 105 (4): 1025–1102.

Buzea, C., Pacheco, I.I. and Robbie, K. 2007. Nanomaterials and nanoparticles: Sources and toxicity. *Biointerphases* 2 (4): MR17–MR71.

Byrne, R.H. 2002. Inorganic speciation of dissolved elements in seawater: The influence of pH on concentration ratios. *Geochemical Transactions* 3: 11–16.

Chen, S.F., Zhang, H. and Lin, Q.Y. 2013. Effect of different water conditions on dissolution of nanosilver. *Water Science and Technology* 68 (8): 1745–1750.

Choi, O., Deng, K.K., Kim, N.J., Ross, L., Surampalli, R.Y. and Hu, Z. 2008. The inhibitory effects of silver nanoparticles, silver ions, and silver chloride colloids on microbial growth. *Water Research* 42 (12): 3066–3074.

Chung, K. 1999. Toxicity of cadmium, DDT, and fluoranthene to juvenile

Mercenaria mercenaria in aqueous and sediment bioassays.pp.

Chung, K.W., Fulton, M.H. and Scott, G.I. 2007. Use of the juvenile clam, Mercenaria mercenaria, as a sensitive indicator of aqueous and sediment toxicity. *Ecotoxicology and Environmental Safety* 67 (3): 333–340.

Collera-Zúñiga, O., García Jiménez, F. and Meléndez Gordillo, R. 2005. Comparative study of carotenoid composition in three mexican varieties of Capsicum annuum L. *Food Chemistry* 90 (1–2): 109–114.

Colvin, V.L. 2003. The potential environmental impact of engineered nanomaterials. *Nature Biotechnology* 21 (10): 1166–1170.

Croteau, M.N. and Luoma, S.N. 2005. Delineating copper accumulation pathways for the freshwater bivalve Corbicula using stable copper isotopes. *Environmental Toxicology and Chemistry* 24 (11): 2871–2878.

Cushing, B.L., Kolesnichenko, V.L. and O'Connor, C.J. 2004. Recent advances in the liquid-phase syntheses of inorganic nanoparticles. *Chemical Reviews* 104 (9): 3893–3946.

Dabbousi, B.O., Rodriguez-Viejo, J., Mikulec, F. V., Heine, J.R., Mattoussi, H., Ober, R., Jensen, K.F. and Bawendi, M.G. 1997. (CdSe)ZnS core-shell quantum dots: Synthesis and characterization of a size series of highly luminescent nanocrystallites. *Journal of Physical Chemistry B* 101 (46): 9463–9475.

DeLuca, T., Kaszuba, M. and Mattison, K. 2006. Optimizing silicone emulsion stability using zeta potential. *American Laboratory* 38 (13): 14–15.

Deonarine, A., Lau, B.L.T., Aiken, G.R., Ryan, J.N. and Hsu-Kim, H. 2011. Effects of humic substances on precipitation and aggregation of zinc sulfide nanoparticles. *Environmental Science and Technology* 45 (8): 3217–3223.

Dillon, R.T. and Manzi, J.J. 1989. Genetics and shell morphology in a hybrid zone between the hard clams Mercenaria mercenaria and M. campechiensis. *Marine Biology* 100 (2): 217–222.

Dobias, J. and Bernier-Latmani, R. 2013. Silver release from silver nanoparticles in natural waters. *Environmental Science and Technology* 47 (9): 4140–4146.

Doherty, F.G. 1990. The Asiatic clam, Corbicula spp., as a biological monitor in freshwater environments. *Environmental Monitoring and Assessment* 15 (2): 143–181.

Dowling, a, Clift, R., Grobert, N., Hutton, D., Oliver, R., O'neill, O., Pethica, J., Pidgeon, N., Porritt, J., Ryan, J. and Et Al. 2004. Nanoscience and nanotechnologies : opportunities and uncertainties. *London The Royal Society The Royal Academy of Engineering Report* 46 (July): 618–618.

Dwivedi, A.D., Dubey, S.P., Sillanpää, M., Kwon, Y.N., Lee, C. and Varma, R.S. 2015. Fate of engineered nanoparticles: Implications in the environment.

Coordination Chemistry Reviews 287: 64–78.

El-Rafie, H.M., El-Rafie, M.H. and Zahran, M.K. 2013. Green synthesis of silver nanoparticles using polysaccharides extracted from marine macro algae. *Carbohydrate Polymers* 96 (2): 403–410.

Evanoff, D.D. and Chumanov, G. 2005. Synthesis and optical properties of silver nanoparticles and arrays. *ChemPhysChem* 6 (7): 1221–1231.

Fabrega, J., Fawcett, S.R., Renshaw, J.C. and Lead, J.R. 2009. Silver nanoparticle impact on bacterial growth: Effect of pH, concentration, and organic matter. *Environmental Science and Technology* 43 (19): 7285–7290.

Fabrega, J., Luoma, S.N., Tyler, C.R., Galloway, T.S. and Lead, J.R. 2011. Silver nanoparticles: Behaviour and effects in the aquatic environment. *Environment International* 37 (2): 517–531.

Farkas, J., Cappadona, V., Olsen, A.J., Hansen, B.H., Posch, W., Ciesielski, T.M., Goodhead, R., Wilflingseder, D., Blatzer, M., Altin, D., Moger, J., Booth, A.M. and Jenssen, B.M. 2020. Combined effects of exposure to engineered silver nanoparticles and the water-soluble fraction of crude oil in the marine copepod Calanus finmarchicus. *Aquatic Toxicology* 227.

Fauconnier, N., Pons, J.N., Roger, J. and Bee, A. 1997. Thiolation of maghemite nanoparticles by dimercaptosuccinic acid. *Journal of Colloid and Interface Science* 194 (2): 427–433.

Foltynowicz, Z., Gwiazdowska, D., Rodewald, D., Nowaczyk, A. and Filipiak, M. 2013. Antimicrobial properties of socks protected with silver nanoparticles. *Fibres and Textiles in Eastern Europe* 101 (5): 91–96.

Gatoo, M.A., Naseem, S., Arfat, M.Y., Mahmood Dar, A., Qasim, K. and Zubair, S. 2014. Physicochemical properties of nanomaterials: Implication in associated toxic manifestations. *BioMed Research International* 2014.

Georgantzopoulou, A. 2015. Effects of silver nanoparticles and ions and interactions with first line of defense.Wageningen University, 186pp.

Georgantzopoulou, A., Balachandran, Y.L., Rosenkranz, P., Dusinska, M., Lankoff, A., Wojewodzka, M., Kruszewski, M., Guignard, C., Audinot, J.N., Girija, S., Hoffmann, L. and Gutleb, A.C. 2013. Ag nanoparticles: Size- and surface-dependent effects on model aquatic organisms and uptake evaluation with NanoSIMS. *Nanotoxicology* 7 (7): 1168–1178.

Georgieva, J. V., Kalicharan, D., Couraud, P.O., Romero, I.A., Weksler, B., Hoekstra, D. and Zuhorn, I.S. 2011. Surface characteristics of nanoparticles determine their intracellular fate in and processing by human blood-brain barrier endothelial cells in vitro. *Molecular Therapy* 19 (2): 318–325.

Ghoul, M., Bacquet, M. and Morcellet, M. 2003. Uptake of heavy metals from synthetic aqueous solutions using modified PEI - Silica gels. *Water Research* 37 (4): 729–734.

Gnach, A., Lipinski, T., Bednarkiewicz, A., Rybka, J. and Capobianco, J.A. 2015. Upconverting nanoparticles: Assessing the toxicity. *Chemical Society Reviews* 44 (6): 1561–1584.

Gong, N., Shao, K., Feng, W., Lin, Z., Liang, C. and Sun, Y. 2011. Biotoxicity of nickel oxide nanoparticles and bio-remediation by microalgae Chlorella vulgaris. *Chemosphere* 83 (4): 510–516.

Gosling, E. 2003. *Bivalve Molluscs Biology, Ecology and Culture*. .

Goswami, L., Kim, K.H., Deep, A., Das, P., Bhattacharya, S.S., Kumar, S. and Adelodun, A.A. 2017. Engineered nano particles: Nature, behavior, and effect on the environment. *Journal of Environmental Management* 196: 297–315.

Grassian, V.H., O'Shaughnessy, P.T., Adamcakova-Dodd, A., Pettibone, J.M. and Thorne, P.S. 2007. Inhalation exposure study of Titanium dioxide nanoparticles with a primary particle size of 2 to 5 nm. *Environmental Health Perspectives* 115 (3): 397–402.

Griffitt, R.J., Luo, J., Gao, J., Bonzongo, J.-C.C. and Barber, D.S. 2008. Effects of particle composition and species on toxicity of metallic nanomaterials in aquatic organisms. *Environmental Toxicology and Chemistry* 27 (9): 1972–1978.

Gu, H. and Soucek, M.D. 2007. Preparation and characterization of monodisperse cerium oxide nanoparticles in hydrocarbon solvents. *Chemistry of Materials* 19 (5): 1103–1110.

Guillard, R.R.L. 1975. Culture of phytoplankton for feeding marine invertebrates. *In*: Smith, M.L. and Chanley, M.H. (ed.), *Culture of Marine Invertebrate Animals*, 29–60. Plenum Press.

Guo, L. and Santschi, P.H. 2007. Ultrafiltration and its Applications to Sampling and Characterisation of Aquatic Colloids. *In*: *Environmental Colloids and Particles: Behaviour, Separation and Characterisation*, 159–221. wiley.

Guzman, K.A.D., Finnegan, M.P. and Banfield, J.F. 2006. Influence of surface potential on aggregation and transport of titania nanoparticles. *Environmental Science and Technology* 40 (24): 7688–7693.

Handy, R.D., Von Der Kammer, F., Lead, J.R., Hassellöv, M., Owen, R. and Crane, M. 2008. The ecotoxicology and chemistry of manufactured nanoparticles. *Ecotoxicology* 17 (4): 287–314.

Hartland, A., Fairchild, I.J.I.J., Lead, J.R.J.R., Borsato, A., Baker, A., Frisia, S. and Baalousha, M. 2012. From soil to cave: Transport of trace metals by natural organic matter in karst dripwaters. *Chemical Geology* 304–305: 68–82.

Hartmann, N.I.B., Skjolding, L.M., Hansen, S.F., Baun, A., Kjølholt, J. and Gottschalk, F. 2014. Environmental fate and behaviour of nanomaterials: new knowledge on important transfomation processes. .

Ismail, H., Sam, S.T., Mohd Noor, A.F. and Bakar, A.A. 2007. Properties of ferrite-filled natural rubber composites. *Polymer - Plastics Technology and Engineering* 46 (6): 641–650.

Jana, N.R., Gearheart, L. and Murphy, C.J. 2001. Wet chemical synthesis of silver nanorods and nanowires of controllable aspect ratio. *Chemical Communications* (7): 617–618.

Jeevanandam, J., Barhoum, A., Chan, Y.S., Dufresne, A. and Danquah, M.K. 2018. Review on nanoparticles and nanostructured materials: History, sources, toxicity and regulations. *Beilstein Journal of Nanotechnology* 9 (1): 1050–1074.

Jha, A., Prasad, K. and Kulkarni, and A. 2008. Yeast Mediated Synthesis of Silver Nanoparticles. *International Journal of Nanoscience and Nanotechnology* 4 (1): 17–22.

Jin, S. and Ye, K. 2007. Nanoparticle-mediated drug delivery and gene therapy. *Biotechnology Progress* 23 (1): 32–41.

Johari, S.A., Kalbassi, M.R., Soltani, M. and Yu, I.J. 2013. Toxicity comparison of colloidal silver nanoparticles in various life stages of rainbow trout (Oncorhynchus mykiss). *Iranian Journal of Fisheries Sciences* 12 (1): 76–95.

Ju-Nam, Y. and Lead, J.R. 2008. Manufactured nanoparticles: An overview of their chemistry, interactions and potential environmental implications. *Science of the Total Environment* 400 (1–3): 396–414.

K, a, Gorzela, K. and Bugla-p, G. 2013. Positive and Negative Aspects of Silver Nanoparticles Usage. *Biology International* 53: 10.

Kim, S. Il, Reeve, J. and Bong, M. 2016. Introduction to motivational neuroscience. *Advances in Motivation and Achievement* 19: 1–19.

Kirschling, T.L., Golas, P.L., Unrine, J.M., Matyjaszewski, K., Gregory, K.B., Lowry, G. V. and Tilton, R.D. 2011. Microbial bioavailability of covalently bound polymer coatings on model engineered nanomaterials. *Environmental Science and Technology* 45 (12): 5253–5259.

Klaine, S.J., Alvarez, P.J.J., Batley, G.E., Fernandes, T.F., Handy, R.D., Lyon, D.Y., Mahendra, S., McLaughlin, M.J. and Lead, J.R. 2008. *(4) (PDF) Nanomaterials in the environment: Behavior, fate, bioavailability, and effects*. Environmental Toxicology and Chemistry. Downloaded from https://www.researchgate.net/publication/23666951_Nanomaterials_in_the_ environment_Behavior_fate_bioavailability_and_effects on 19 May 2021. Environ Toxicol Chem.

Kreyling, W.G., Semmler-Behnke, M. and Chaudhry, Q. 2010. A complementary definition of nanomaterial. *Nano Today* 5 (3): 165–168.

Krishnaraj, C., Harper, S.L. and Yun, S. Il. 2016. In Vivo toxicological assessment of biologically synthesized silver nanoparticles in adult Zebrafish (Danio rerio).

Journal of Hazardous Materials 301: 480–491.

Kroto, H.W., Heath, J.R., O'Brien, S.C., Curl, R.F. and Smalley, R.E. 1985. C60: Buckminsterfullerene. *Nature* 318 (6042): 162–163.

Kumar, N. and Kumbhat, S. 2016. Chapter 5. Carbon-based nanomaterials. *Essentials in Nanoscience and Nanotechnology* (2016): 189–236.

Kumar, S.A., Abyaneh, M.K., Gosavi, S.W., Kulkarni, S.K., Pasricha, R., Ahmad, A. and Khan, M.I. 2007. Nitrate reductase-mediated synthesis of silver nanoparticles from AgNO 3. *Biotechnology Letters* 29 (3): 439–445.

Kwok, K.W.H., Auffan, M., Badireddy, A.R., Nelson, C.M., Wiesner, M.R., Chilkoti, A., Liu, J., Marinakos, S.M. and Hinton, D.E. 2012. Uptake of silver nanoparticles and toxicity to early life stages of Japanese medaka (Oryzias latipes): Effect of coating materials. *Aquatic Toxicology* 120–121: 59–66.

Laborda, F., Jiménez-Lamana, J., Bolea, E. and Castillo, J.R. 2013. Critical considerations for the determination of nanoparticle number concentrations, size and number size distributions by single particle ICP-MS. *Journal of Analytical Atomic Spectrometry* 28 (8): 1220–1232.

Lapresta-Fernández, A., Fernández, A. and Blasco, J. 2012. Nanoecotoxicity effects of engineered silver and gold nanoparticles in aquatic organisms. *TrAC - Trends in Analytical Chemistry* 32: 40–59.

Law, N., Ansari, S., Livens, F.R., Renshaw, J.C. and Lloyd, J.R. 2008. Formation of nanoscale elemental silver particles via enzymatic reduction by Geobacter sulfurreducens. *Applied and Environmental Microbiology* 74 (22): 7090–7093.

Lead, J.R., Muirhead, D. and Gibson, C.T. 2005. Characterization of freshwater natural aquatic colloids by atomic force microscopy (AFM). *Environmental Science and Technology* 39 (18): 6930–6936.

Lead, J.R., Batley, G.E., Alvarez, P.J.J., Croteau, M.N., Handy, R.D., McLaughlin, M.J., Judy, J.D. and Schirmer, K. 2018. Nanomaterials in the environment: Behavior, fate, bioavailability, and effects—An updated review. *Environmental Toxicology and Chemistry* 37 (8): 2029–2063.

Lee, W.S., Kim, E., Cho, H.J., Kang, T., Kim, B., Kim, M.Y., Kim, Y.S., Song, N.W., Lee, J.S. and Jeong, J. 2018. The relationship between dissolution behavior and the toxicity of silver nanoparticles on zebrafish embryos in different ionic environments. *Nanomaterials* 8 (9).

Lei, C., Sun, Y., Tsang, D.C.W. and Lin, D. 2018. Environmental transformations and ecological effects of iron-based nanoparticles. *Environmental Pollution* 232: 10–30.

Levard, C., Hotze, E.M., Lowry, G. V. and Brown, G.E. 2012. Environmental transformations of silver nanoparticles: Impact on stability and toxicity. *Environmental Science and Technology* 46 (13): 6900–6914.

Levard, C., Reinsch, B.C., Michel, F.M., Oumahi, C., Lowry, G. V. and Brown, G.E. 2011. Sulfidation processes of PVP-coated silver nanoparticles in aqueous solution: Impact on dissolution rate. *Environmental Science and Technology* 45 (12): 5260–5266.

Li, X. and Lenhart, J.J. 2012. Aggregation and dissolution of silver nanoparticles in natural surface water. *Environmental Science and Technology* 46 (10): 5378–5386.

Li, X., Lenhart, J.J. and Walker, H.W. 2012. Aggregation kinetics and dissolution of coated silver nanoparticles. *Langmuir* 28 (2): 1095–1104.

Liu, J. and Hurt, R.H. 2010. Ion release kinetics and particle persistence in aqueous nano-silver colloids. *Environmental Science and Technology* 44 (6): 2169–2175.

Liu, J., Sonshine, D.A., Shervani, S. and Hurt, R.H. 2010. Controlled release of biologically active silver from nanosilver surfaces. *ACS Nano* 4 (11): 6903–6913.

Lovrić, J., Cho, S.J., Winnik, F.M. and Maysinger, D. 2005. Unmodified cadmium telluride quantum dots induce reactive oxygen species formation leading to multiple organelle damage and cell death. *Chemistry and Biology* 12 (11): 1227–1234.

Lowry, G. V., Gregory, K.B., Apte, S.C. and Lead, J.R. 2012. Transformations of nanomaterials in the environment. *Environmental Science and Technology* 46 (13): 6893–6899.

MacCuspie, R.I. 2011. Colloidal stability of silver nanoparticles in biologically relevant conditions. *Journal of Nanoparticle Research* 13 (7): 2893–2908.

Maynard, A.D., Aitken, R.J., Butz, T., Colvin, V., Donaldson, K., Oberdörster, G., Philbert, M.A., Ryan, J., Seaton, A., Stone, V., Tinkle, S.S., Tran, L., Walker, N.J. and Warheit, D.B. 2006. Safe handling of nanotechnology. *Nature* 444 (7117): 267–269.

Mcleod, P.B., Luoma, S.N. and Luthy, R.G. 2008. Biodynamic modeling of PCB uptake by Macoma balthica and Corbicula fluminea from sediment amended with activated carbon. *Environmental Science and Technology* 42 (2): 484–490.

Mehennaoui, K., Georgantzopoulou, A., Felten, V., Andreï, J., Garaud, M., Cambier, S., Serchi, T., Pain-Devin, S., Guérold, F., Audinot, J.N., Giambérini, L. and Gutleb, A.C. 2016. Gammarus fossarum (Crustacea, Amphipoda) as a model organism to study the effects of silver nanoparticles. *Science of the Total Environment* 566–567: 1649–1659.

Miller, W.A., Gardner, I.A., Atwill, E.R., Leutenegger, C.M., Miller, M.A., Hedrick, R.P., Melli, A.C., Barnes, N.M. and Conrad, P.A. 2006. Evaluation of methods for improved detection of Cryptosporidium spp. in mussels (Mytilus

californianus). *Journal of Microbiological Methods* 65 (3): 367–379.

Mishra, G., Singh, D., Yadawa, P.K., Verma, S.K. and Yadav, R.R. 2013. Study of Copper/Palladium Nanoclusters Using Acoustic Particle Sizer. *Platinum Metals Review* 57 (3): 186–191.

Mitrano, D.M., Limpiteeprakan, P., Babel, S. and Nowack, B. 2016. Durability of nano-enhanced textiles through the life cycle: Releases from landfilling after washing. *Environmental Science: Nano* 3 (2): 375–387.

Mohanpuria, P., Rana, N.K. and Yadav, S.K. 2008. Biosynthesis of nanoparticles: Technological concepts and future applications. *Journal of Nanoparticle Research* 10 (3): 507–517.

Montaño, M.D., Olesik, J.W., Barber, A.G., Challis, K. and Ranville, J.F. 2016. Single Particle ICP-MS: Advances toward routine analysis of nanomaterials. *Analytical and Bioanalytical Chemistry* 408 (19): 5053–5074.

Moore, K. 2006. A new silver dressing for wounds with delayed healing. *Wounds UK* 2 (2): 70–78.

Moore, T.L., Rodriguez-Lorenzo, L., Hirsch, V., Balog, S., Urban, D., Jud, C., Rothen-Rutishauser, B., Lattuada, M. and Petri-Fink, A. 2015. Nanoparticle colloidal stability in cell culture media and impact on cellular interactions. *Chemical Society Reviews* 44 (17): 6287–6305.

Morgan, T.P., Grosell, M., Playle, R.C. and Wood, C.M. 2004. The time course of silver accumulation in rainbow trout during static exposure to silver nitrate: Physiological regulation or an artifact of the exposure conditions? *Aquatic Toxicology* 66 (1): 55–72.

Mudunkotuwa, I.A., Pettibone, J.M. and Grassian, V.H. 2012. Environmental implications of nanoparticle aging in the processing and fate of copper-based nanomaterials. *Environmental Science and Technology* 46 (13): 7001–7010.

Mukherjee, P., Ahmad, A., Mandal, D., Senapati, S., Sainkar, S.R., Khan, M.I., Parishcha, R., Ajaykumar, P. V., Alam, M., Sastry, M., Kumar, R. and Sastry, M. 2001. Fungus-Mediated Synthesis of Silver Nanoparticles and Their Immobilization in the Mycelial Matrix: A Novel Biological Approach to Nanoparticle Synthesis. *Nano Letters* 1 (10): 515–519.

Murdock, R.C., Braydich-Stolle, L., Schrand, A.M., Schlager, J.J. and Hussain, S.M. 2008. Characterization of nanomaterial dispersion in solution prior to in vitro exposure using dynamic light scattering technique. *Toxicological Sciences* 101 (2): 239–253.

Nair, P.M.G., Park, S.Y. and Choi, J. 2013. Evaluation of the effect of silver nanoparticles and silver ions using stress responsive gene expression in Chironomus riparius. *Chemosphere* 92 (5): 592–599.

Narayanan, K.B. and Sakthivel, N. 2010. Biological synthesis of metal nanoparticles by microbes. *Advances in Colloid and Interface Science* 156 (1–

2): 1–13.

Navarro, E., Piccapietra, F., Wagner, B., Marconi, F., Kaegi, R., Odzak, N., Sigg, L. and Behra, R. 2008a. Toxicity of silver nanoparticles to Chlamydomonas reinhardtii. *Environmental Science and Technology* 42 (23): 8959–8964.

Navarro, E., Baun, A., Behra, R., Hartmann, N.B., Filser, J., Miao, A.J., Quigg, A., Santschi, P.H. and Sigg, L. 2008b. Environmental behavior and ecotoxicity of engineered nanoparticles to algae, plants, and fungi. *Ecotoxicology* 17 (5): 372–386.

Nel, A., Xia, T., Mädler, L. and Li, N. 2006. Toxic potential of materials at the nanolevel. *Science* 311 (5761): 622–627.

Nichols, G., Byard, S., Bloxham, M.J., Botterill, J., Dawson, N.J., Dennis, A., Diart, V., North, N.C. and Sherwood, J.D. 2002. A review of the terms agglomerate and aggregate with a recommendation for nomenclature used in powder and particle characterization. *Journal of Pharmaceutical Sciences* 91 (10): 2103–2109.

Niemeyer, C.M. 2010. ChemInform Abstract: Nanoparticles, Proteins, and Nucleic Acids: Biotechnology Meets Materials Science. *ChemInform* 33 (13): no-no.

Nowack, B. and Bucheli, T.D. 2007. Occurrence, behavior and effects of nanoparticles in the environment. *Environmental Pollution* 150 (1): 5–22.

Nowack, B., Ranville, J.F., Diamond, S., Gallego-Urrea, J.A., Metcalfe, C., Rose, J., Horne, N., Koelmans, A.A. and Klaine, S.J. 2012. Potential scenarios for nanomaterial release and subsequent alteration in the environment. *Environmental Toxicology and Chemistry* 31 (1): 50–59.

Ocsoy, I., Gulbakan, B., Chen, T., Zhu, G., Chen, Z., Sari, M.M., Peng, L., Xiong, X., Fang, X. and Tan, W. 2013a. DNA-guided metal-nanoparticle formation on graphene oxide surface. *Advanced Materials* 25 (16): 2319–2325.

Ocsoy, I., Paret, M.L., Ocsoy, M.A., Kunwar, S., Chen, T., You, M. and Tan, W. 2013b. Nanotechnology in plant disease management: DNA-directed silver nanoparticles on graphene oxide as an antibacterial against Xanthomonas perforans. *ACS Nano* 7 (10): 8972–8980.

Ouali, L. and Pefferkorn, E. 1994. Fragmentation of colloidal aggregates induced by polymer adsorption. *Journal of Colloid And Interface Science* 168 (2): 315–322.

Oza, G., Reyes-Calderón, A., Mewada, A., Arriaga, L.G., Cabrera, G.B., Luna, D.E., Iqbal, H.M.N., Sharon, M. and Sharma, A. 2020. Plant-based metal and metal alloy nanoparticle synthesis: a comprehensive mechanistic approach. *Journal of Materials Science* 55 (4): 1309–1330.

Pal, T., Sau, T.K. and Jana, N.R. 1997. Reversible formation and dissolution of silver nanoparticles in aqueous surfactant media. *Langmuir* 13 (6): 1481–1485.

Patakfalvi, R., Papp, S. and Dékány, I. 2007. The kinetics of homogeneous nucleation of silver nanoparticles stabilized by polymers. *Journal of Nanoparticle Research* 9 (3): 353–364.

Peijnenburg, W.J.G.M.G.M., Baalousha, M., Chen, J., Chaudry, Q., Von Der Kammer, F., Kuhlbusch, T.A.J.J., Lead, J., Nickel, C., Quik, J.T.K.K., Renker, M., Wang, Z. and Koelmans, A.A. 2015. A Review of the Properties and Processes Determining the Fate of Engineered Nanomaterials in the Aquatic Environment. *Critical Reviews in Environmental Science and Technology* 45 (19): 2084–2134.

Pietroiusti, A., Massimiani, M., Fenoglio, I., Colonna, M., Valentini, F., Palleschi, G., Camaioni, A., Magrini, A., Siracusa, G., Bergamaschi, A., Sgambato, A. and Campagnolo, L. 2011. Low doses of pristine and oxidized single-wall carbon nanotubes affect mammalian embryonic development. *ACS Nano* 5 (6): 4624–4633.

Prabhu, S. and Poulose, E.K. 2012. Silver nanoparticles: mechanism of antimicrobial action, synthesis, medical applications, and toxicity effects. *International Nano Letters* 2 (1): 1–10.

Pyatenko, A., Yamaguchi, M. and Suzuki, M. 2007. Synthesis of spherical silver nanoparticles with controllable sizes in aqueous solutions. *Journal of Physical Chemistry C* 111 (22): 7910–7917.

Rama, P., Kaur, B.S., Mausam, V., Y., S.R. and C., Z.T. 2021. Behavior and Fate of Natural and Engineered Nanomaterials in Soils. *Nanomaterials in the Environment*: 291–314.

Rhodes, E. W. and Landers, W.C. 1974. Growth of oyster larva Grassorted virginica of various sizes in different concentrations of the Chrysophyte Isochrysis galbana. *Proc. Natn. Shellfish Assoc.,* 63: 53–59.

Ringwood, A.H., McCarthy, M., Bates, T.C. and Carroll, D.L. 2010. The effects of silver nanoparticles on oyster embryos. *Marine Environmental Research* 69 (SUPPL. 1): S49–S51.

Samadi, N., Golkaran, D., Eslamifar, A., Jamalifar, H., Fazeli, M.R. and Mohseni, F.A. 2009. Intra/extracellular biosynthesis of silver nanoparticles by an autochthonous strain of Proteus mirabilis isolated from photographic waste. *Journal of Biomedical Nanotechnology* 5 (3): 247–253.

Schmid, G., Decker, M. and Ernst, H. 2003. Small dimensions and material properties. *Graue Reihe* 35 (November): 1–125.

Scott, A.P. and Middleton, C. 1979. Unicellular algae as a food for turbot (Scophthalmus maximus L.) larvae - The importance of dietary long-chain polyunsaturated fatty acids. *Aquaculture* 18 (3): 227–240.

Seaton, A. and Donaldson, K. 2005. Nanoscience, nanotoxicology, and the need to think small. *Lancet* 365 (9463): 923–924.

Sikder, M., Eudy, E., Chandler, G.T. and Baalousha, M. 2018. Comparative study of dissolved and nanoparticulate Ag effects on the life cycle of an estuarine meiobenthic copepod, Amphiascus tenuiremis. *Nanotoxicology* 12 (5): 375–389.

Singhal, G., Bhavesh, R., Kasariya, K., Sharma, A.R., Singh, R.P. and Singh, P.R. 2011. Biosynthesis of silver nanoparticles using Ocimum sanctum (Tulsi) leaf extract and screening its antimicrobial activity. *Journal of Nanoparticle Research* 13 (7): 2981–2988.

Sintubin, L., Verstraete, W. and Boon, N. 2012. Biologically produced nanosilver: Current state and future perspectives. *Biotechnology and Bioengineering* 109 (10): 2422–2436.

Sintubin, L., De Windt, W., Dick, J., Mast, J., Van Der Ha, D., Verstraete, W. and Boon, N. 2009. Lactic acid bacteria as reducing and capping agent for the fast and efficient production of silver nanoparticles. *Applied Microbiology and Biotechnology* 84 (4): 741–749.

Sohn, E.K., Johari, S.A., Kim, T.G., Kim, J.K., Kim, E., Lee, J.H., Chung, Y.S. and Yu, I.J. 2015. Aquatic toxicity comparison of silver nanoparticles and silver nanowires. *BioMed Research International* 2015.

Stolpe, B. and Hassellöv, M. 2007. Changes in size distribution of fresh water nanoscale colloidal matter and associated elements on mixing with seawater. *Geochimica et Cosmochimica Acta* 71 (13): 3292–3301.

Sugimoto, T. 1987. Preparation of monodispersed colloidal particles. *Advances in Colloid and Interface Science* 28 (C): 65–108.

Thompson, M., Nel, A.E., Somasundaran, P., Mädler, L., Klaessig, F., Velegol, D., Hoek, E.M. V., Castranova, V. and Xia, T. 2009. Understanding biophysicochemical interactions at the nano–bio interface. *Nature Materials* 8 (7): 543–557.

Tian, J., Wong, K.K.Y., Ho, C.M., Lok, C.N., Yu, W.Y., Che, C.M., Chiu, J.F. and Tam, P.K.H. 2007. Topical delivery of silver nanoparticles promotes wound healing. *ChemMedChem* 2 (1): 129–136.

Torkamani, S., Wani, S.N., Tang, Y.J. and Sureshkumar, R. 2010. Plasmon-enhanced microalgal growth in miniphotobioreactors. *Applied Physics Letters* 97 (4): 43703.

Tourinho, P.S., van Gestel, C.A.M., Lofts, S., Svendsen, C., Soares, A.M.V.M. and Loureiro, S. 2012. Metal-based nanoparticles in soil: Fate, behavior, and effects on soil invertebrates. *Environmental Toxicology and Chemistry* 31 (8): 1679–1692.

UDFDA. 2011. Guidance for industry considering whether an FDA-regulated product involves the application of nanotechnology. *Biotechnology Law Report* 30 (5): 613–616.

US EPA. 2010. *Indoor Air Quality (IAQ)* | *US EPA*. Building Air Quality (BAQ): A Guide for Building Owners and Facility Managers. Downloaded from https://www.epa.gov/indoor-air-quality-iaq on 24 May 2021.

US EPA. . *EPA Regional Office and State Indoor Air Quality Information*. Downloaded from https://www.epa.gov/indoor-air-quality-iaq/epa-regional-office-and-state-indoor-air-quality-information on 24 May 2021.

Vanhaecke, F., Vanhoe, H., Dams, R. and Vandecasteele, C. 1992. The use of internal standards in ICP-MS. *Talanta* 39 (7): 737–742.

Veerakumar, P., Lu, Z.Z., Velayudham, M., Lu, K.L. and Rajagopal, S. 2010. Alumina supported nanoruthenium as efficient heterogeneous catalyst for the selective H2O2 oxidation of aliphatic and aromatic sulfides to sulfoxides. *Journal of Molecular Catalysis A: Chemical* 332 (1–2): 128–137.

Veerasamy, R., Xin, T.Z., Gunasagaran, S., Xiang, T.F.W., Yang, E.F.C., Jeyakumar, N. and Dhanaraj, S.A. 2011. Biosynthesis of silver nanoparticles using mangosteen leaf extract and evaluation of their antimicrobial activities. *Journal of Saudi Chemical Society* 15 (2): 113–120.

Wagner, S., Gondikas, A., Neubauer, E., Hofmann, T. and Von Der Kammer, F. 2014. Spot the difference: Engineered and natural nanoparticles in the environment-release, behavior, and fate. *Angewandte Chemie - International Edition* 53 (46): 12398–12419.

Wood, B.J.B. 1974. Fatty acids and saponifiable lipids. *In*: Stewart, W.D.. (ed.), *Algal Physiology and Biochemistry*, Blackwell Scientific Publications.

Wu, Y., Zhou, Q., Li, H., Liu, W., Wang, T. and Jiang, G. 2010. Effects of silver nanoparticles on the development and histopathology biomarkers of Japanese medaka (Oryzias latipes) using the partial-life test. *Aquatic Toxicology* 100 (2): 160–167.

Xu, J. 2011. Biomolecules Produced by Mangrove-Associated Microbes. *Current Medicinal Chemistry* 18 (34): 5224–5266.

Yang, X., Gondikas, A.P., Marinakos, S.M., Auffan, M., Liu, J., Hsu-Kim, H. and Meyer, J.N. 2012. Mechanism of silver nanoparticle toxicity is dependent on dissolved silver and surface coating in caenorhabditis elegans. *Environmental Science and Technology* 46 (2): 1119–1127.

Yoon, K.Y., Hoon Byeon, J., Park, J.H. and Hwang, J. 2007. Susceptibility constants of Escherichia coli and Bacillus subtilis to silver and copper nanoparticles. *Science of the Total Environment* 373 (2–3): 572–575.

Zar, J.H. 1996. *Biostatistical Analysis*. Prentice Hall, Inc, .

Zhang, H. 2013. Application of silver nanoparticles in drinking water purification.Paper 200pp.

Zhang, W., Yao, Y., Sullivan, N. and Chen, Y. 2011. Modeling the primary size

effects of citrate-coated silver nanoparticles on their ion release kinetics. *Environmental Science and Technology* 45 (10): 4422–4428.

Zhou, K., Boggs, S.A., Ramprasad, R., Aindow, M., Erkey, C. and Alpay, S.P. 2008. Dielectric response and tunability of a dielectric-paraelectric composite. *Applied Physics Letters* 93 (10): 102908.

WHO | Indoor air pollution and household energy. Downloaded from https://www.who.int/heli/risks/indoorair/indoorair/en/ on 24 May 2021.